

Goddard-Problem Variants

by

Panagiotis Tsiotras

Thesis submitted to the Faculty of the
Virginia Polytechnic Institute and State University
in partial fulfillment of the requirements for the degree of
Master of Science
in
Aerospace Engineering

APPROVED:

Henry J. Kelley

Eugene M. Cliff

Harold L. Stalford

November, 1987

Blacksburg, Virginia

Goddard-Problem Variants

by

Panagiotis Tsiotras

Henry J. Kelley

Aerospace Engineering

(ABSTRACT)

The problem of maximizing the altitude of a rocket in vertical flight has been extensively analyzed by many writers since the early days of rocketry. In the beginning, solutions were obtained using the classical theory of the Calculus of Variations, and later using Optimal Control theory. For strict assumptions on the drag law and the thrust, solutions were found, even in a closed, analytic form. Nevertheless, for more realistic conditions, the problem becomes a very complex one, and the solution is far from complete. In addition to this, complexity increases if an isoperimetric constraint is added to the problem. Such a case is, for example, the problem of extremizing the rise in altitude for a given time. In the present work an attempt is made to treat the problem under the most realistic assumptions used so far, for both the system of equations and the drag model. The analysis of the problem reveals that a more complex thrust history exists than the classical sequence of full-singular-coast subarcs, for both the time-constrained case, and for the case of a drag model with a sharp rise in the transonic region. In the first case, a second full-thrust subarc is generated at the end of the singular subarc, owing to the boundedness of the thrust, while,

in the second case, a full-thrust subarc appears in transition from the subsonic to the supersonic branch of the singular path. Both are new results, at least for the bounded-thrust case, and the drag law assumed, insofar as the author knows. Discussion is also provided for the limitations of such a switching structure, and it is shown that the composition of an optimal trajectory is heavily dependent on the assumed drag law.

Acknowledgments

I would like to express my deepest gratitude to my thesis advisor, and professor, Dr. Henry J. Kelley, for providing guidance, encouragement, and for trying to teach me his invaluable insight for optimal control problems.

I would like to extend my sincere appreciation to Dr. Eugene M. Cliff for his valuable suggestions and remarks during my research, and especially for his help during the literature survey. I wish to thank also Dr. Harold L. Stalford for serving on my committee.

Last but not least, I would like to use this opportunity to thank all of my friends for their support and inspiration during my work, and especially Hans Seywald and Renjith Kumar for the creative discussions we had, but most important, for their friendship.

Support for this research work was partially provided by the USAF Armament Laboratory, Eglin AFB, Florida under contract F08635-86-K-0390, which is gratefully acknowledged.

Dedicated to the
memory of my father

Table of Contents

Chapter 1. Introduction.....	1
Historical Review	1
Motivation and Objectives	3
Chapter 2. Problem Formulation	5
Statement of Problem.....	5
Basic Assumptions.....	5
Equations of Motion	7
Boundary and Transersality Conditions.....	9
Problem Analysis.....	10
Evaluation of Singular Control.....	12
Construction of the Singular Surface.....	14

Chapter 3. Case of Constant Drag Coefficient.....	17
Numerical Data.....	17
Numerical Solution and Computational Results.....	18
Chapter 4. Necessary Conditions for Optimality.....	23
Overview.....	23
Kelley Condition.....	24
Transformation to Reduced State-space.....	24
Junction Conditions.....	30
Jacobi and Jacobi-like Conditions.....	32
Chapter 5. Mach-Dependent Drag Coefficient.....	35
Problem Formulation.....	35
Control-Logic Analysis.....	37
Composite Optimal Trajectory.....	39
Numerical Solution and Computational Results.....	40
Chapter 6. Conclusions.....	42
Suggestions for Future Research.....	43
List of References.....	45
Tables.....	50

Figures.....	53
Vita.....	99

LIST OF FIGURES

<u>Fig.</u>	<u>Title</u>
1	Singular surface in h,m,v space
2	Variation of Hamiltonian with final time
3	Variation of final altitude with final time
4	Variation of final velocity with final time
5	Variation of full-thrust subarc with final time
6	Variation of singular-thrust subarc with final time
7	Variation of zero-thrust subarc with final time
8	Variation of altitude h with time
9	Variation of velocity v with time
10	Variation of mass m with time
11	Variation of thrust P with time
12	Variation of thrust P with time for full-singular-full sequence
13	Variation of costate λ_h with time
14	Variation of costate λ_v with time
15	Variation of costate λ_m with time
16	Variation of mass m with velocity v
17	Variation of altitude h with velocity v
18	Switching function \mathcal{H}_1 vs. time for full-coast sequence

- 19 Switching function \mathcal{H}_1 vs. time for full-singular-full-coast sequence
- 20 Switching function \mathcal{H}_1 vs. time for full-singular-coast sequence
- 21 Variation of z_1 with z_3
- 22 Variation of z_1 with time
- 23 Variation of z_3 with time
- 24 Variation of drag coefficient with Mach number
- 25 Variation of $\frac{\partial C_D}{\partial M}$ with Mach number
- 26 Variation of $\frac{\partial^2 C_D}{\partial M^2}$ with Mach number
- 27 Variation of Drag with Mach number
- 28 Variation of $\frac{\partial D}{\partial v}$ with Mach number
- 29 Variation of $\frac{\partial^2 D}{\partial v^2}$ with Mach number
- 30 Variation of $v(\frac{\partial^2 D_o}{\partial v^2} + \frac{\partial D_o}{c \partial v} c^{-1}) + \frac{D_o}{c}$ with Mach number
- 31 Singular surface for Mach dependent drag coefficient
- 32 Projection of singular path on mass-velocity plane
- 33 Projection of singular path on altitude-velocity plane
- 34 Variation of $-\tilde{\mathcal{H}}$ with $z_2 = v$ in the reduced state-space
- 35 Projection of the trajectory on mass-velocity plane for $P_{\max} = \infty$
- 36 Projection of the trajectory on altitude-velocity plane for $P_{\max} = \infty$
- 37 Variation of altitude h with time for $P_{\max} = 6$
- 38 Variation of velocity v with time for $P_{\max} = 6$
- 39 Variation of mass m with time for $P_{\max} = 6$
- 40 Variation of costate λ_h with time for $P_{\max} = 6$

- 41 Variation of costate λ_v with time for $P_{\max} = 6$
- 42 Variation of costate λ_m with time for $P_{\max} = 6$
- 43 Switching function \mathcal{H}_1 vs. time for $P_{\max} = 6$
- 44 Switching function \mathcal{H}_1 vs. time for full-singular-full-singular sequence

NOMENCLATURE

\tilde{c}	Exhaust Velocity, Dimensionalized
c	Exhaust Velocity, Non-Dimensionalized
C_D	Drag Coefficient
\tilde{D}	Aerodynamic Drag, Dimensionalized
D	Aerodynamic Drag, Non-Dimensionalized
D_o	Part of Drag, depending only on the Velocity
\tilde{g}	Acceleration due to Gravity
G	Gravitational Constant
\tilde{h}	Altitude, Dimensionalized
h	Altitude, Non-Dimensionalized
h_0	Initial Altitude
\mathcal{H}	Hamiltonian
$\tilde{\mathcal{H}}$	Hamiltonian in Transformed State Space
\mathcal{H}_1	Switching Function
$\tilde{\mathcal{H}}_1$	Switching Function in Transformed State Space
\mathcal{H}_0	Part of the Hamiltonian Independent of the Thrust
J	Cost Function
J	Jacobian of the Transformation
\tilde{m}	Mass of Vehicle, Dimensionalized
m	Mass of Vehicle, Non-Dimensionalized

m_0	Launching Mass of Vehicle
m_f	Final Mass of Vehicle
\tilde{P}	Thrust, Dimensionalized
P	Thrust, Non-Dimensionalized
P_{\max}	Upper Bound on the Thrust
P^*	Optimum Thrust Program
ϕ	Admissible Set for the Optimal Control
q	Order of Singular Arc
R_e	Radius of the Earth
t_c	Prescribed Duration of Flight
t_f	Final Time
t_{free}	Final Time, Free-Time Case
\tilde{v}	Vehicle Velocity, Dimensionalized
v	Vehicle Velocity, Non-Dimensionalized
v	Initial Velocity
\vec{x}	State Vector in Original State Space
\vec{z}	State Vector in Transformed State Space
z_1, z_2, z_3	Components of the \vec{z} Vector

Greek symbols

$\vec{\kappa}$Co-state Vector in the Transformed State Space

$\kappa_{z_1}, \kappa_{z_2}, \kappa_{z_3}$Components of the $\vec{\kappa}$ Vector

$\vec{\lambda}$Co-state Vector

λ_hCo-state Variable of Altitude

λ_vCo-state Variable of Velocity

λ_mCo-state Variable of Mass

1. Introduction

Historical Review

In 1919 R.H.Goddard, in his classical paper, "A Method of Reaching Extreme Altitudes" [1], proposed the problem of minimizing the mass of a given propellant required to transfer a rocket along a vertical path from rest on the earth to an assigned maximal height. He identified this as an unsolved problem of the Calculus of Variations, but he attempted neither a solution nor a precise formulation. Consequently, he abandoned a rigorous approach, and constructed an approximate numerical solution.

Almost a decade after the publication of Goddard's paper, Hamel [2] in a very brief 1927 publication, objected to the lack of rigor in Goddard's analysis, and pointed out the existence of a solution by means of the Calculus of Variations, based on the fact that the mass of the rocket enters linearly in the equation of motion. However, it was not until 1951 that Tsien and Evans [3], using his results, treated the problem in detail, and carried out the computations of the

trajectories for two particular cases, namely, one with linear drag dependence on velocity, and the other with quadratic drag dependence on velocity.

Leitmann [4-7] later extended their results and derived necessary conditions for the solution. He carried out a similar study for the equivalent problem where the case of the rocket is consumed along with the fuel, changing the area factor in the drag function--an assumption used also by Goddard--treating it as a problem of Mayer with two differential equations. Especially Leitmann's work revealed numerous gaps in the theory that remained to be filled. As Leitmann [8] pointed out, the problem's solution continued to be far from complete, mainly due to the difficulty arising from the requirement that the mass be monotonic non-increasing. In [8] the possibility was suggested of a more complex sequence of subarcs for the case of sharp transonic drag-rise.

Solutions that meet this requirement have been obtained only in few special cases, typified by the work of Miele & Cavoti [9], Miele himself [10], who treated the case of flight in vacuum and the power law of drag, and later by Bryson and Ross [11]. Miele also [12], using a totally different approach, proved the *sufficiency* of the optimal solution established by his predecessors i.e., that the optimal burning program involves a rapid boost at the beginning of the flight, usually followed by a period of continuous burning (sustain phase) and ending with a zero-thrust period. Unfortunately his method, based on Green's theorem, is applicable only to a few cases, those for which the index of performance can be written as a line integral in a plane. Miele was also the first to extend the previous results to the case in which a time constraint is imposed, and the first to suggest the possibility of a more complex sequence of subarcs for the case of a general drag model [13].

One of the most complete works on Goddard's problem, perhaps, is the extensive treatment by Garfinkel [14], who proved that with impulsive boosts in the velocity admitted, and for the case of a general drag model, the solution contains a finite number of such boosts in the transonic region of the rocket

velocity, and contains no coasting arcs except the terminal stage; thus, under certain assumptions a typical solution is characterized by the structural formula

$$(IB)_{N+1}C \quad (1.1)$$

where I,B and C denote the impulsive boost, the burning stage and the terminal coasting period respectively. His solution therefore includes as a special case the results of Tsien & Evans, with $N=0$.

Later on, Munick [15], and Lee & Markus [16], gave the rigorous proof of 4 lemmas, which govern the composition of subarcs for an optimal trajectory.

Motivation and Objectives

As mentioned so far, the problem of optimum thrust programming for maximizing the altitude of a rocket in vertical flight, for given amount of propellant, has been extensively analyzed from the early days of rocketry. However, although this problem, in one version or another, has interested many writers, solutions were obtained only under the convenient assumption that thrust has no upper bound or, equivalently, that the upper bound of the thrust is of a sufficiently high magnitude.

Furthermore, with the exception of the very brief work by Miele [17,18] attention was confined to the free-final-time case, assuming that the results extend gracefully to the fixed-final-time case [19]. Under these assumptions the optimal control--when it exists--consists, at the most, of the classical sequence of three subarcs, i.e., an initial full-thrust subarc followed by a variable-thrust subarc, and finally a coasting subarc until maximum altitude has been reached. This however, may not be the case when a constraint of isoperimetric type is added to the problem. Such a case could be, for instance, the problem of extremizing the rise in altitude for a given time, or alternatively the problem of extremizing the time of flight for given altitude increase. In the present work the

first case is studied, recognizing the reciprocity of the two cases. If such a case is under study, it can be shown that the optimal control may have a more complex switching structure, mainly due to the possibility of appearance of a second full-thrust subarc following a singular period of burning. The solution is applied to two special cases, one with constant drag coefficient and the other with drag coefficient dependent on the Mach number.

Indeed, drag plays an important role in the switching structure of the problem. In particular, it can be shown [3,9] that for the special case when drag is ideally zero, the variable-thrust subarc disappears from the extremal solution, which consequently reduces to subarcs flown with maximum engine output and coasting subarcs. Moreover, the approximation $C_D \approx \text{const.}$ may be of use at low altitudes, when the speed of optimum climb still belongs to the region of quasi-incompressible flow. As the altitude increases, both the velocity and the Mach number increase with such a rapidity that the hypothesis $\partial C_D / \partial M = 0$ is soon no longer satisfied, and a more accurate drag model should be used. Constant drag coefficient C_D is then replaced by a Mach-dependent drag coefficient featuring a sharp increase in the transonic region. When such a model is used, two optimal solutions for the singular surface arise: one in the subsonic-transonic region, and the other in the supersonic region of the velocity [13]. Analysis shows that the requirement of the monotonicity of the mass may generate another full-thrust subarc during transition from the subsonic to supersonic region. The results are then compared with the results of constant C_D , and complete numerical data are given.

2. Problem Formulation

Statement of Problem

The problem is to determine the optimum trajectory of a rocket in vertical flight, from an assigned initial position on the surface of the earth to the final position where the altitude reaches its maximum value, time-of-flight being pre-determined. The guidance of the rocket is achieved by means of the magnitude of the thrust, which is considered a control variable with upper and lower bounds.

Basic Assumptions

The following assumptions are made in order to simplify the physics of the problem:

1. The rocket-powered aircraft is ideally regarded as a particle of variable mass
2. Flat, stationary earth with Newtonian central gravitational field of inverse-square-law form
3. Single-stage rocket
4. Constant exhaust velocity
5. Air density exponential with altitude
6. Isothermal atmosphere
7. The rocket is stabilized so that its axis is always parallel to the flight path
8. The mass is monotonically non-increasing
9. Drag obeys certain restrictions with respect to the velocity, listed below
10. An optimal control exists

Assumption 9 is perhaps the most important one, because, as shown in [20], without essential restrictions on the drag, there may not even exist an optimal program. We adopt the restrictions on the drag of [20], briefly stated below:

- $-D(-v, h) = D(v, h) \geq 0$ for $v \geq 0$
- $vD(v, h) \geq 0$ for $v \geq 0$
- $|D(v_1, h)| \geq |D(v_2, h)|$ if $|v_1| \geq |v_2|$
- $D(v, h) = D_o(v) \exp(-\beta h)$
- D_o is of class C^m , that is, D_o is continuous
- $D'_o(0) = 0$
- $D''_o(0) \geq 0$

Under these restrictions, assumption 10 is valid [16,20].

Equations of motion

The flight path of the rocket obeys the following system of equations:

$$\ddot{h} = \tilde{v} \quad (2.1)$$

$$\dot{\tilde{v}} = \frac{(\tilde{P} - \tilde{D})}{\tilde{m}} - \tilde{g} \quad (2.2)$$

$$\dot{\tilde{m}} = -\frac{\tilde{P}}{\tilde{c}} \quad (2.3)$$

These three equations correspond to force equilibrium and kinematics along the direction of flight. In these equations \tilde{h} is the altitude, \tilde{v} is the velocity of the vehicle, \tilde{m} the mass of the vehicle, \tilde{P} the thrust and \tilde{D} the aerodynamic drag.

The above system of equations can be suitably non-dimensionalized using the following quantities:

$$\hat{h} = R_e$$

$$\hat{t} = G^{-\frac{1}{2}} \hat{h}^{\frac{3}{2}}$$

$$\hat{v} = G^{-\frac{1}{2}} \hat{h}^{-\frac{1}{2}}$$

$$\hat{g} = G \hat{h}^{-2}$$

$$\hat{m} = m_0$$

Here R_e denotes the radius of the earth, G the gravitational constant, \hat{g} the acceleration due to gravity at the surface of the earth, and \hat{m} the launching mass of the vehicle. Consequently, the forces are non-dimensionalized by the quantity $\hat{m}\hat{g}$, the initial weight.

The above equations of motion, the notation and the non-dimensionalization factors are taken from [21]. The non-dimensionalized equations of motion become therefore as follows:

$$\dot{\hat{h}} = \hat{v} \tag{2.4}$$

$$\dot{\hat{v}} = \frac{\hat{P} - \hat{D}}{\hat{m}} - \hat{h}^{-2} \tag{2.5}$$

$$\dot{\hat{m}} = -\frac{\hat{P}}{c} \tag{2.6}$$

Furthermore, the thrust is bounded according to the inequality:

$$0 \leq P \leq P_{\max} \quad (2.7)$$

Boundary and Transversality Conditions

The initial conditions are specified for the three states and are given as :

$$h(0) = h_0, \quad v(0) = v_0, \quad \text{and} \quad m(0) = m_0 \quad (2.8)$$

The final value of the mass is also given:

$$m(t_f) = m_f \quad (2.9)$$

The problem is to maximize the altitude at the terminal time:

$$J = h(t_f) \quad (2.10)$$

subject to the prescribed boundary conditions (2.8)-(2.9), the dynamic equality constraints given by eqs.(2.4)-(2.6) and the isoperimetric constraint on time:

$$t_c = \int_0^{t_f} dt \quad (2.11)$$

The control--a piecewise smooth function of time--may exhibit jumps, and is bounded as in eq.(2.7). The problem is formulated as a problem of Mayer, i.e., no additional differential equation or integral for the cost is required for the solution [22].

The transversality condition requires that for the unspecified states at the terminal time, the following relation to be satisfied by their associated co-states:

$$\lambda_i(t_f) = \left. \frac{\partial J}{\partial x_i} \right|_{t_f} \quad (2.12)$$

which for our problem implies that

$$\lambda_h(t_f) = 1 \quad (2.13)$$

$$\lambda_v(t_f) = 0 \quad (2.14)$$

The time does not appear explicitly in the equation of motion, therefore the Hamiltonian is a first integral, remaining constant throughout the trajectory

$$\mathcal{H} = C_1 \quad (0 \leq t \leq t_f) \quad (2.15)$$

where C_1 is a constant to be determined, satisfying the conditions

$$\begin{aligned} C_1 > 0 & \quad \text{when} \quad t_f < t_{free} \\ C_1 = 0 & \quad \text{when} \quad t_f = t_{free} \\ C_1 < 0 & \quad \text{when} \quad t_f > t_{free} \end{aligned} \quad (2.16)$$

For the minimum-time problem $C_1 = +1$ and for the maximum-time problem $C_1 = -1$.

Since some of the states are known at the initial time, while others are known at the final time, the problem is a so-called Two-Point-Boundary-Value Problem (TPBVP).

Problem analysis

Define the state vector $\vec{x} = \text{col}(h, v, m)$, and the co-state vector $\vec{\lambda} = \text{col}(\lambda_h, \lambda_v, \lambda_m)$. Then the Hamiltonian takes the form:

$$\mathcal{H}(\vec{\lambda}, \vec{x}, P) = \lambda_h \dot{h} + \lambda_v \dot{v} + \lambda_m \dot{m} \quad (2.17)$$

Using the eqs.(2.4)-(2.6) and noting that the control P appears linearly in the equations of motion, one obtains for the Hamiltonian the following form:

$$\mathcal{H} - C_1 = \mathcal{H}_0 + P \mathcal{H}_1 = 0 \quad (2.18)$$

where \mathcal{H}_0 and \mathcal{H}_1 are given by:

$$\mathcal{H}_0 = \lambda_h v - \lambda_v \left(\frac{D}{m} + h^{-2} \right) - C_1 \quad (2.19)$$

$$\mathcal{H}_1 = \frac{\lambda_v}{m} - \frac{\lambda_m}{c} \quad (2.20)$$

\mathcal{H}_1 is the "switching function" and governs the history of the control.

The co-states satisfy the following system of differential equations

$$\dot{\lambda}_i = - \frac{\partial \mathcal{H}}{\partial x_i} \quad (2.21)$$

The components of the co-state vector are given analytically by

$$\dot{\lambda}_h = - \frac{\partial \mathcal{H}}{\partial h} = \frac{\lambda_v}{m} \frac{\partial D}{\partial h} - 2\lambda_v h^{-3} \quad (2.22)$$

$$\dot{\lambda}_v = - \frac{\partial \mathcal{H}}{\partial v} = \frac{\lambda_v}{m} \frac{\partial D}{\partial v} - \lambda_h \quad (2.23)$$

$$\dot{\lambda}_m = - \frac{\partial \mathcal{H}}{\partial m} = \frac{\lambda_v}{m^2} (P - D) \quad (2.24)$$

It is known that the maximum of \mathcal{H} with respect to all controls in the admissible set $\wp = [0, P_{\max}]$, is a necessary condition for optimal control [23]. This Maximum Principle can be stated as follows :

$$\mathcal{H}(P^*) = \max_{P \in \wp} \mathcal{H}(P) \equiv 0 \quad (0 \leq t \leq t_f) \quad (2.25)$$

Controls which satisfy the necessary condition of eq.(2.25) are called "extremal controls", and the trajectory produced by a system subjected to extremal control is called an "extremal path" or, simply, an "extremal".

From eqs.(2.7) and (2.25) three possibilities exist for an extremal control, depending on the sign of the switching function:

$$\begin{aligned}
 P^* &= P_{\max} && \text{when } \mathcal{H}_1 > 0 \\
 0 \leq P^* &\leq P_{\max} && \text{when } \mathcal{H}_1 = 0 \\
 P^* &= 0 && \text{when } \mathcal{H}_1 < 0
 \end{aligned} \tag{2.26}$$

The second case corresponds to the existence of an interval of singular control i.e., an interval of control effort with $\mathcal{H}(P)$ stationary. Along an interval of singular control (singular arc) a positive δ exists, so that the switching function vanishes for each t in $t^* - \delta \leq t \leq t^* + \delta$. Hence, the following relationships are fulfilled simultaneously on a singular arc:

$$\mathcal{H}_1 = \dot{\mathcal{H}}_1 = \ddot{\mathcal{H}}_1 = \dots \equiv 0 \tag{2.27}$$

Evaluation of Singular Control

Along a singular extremal the graph of the Hamiltonian vs. the control is a horizontal line, and the Maximum Principle gives no information about the optimal control because all admissible controls qualify. A singular control can however be determined from the equation

$$\frac{d^{2q}}{dt^{2q}} \left(\frac{\partial \mathcal{H}}{\partial P} \right) = 0 \tag{2.28}$$

where q is the smallest integer for which P enters explicitly into the left-hand side of the above equation. The value of q also denotes the order of the singular arc. Using eqs.(2.4)-(2.6) and eqs.(2.22)-(2.24) the first derivative of \mathcal{H}_1 takes the following form:

$$\dot{\mathcal{H}}_1 = \frac{\lambda_v}{m^2} \left(\frac{\partial D}{\partial v} + \frac{D}{c} \right) - \frac{\lambda_h}{m} = 0 \quad (2.29)$$

and the value of the singular control is evaluated from the second derivative of \mathcal{H}_1 which, it can be shown, has the form:

$$\ddot{\mathcal{H}}_1 = A + P_0 B = 0 \quad (2.30)$$

resulting in the singular control

$$P_0 = -\frac{A}{B} \quad (2.31)$$

The value of q is 1 and the singular arc is of first order.

The equations for A and B are given below:

$$A = \sum_{i=1}^4 Q_i \quad (2.32)$$

$$B = \sum_{i=1}^3 R_i \quad (2.33)$$

where

$$Q_1 = -\frac{D}{mc} \left(\frac{D}{c} + \frac{\partial D}{\partial v} \right)$$

$$Q_2 = \frac{\partial}{\partial h} \left(\frac{\partial D}{\partial v} \right) v - \frac{\partial}{\partial v} \left(\frac{\partial D}{\partial v} \right) \left(\frac{D}{m} + h^{-2} \right)$$

$$Q_3 = \frac{1}{c} \left[\frac{\partial D}{\partial h} v - \frac{\partial D}{\partial v} \left(\frac{D}{m} + h^{-2} \right) \right]$$

$$Q_4 = -\frac{\partial D}{\partial h} + 2mh^{-3}$$

and R_i given by

$$R_1 = \frac{1}{mc} \left(\frac{\partial D}{\partial v} + \frac{D}{c} \right)$$

$$R_2 = \frac{\partial}{\partial v} \left(\frac{\partial D}{\partial v} \right) m^{-1}$$

$$R_3 = \frac{1}{mc} \frac{\partial D}{\partial v}$$

Notice that the singular control is in state feedback form.

Construction of the Singular Surface

The study of problems in which singular solutions appear is significantly simplified if it is possible to determine a surface S which represents the conditions

$$\mathcal{H}_0 = \dot{\mathcal{H}}_0 = \dots \equiv 0 \quad (2.34)$$

$$\mathcal{H}_1 = \dot{\mathcal{H}}_1 = \dots \equiv 0 \quad (2.35)$$

in the state space of the original state variables.

This surface S may be called the "singular control surface", since the state-variable trajectory corresponding to the singular control P_0 must lie on this surface. For this reason, only those regions of S corresponding to $P_0 \in \wp$ are considered. Note that S is also the "singular control switching boundary" [24] since any point of the state space which is not on S must feature a bang-bang control. Sometimes--especially in high order systems--it is convenient to construct projections of the hypersurface S upon various state-variable planes.

Moreover, if an expression

$$S(\bar{x}) = 0 \quad (2.36)$$

for the singular control surface can be obtained, then the singular control in (2.24) is a function only of state variables. It should be noted, however, that the existence and location of the singular control surface S is not dependent upon the particular boundary conditions of the problem.

For our problem, along the singular surface the expressions given by eqs.(2.19),(2.20) and (2.29) vanish. Solving eq.(2.29) for λ_h and replacing it in eq.(2.19) one obtains:

$$\lambda_v \left[\frac{v}{m} \left(\frac{\partial D}{\partial v} + \frac{D}{c} \right) - \left(\frac{D}{m} + h^{-2} \right) \right] = C_1 \quad (2.37)$$

or equivalently,

$$E = v \left(\frac{\partial D}{\partial v} + \frac{D}{c} \right) - D - mh^{-2} - \frac{C_1}{\lambda_v} m = 0 \quad (2.38)$$

which is the equation of the singular surface.

It is noted that for the particular case of free final time, when $C_1 = 0$, the previous equation agrees with the results obtained by Munick, Tsien and Evans, et al. Therefore, a one-parameter family of singular surfaces is generated according to the value of the constant C_1 .

From eq.(2.23) and eq.(2.29) a simple relationship can be found for the propagation of λ_v along the singular arc: If one solves for λ_h from eq.(2.29) and substitute in eq.(2.23) one obtains that:

$$\dot{\lambda}_v = -\lambda_v \frac{D}{mc} \quad (2.39)$$

which, integrated along with eqs.(2.4)-(2.6), will generate the optimal path on the singular surface. The values of the co-states λ_h and λ_m then can be found by direct substitution of λ_v into eq.(2.20) and eq.(2.29).

3. Case of Constant Drag Coefficient

Numerical Data

The aerodynamic drag assumes the following form:

$$D = C_D b v |v| \exp(\beta(1 - h)) \quad (3.1)$$

where the factor $b v |v| \exp(\beta(1 - h))$ is numerically equal to the product of the velocity head and the characteristic area of the aircraft, b , β are constants, and C_D is the zero-lift drag coefficient.

The aerodynamic data and vehicle's parameters, with the exception of the value of P_{\max} , were taken from [21]. Their values are listed below:

$$C_D = 0.05$$

$$b = 6200$$

$$\beta = 500$$

$$P_{\max} = 3.5$$

These correspond roughly to the Soviet SA-2 surface-to-air missile, NATO code-name GUIDELINE [25]. The non-dimensionalized initial and final values of the state variables are given below [21]:

$$\begin{aligned}h(t_0) &= 1 \\v(t_0) &= 0 \\m(t_0) &= 1 \\m(t_f) &= 0.6\end{aligned}$$

For the drag model of eq.(3.1) the partial derivatives required for the solution (see eqs.(2.21)-(2.23) and eqs.(2.30)) are given as follows:

$$\frac{\partial D}{\partial v} = 2C_D b |v| \exp(\beta(1 - h)) \quad (3.2)$$

$$\frac{\partial D}{\partial h} = -C_D b v |v| \beta \exp(\beta(1 - h)) \quad (3.3)$$

$$\frac{\partial}{\partial v} \left(\frac{\partial D}{\partial v} \right) = \frac{\partial^2 D}{\partial v^2} = 2 \operatorname{sgn}(v) C_D b \exp(\beta(1 - h)) \quad (3.4)$$

$$\frac{\partial}{\partial h} \left(\frac{\partial D}{\partial v} \right) = -2C_D b |v| \beta \exp(\beta(1 - h)) \quad (3.5)$$

where sgn denotes the signum function defined by

$$\operatorname{sgn}(v) = \begin{cases} +1 & \text{if } v > 0 \\ -1 & \text{if } v < 0 \end{cases} \quad (3.6)$$

Numerical Solution and Computational Results

In the analysis of the problem it is tacitly assumed that the experiment has no meaning for $t_f < \bar{t}$, where

$$\bar{t} = (m_0 - m_f) \frac{c}{P} \quad (3.7)$$

therefore, only problems of maximizing the altitude for times greater or equal to \bar{t} are considered.

Three cases of the switching structure may arise according to the specified value of the final time (table 1):

1. Full thrust, singular thrust, and zero thrust.
2. Full thrust, singular thrust, full thrust, and zero thrust.
3. Full thrust and zero thrust.

The free-terminal-time problem corresponds to the classical first case of switching structure listed above, which also yields the absolute maximum final altitude for every other value of flight time (fig.3). This is not a surprising result, since it corresponds to minimum flight time with unconstrained final altitude (table 2).

The switching structure remains unchanged when the final time is increased, with the singular subarc occupying a greater portion of the solution of the whole optimal trajectory, as a result of the requirement to reach the final altitude later. Hence, the rocket consumes its fuel at a slower rate, as well (fig.6). The case of time-of-flight larger than the free-final-time case corresponds, due to Mayer reciprocity, to the rather unusual maximum-time problem. For this problem the optimality of the previous switching structure was tested, with respect to neighboring trajectories of a more complex sequence, including an initial coast before the full-thrust subarc.

However the history of the thrust is considerably different for the case of shortened flight, and the appearance of a second full-thrust subarc, following the variable-thrust subarc, becomes inevitable for sufficiently small values of final time. The main reason for this is the fact that for small values of the flight time

the singular thrust tends to hit its upper bound. Such a situation is not allowed, from eq.(2.7), and therefore, the trajectory must depart from singular control, and a bang-bang control must be used. If one allows the control to saturate above, in following the singular subarc, then only a zero-thrust subarc is possible to satisfy the McDanell and Powers necessary condition for joining optimal singular and non-singular subarcs [37]. In such a case, the mass will not meet its terminal boundary condition (i.e., there is still fuel to be burnt). The only appropriate choice is, evidently, a second full-thrust subarc in order to make use of the remaining propellant. Departure from the singular surface, however, must occur at a point in time so that the switching function becomes zero at the time when fuel is exhausted. Switching then takes place to a coast which extends to the final time.

The second full-thrust subarc reveals the necessity of burning the fuel at an increasing rate for the case of small values of final time. In fact, the first and second full-thrust subarcs occupy an increasing portion of the whole trajectory as the final time decreases, while the intermediate variable-thrust subarc decreases.

Thus, the third case arises when the two full-thrust subarcs join, and the singular subarc is totally absent from the composite. A limiting case of this switching structure is the case when no coasting subarc is present, and the trajectory is composed totally by a full-thrust arc. This is the case when $t_f = \bar{t}$.

It should be noted however, that the possibility of appearance of any of the aforementioned cases in an optimal solution does not depend merely on the final time, but on the value of the upper bound of the thrust, as well. It is possible, for instance, that a second full-thrust be required, even for the free-final-time case, if the thrust is bounded above by a small value, whereas, on the other hand, with a very high upper bound on the thrust ($P_{\max} \rightarrow \infty$) the optimal trajectory is composed according to the classical sequence: full, singular and coast. In fact, for the limiting case, when $P_{\max} = \infty$, the first case is the only possible one [3,4].

Notice that the terminal velocity is positive for $t_f < t_{free}$, and is negative for $t_f > t_{free}$. Obviously $v=0$ for $t_f = t_{free}$. This is hardly surprising; from eqs.(2.17)-(2.19) and eqs.(2.13)-(2.14) for the coasting subarc ($P=0$) the following relationship must hold at the terminal time:

$$C_1 = v(t_f) \quad (3.8)$$

and, using eq.(2.16), the proof is complete.

The numerical solution was obtained, using the two-point-boundary-value problem solver, BOUNDSOL [26]. However, the convergence of the solution algorithm is experienced only if the initial guesses for the trajectory are reasonably "good". A method for obtaining very accurate first guesses for BOUNDSOL will be described as follows:

Given a initial guess for the ratio

$$\lambda'_v = \frac{\lambda_v}{C_1} \quad (3.9)$$

one may integrate forward the state eqs.(2.4)-(2.6) with the assigned initial boundary values of the states, until eq.(2.37) is satisfied. Solving the system of eqs.(2.17)-(2.19) one finds the values of the co-states at the entry of the singular arc, given by:

$$\lambda'_h = \frac{\lambda'_v}{m} \left(\frac{\partial D}{\partial v} + \frac{D}{c} \right) \quad (3.10)$$

$$\lambda'_m = \lambda'_v \frac{m}{c} \quad (3.11)$$

These relations assume that the constant C_1 has been used as a scaling factor of the co-states, due to the linearity of eqs.(2.17)-(2.19).

The values of the co-states at the initial time can then be found by backward integration of the state-Euler system, eqs.(2.4)-(2.6), and eqs.(2.21)-(2.23) using these values of $\lambda'_v, \lambda'_h, \lambda'_m$.

Once on the singular arc, one can integrate forward using the singular thrust from eq.(2.31). Integration is continued along the singular arc, checking that the inequality constraint $0 \leq P_0 \leq P_{\max}$ is not violated.

Exit from the singular arc is made at the time when the mass criterion is satisfied. In the case when the singular thrust saturates on its upper bound, the time for the departure is taken so that, at the end of the second full-thrust, both conditions

$$\mathcal{H}_1 = 0 \quad \text{and} \quad m_f = 0.6 \quad (3.12)$$

are satisfied.

A final coasting arc follows until $\lambda_v = 0$. Once the final conditions on the state variables have been satisfied, the final value of the co-state variable λ_h is used to scale the values of all the components of the co-state manifold throughout the trajectory. This ensures the satisfaction of the transversality condition $\lambda_h(t_f) = 1$.

A direct relation between the constant C_1 and the final time t_f is evident. Every value of C_1 corresponds to a unique value of the final time. The graph of C_1 vs. t_f appears in fig.2.

Notice that the whole procedure involves two successive scalings of the co-states i.e., first using C_1 , and the final scaling using $\lambda_h(t_f)$. With these initial guesses, BOUNDSOL converged within one or two iterations. With a converged solution, small perturbations in the final time can generate the whole family of trajectories.

4. Necessary Conditions for Optimality

Overview

The Pontryagin maximum principle states that the optimal control provides an absolute maximum of the generalized Hamiltonian. If the maximum principle determines a unique control, the extremal is called "nonsingular". If on the other hand, the graph of the Hamiltonian vs. the control is a horizontal line, then all admissible controls qualify, and if this line remains horizontal during a nonvanishing time interval, a singular extremal is generated. Of course some solutions are composed of both singular and nonsingular subarcs. When an extremal compares favorably only to curves that have neighboring values of state-rate, it is said to be a candidate to provide a weak maximum. When this restriction is removed, the extremal is said to be a candidate to provide a strong maximum.

It is of interest to find conditions whose satisfaction furnishes not merely a stationary value, but a relative maximum.

Kelley Condition

It should be noted that the fact that a trajectory satisfies the Euler differential equations and the other first-order necessary conditions only guarantees its stationary character. To determine whether a maximum is attained, further investigation is in order. Thus the Legendre-Clebsch, Weierstrass and Jacobi conditions must be checked. Each of these three conditions is a necessary condition for a maximum. All of them, suitably strengthened, in combination with the first-order necessary conditions, provide a sufficient condition.

The appearance of singular subarcs in Goddard's problem was confirmed by the research of Tsien and Evans, Hamel, Leitmann, et al. However, it was not until 1964 that a new necessary condition for screening singular extremals became available [27]. Kelley's result was generalized by Robbins [28,29], Tait, and Kopp and Moyer [30], to give what is now known as the generalized Legendre-Clebsch condition, or the Kelley-Contensou condition.

This condition can be stated as follows:

$$(-1)^q \frac{\partial}{\partial P} \left[\frac{d^{2q}}{dt^{2q}} \left(\frac{\partial \mathcal{H}}{\partial P} \right) \right] \leq 0 \quad (4.1)$$

where q is the order of the singularity of the arc, as in eq.(2.28). For the problem under study, this inequality virtue of eq.(2.30) reduces to the inequality

$$B \geq 0 \quad (4.2)$$

Transformation to Reduced State-space

A transformation approach suggested by Kelley [31] is sometimes very helpful in permitting analysis of singular problems in a state space of reduced dimension. The singular arcs then become nonsingular, so that existing necessary conditions

are applicable. This approach has the practical shortcoming of requiring the solution of a system of nonlinear differential equations, required for synthesis of the transformation, in "closed form". Fortunately, this transformation technique can be obtained rather easily for the present problem, allowing the structure of the accessory problem to be studied in a reduced, two-dimensional, state space. This is quite attractive; the complete family of singular extremals for given initial conditions can be pictured in two-dimensional space.

Omitting for brevity the theory of the transformation, it can be shown [30,31] that the transformation of the original state vector \vec{x} to the canonical form leads to the new state vector \vec{z} with components

$$z_1 = h \quad z_2 = v \quad z_3 = me^{v/c} \quad (4.3)$$

The quantity $z_3 = me^{v/c}$ remains constant during an impulsive burning [3], therefore

$$u = c \ln z_3 = v + c \ln m \quad (4.4)$$

has the properties of a "potential velocity", since it is the velocity that could be attained at any point in flight by burning the rest of the fuel instantaneously i.e., decreasing m to m_f [11]. Such an instantaneous "boost", while not physically possible, is a convenient idealization to a very rapid burning of fuel. The above equation gives us the possibility to find an upper bound for the--theoretically-attainable--velocities along an optimal trajectory: the largest value for u from eq.(4.4) is obtained for the largest amount of fuel to be burned i.e., the initial value, therefore,

$$v_{\max} = -c \ln m_f \quad (4.5)$$

and this maximum attainable velocity could be achieved if all of the fuel were burned instantaneously, at the beginning of the flight. This is the same result obtained by Munick [15], Lee and Markus [16], and Ewing and Hazeltine [20], although using a slightly different approach.

The differential equations in the new state space are derived directly from eqs.(2.4)-(2.6) and eq.(4.3)

$$\begin{aligned}\dot{z}_1 &= z_2 \\ \dot{z}_2 &= \frac{P-D}{z_3} \exp(z_2/c) - z_1^{-2} \\ \dot{z}_3 &= -\frac{D}{c} \exp(z_2/c) - \frac{z_3}{c} z_1^{-2}\end{aligned}\tag{4.6}$$

The Hamiltonian for the new system is given by

$$\tilde{\mathcal{H}} = \kappa_{z_1} \dot{z}_1 + \kappa_{z_2} \dot{z}_2 + \kappa_{z_3} \dot{z}_3\tag{4.7}$$

where $\vec{\kappa} = \text{col}(\kappa_{z_1}, \kappa_{z_2}, \kappa_{z_3})$ is the co-state vector of the new state-space, satisfying the differential equations

$$\dot{\kappa}_{z_1} = \frac{\kappa_{z_3}}{c} \left[\exp(z_2/c) \frac{\partial D}{\partial z_1} - 2z_3 z_1^{-3} \right] - \kappa_{z_2} \left[-z_3^{-1} \frac{\partial D}{\partial z_1} \exp(z_2/c) + 2z_1^{-3} \right]\tag{4.8}$$

$$\begin{aligned}\dot{\kappa}_{z_2} &= -\kappa_{z_1} + \frac{\kappa_{z_3}}{c} \exp(z_2/c) \left[\frac{\partial D}{\partial z_2} + \frac{D}{c} \right] \\ &\quad - \kappa_{z_2} \frac{\exp(z_2/c)}{z_3} \left[-\frac{\partial D}{\partial z_2} + \frac{P-D}{c} \right]\end{aligned}\tag{4.9}$$

$$\dot{\kappa}_{z_3} = \frac{\kappa_{z_3}}{c} z_1^{-2} - \kappa_{z_2} \left[-\frac{P-D}{z_3^2} \exp(z_2/c) \right]\tag{4.10}$$

Notice that the control P appears only in one equation, namely in the equation for \dot{z}_2 . We can therefore discard this equation, for the singular portion of the trajectory, and consider the z_2 variable as a new control-like variable, in the reduced state-space of variables z_1 and z_3 . This change occurs through the identical vanishing of the Lagrange multiplier associated with the second

equation of the state z_2 . Indeed, the switching function of the transformed problem is given from eq.(4.7) as

$$\tilde{\mathcal{H}}_1 = \frac{\partial \tilde{\mathcal{H}}}{\partial P} = \frac{\kappa_{z_2}}{z_3} \exp(z_2/c) \quad (4.11)$$

and along a singular arc

$$\kappa_{z_2} \equiv 0 \quad (4.12)$$

because, throughout the trajectory,

$$\exp \frac{(z_2/c)}{z_3} \neq 0 \quad \text{always}$$

The vanishing of κ_{z_2} , along the singular portion of the trajectory, can be verified through an analogous transformation for the co-state vector $\vec{\lambda}$ of the original state space as follows:

Optimal-control theory indicates that the co-state variables have a special meaning [32,33]; the value at time t of the Lagrange multiplier λ_i , associated with the variable x_i is just $\partial J / \partial x_i(t)$, where J -the "payoff" function with t regarded as a starting time. This interpretation of the co-states is very instructive and it will be used extensively later on. Requiring that the cost function and the Hamiltonian remain unchanged under the transformation, and using the chain rule of differentiation, the following relationship must hold along the trajectory [34]:

$$\vec{\lambda} = \frac{\partial J}{\partial \vec{x}} = \frac{\partial \vec{z}}{\partial \vec{x}} \frac{\partial J}{\partial \vec{z}} \quad (4.13)$$

According to the interpretation mentioned earlier,

$$\vec{\kappa} = \frac{\partial J}{\partial \vec{z}} \quad (4.14)$$

is the co-state vector for the new state space and

$$J = \frac{\partial \vec{z}}{\partial \vec{x}} \quad (4.15)$$

is the Jacobian of the transformation, with elements

$$J_{ij} = \frac{\partial z_j}{\partial x_i} \quad i, j = 1, 2, 3 \quad (4.16)$$

Assuming that the transformation is nonsingular, then the inverse of the Jacobian matrix exists, and the system of eq.(4.13) has the unique solution

$$\vec{\kappa} = [J]^{-1} \vec{\lambda} \quad (4.17)$$

which, can be written analytically as

$$\kappa_{z_i} = \sum_{j=1}^3 \frac{\partial z_j}{\partial x_i} \lambda_j \quad i = 1, 2, 3 \quad (4.18)$$

or in matrix notation

$$\begin{bmatrix} \kappa_{z_1} \\ \kappa_{z_2} \\ \kappa_{z_3} \end{bmatrix} = \begin{bmatrix} 1 & 0 & 0 \\ 0 & 1 & -m/c \\ 0 & 0 & e^{-v/c} \end{bmatrix} \begin{bmatrix} \lambda_h \\ \lambda_v \\ \lambda_m \end{bmatrix} \quad (4.19)$$

which, after algebraic manipulations, yields

$$\begin{aligned} \kappa_{z_1} &= \lambda_h \\ \kappa_{z_2} &= \lambda_v - \frac{m}{c} \lambda_m \end{aligned} \quad (4.20)$$

$$\kappa_{z_3} = \lambda_m e^{-v/c}$$

Notice that

$$\det[J] = e^{-v/c} \neq 0 \quad (4.21)$$

hence, the transformation is nonsingular everywhere. From eq.(4.20) the co-state κ_{z_2} is exactly the switching function of the original problem; consequently, along the singular arc the co-state equations reduce to

$$\dot{\kappa}_{z_1} = -\frac{\partial \tilde{\mathcal{H}}}{\partial z_1} = \frac{\kappa_{z_3}}{c} \left[\exp(z_2/c) \frac{\partial D}{\partial z_1} - 2z_3 z_1^{-3} \right] \quad (4.22)$$

$$\dot{\kappa}_{z_3} = -\frac{\partial \tilde{\mathcal{H}}}{\partial z_3} = \frac{\kappa_{z_3}}{c} z_1^{-2} \quad (4.23)$$

where

$$\tilde{\mathcal{H}} = \kappa_{z_1} z_2 - \frac{\kappa_{z_3}}{c} \left[D \exp(z_2/c) + z_3 z_1^{-2} \right] \quad (4.24)$$

Notice that the new control z_2 does not appear linearly in the system of state and co-state equations, and the Maximum Principle and the classical Legendre-Clebsch necessary conditions can be applied successfully in the reduced-state-space problem.

The extremals, then, of the transformed problem are the singular extremals of the original, and those extremals satisfying the strengthened version of the classical Legendre-Clebsch condition are maximizing, at least over short intervals. The stationary solution of the transformed problem corresponding to the singular subarc of the original problem occurs then, when

$$\frac{\partial \tilde{\mathcal{H}}}{\partial z_2} = \kappa_{z_1} - \frac{\kappa_{z_3}}{c} \exp(z_2/c) \left[\frac{D}{c} + \frac{\partial D}{\partial z_2} \right] = 0 \quad (4.25)$$

and the Legendre-Clebsch necessary condition requires, for a maximizing extremal

$$\frac{\partial^2 \tilde{\mathcal{H}}}{\partial z_2^2} = -\frac{\kappa_{z_3}}{c} \exp(z_2/c) \left[\frac{D}{c^2} + \frac{2}{c} \frac{\partial D}{\partial z_2} + \frac{\partial^2 D}{\partial z_2^2} \right] \leq 0 \quad (4.26)$$

The latter relationship assures the convexity of the Hamiltonian in the neighborhood of a solution of eq.(4.24) i.e., an optimal control obtained by eq.(4.24) provides *at least a local* maximum of $\tilde{\mathcal{H}}$. Using the transformation relationships for the state and the co-state variables, one can verify that the above expressions are identical to the eq.(2.29) and eq.(4.2) respectively, already found in the original state space.

Junction Conditions

The three possible cases of subarcs that may appear in the solution of an optimal trajectory have been examined; however, the number and sequence of subarcs which satisfy the specified boundary conditions need to be determined. An admissible control must, of course, satisfy other requirements, in addition to satisfying the given constraints. Other such requirements are the continuity of $\mathcal{H}(t)$ and the continuity of $\vec{\lambda}(t)$. These conditions are referred to in the literature as the *Weierstrass-Erdmann* corner conditions [22,35].

If the solution is totally non-singular, or totally singular, necessary conditions are available in order to prove optimality in a large number of cases. However, the character of optimal trajectories which include both singular and non-singular subarcs is not easily decided. The analysis of such problems is complicated by the fact that the optimal solution, in general, consists of some combination of singular and non-singular subarcs, the number and sequence of which are not known *a priori*. The first results concerning the behavior of the optimal control at a junction between singular and non-singular subarcs were derived by Kelley, Kopp

and Moyer [30], and may be summarized as follows: If q is the order of the singular subarc, then

If q is *odd* a jump discontinuity in control may occur at a junction between a locally minimizing singular subarc, i.e., a subarc on which the generalized Legendre-Clebsch condition is satisfied in strengthened form, with a non-singular subarc.

If q is *even* jump discontinuities in control from singular subarcs satisfying the strengthened form of the generalized Legendre-Clebsch condition are ruled out.

Johnson in [36] recognized the conflict between the generalized Legendre-Clebsch condition and the junction condition for q even, and showed that analytic junctions with jumps can occur only if q is odd, but he did not identify the character of junctions between non-singular and q -even singular subarcs.

In 1971 McDanell and Powers, motivated by the preliminary results obtained by Kelley, Kopp and Moyer, and Johnson, considered the problem concerning the continuity and smoothness properties of the optimal control at a junction between singular and non-singular subarcs in more detail [37], and they generalized the previous conclusions, with one important exception; they proved the possibility of a continuous junction for control saturation with zero slope for q -odd problems, a possibility which had not been included by Kelley, Kopp and Moyer and which was later ruled out for $q > 1$ by Bershchanskiy [38]. Their main result was that--for analytic junctions--the sum of the order of the singular subarc and the order of the lowest time derivative of the control which is discontinuous at the junction must be an odd integer when the strengthened generalized Legendre-Clebsch condition is satisfied.

In the McDanell and Powers results, the assumption that the control is piecewise analytic is not to be taken lightly because the junction is usually

non-analytic (“chattering”) not only for q even, but also for q odd with $q > 1$. In fact, according to Bershchanskiy [38], the McDanell-Powers necessary conditions are useful mainly for $q = 1$, and only for exceptional cases for $q > 1$. As was shown in [38] for q -even problems or for q -odd problems with $q > 1$ the transition from a nonsingular to a singular subarc is associated with *chattering* junctions, i.e., controls that switch rapidly between the upper and the lower bound faster and faster, with a point of accumulation, and which, although measurable, are non-analytic.

All these conditions, though only necessary, help to eliminate some of the possible subarc-sequence candidates.

Jacobi and Jacobi-like Conditions

Despite the necessary conditions mentioned in the preceding section, there is presently no general theory for determining singular subarcs--for determining their roles as subarcs of a composite solution. This is primarily due to the fact that the classical Jacobi theory, which leads to the Jacobi necessary condition--that the extremal must not include a pair of conjugate points--does not apply to singular arcs or to extremals having corners.

The complexity of the theory arises from the fact that a Jacobi-test procedure must be based on the study of the second variation. The main task of such a test is to find a system of non-zero variations which give to the second variation the value zero at some point in time. Then, a conjugate point has been found and the extremal ceases to be optimal past the conjugate point. Several methods have been developed for determining neighboring extremals that provide a system of non-zero variations for the case of non-singular extremals without corners. For instance, in the work of Kelley and Moyer [39], the existence of a non-zero system of variations is tested by the degeneracy of the rank of the transformation matrix M of the linearized system of Euler equations, i.e., a matrix with entries

$$\frac{\partial x_i}{\partial \lambda_j} \tag{4.27}$$

The method is equivalent to finding a vector

$$v_i = (-1)^i \det M_i \quad i = 1, \dots, n \tag{4.28}$$

where M_i is the $(n - 1) \times (n - 1)$ matrix obtained from matrix M by deleting the i^{th} row. Then, at a conjugate point the vector v_i should be either parallel or antiparallel to λ_i . The difficulty of calculating the partial derivatives with respect to the λ_j in eq.(4.27) can be simplified using difference quotients, as suggested by Cicala [33].

Determining extremal contacts with an envelope is even more difficult in the presence of corners. Extremals with corners, or broken extremals, have been studied with generality, detail, and rigor in [40,41], which show that such extremals are nonoptimal after they pass conjugate or reflection points. The latter are defined as the points of contact to an envelope where the slope of the extremal is discontinuous, in contrast to the usual type of conjugate point with continuous state-rates. Moyer, using this idea, extended the previous computational technique in the case of a non-singular extremal exhibiting corners [42] and used this approach successfully at application in [43].

However, the case of an extremal including singular subarcs is more difficult, and most of the few attempts made in this direction are limited to the case of a *totally* singular arc [44]. Very few methods have been also developed for the more complex case of a composite extremal including both singular and non-singular subarcs [45,46]. One fruitful method, although subject to the limitations of a scalar control with a low-dimension state-variable vector, is that proposed by Moyer [47], motivated by Caratheodory's work on broken extremals [48].

Next, the procedure of a Jacobi-like test in the reduced z-space of our problem will be discussed. The transformation offers the advantage that one can plot the extremals, in the z_1, z_3 space. This permits detection of extremals that have contacted an envelope. The method is that proposed by Moyer [42]:

One plots a family of extremals that originate from the same initial conditions in the z-state space i.e., having the same initial values for z_1 , and z_3 , and stops integration at a fixed final time. The locus of endpoints for various t defines curves in z-space called *wavefronts* [42,47]. The co-state vector is normal to the wavefront. If there are two extremals that intersect at a point, then their co-state vectors, being both normal to the wavefront, should be co-linear. This general method for checking for conjugate points is an easy exercise in the case of a two-dimensional state space.

In practice, starting from some point on the singular surface--or in z-space, on the singular "curve"--one integrates backward in time using the eq.(4.24) until the initial condition for z_1 is met, that is, $z_1(t') = 1$. Of course $t' \neq 0$, and $z_3 \neq 1$ at the initial time. In this way one generates an extremal that corresponds to the singular extremal of the original problem, and, moreover, has no corners. The last requirement is a significant one, since the usual Jacobi test does not apply to a extremal possessing corners [22,35]. The neighbouring extremals are then generated by keeping z_1 and z_3 fixed, and changing the ratio of the co-states:

$$\frac{\kappa_{z_1}}{\kappa_{z_3}}$$

This approach is applicable in the impulsive case only, i.e., $P_{\max} = \infty$, and even for this ideal case the test does not include the final coasting subarc. That is because past the corner junction between the singular subarc and the final coast, the solution can no longer be regarded as in z_1, z_3 space (fig.11). Therefore, the test will establish the non-existence of conjugate points only up to the entering the final coasting subarc (figs.21-23).

5. Mach-Dependent Drag Coefficient

Problem Formulation

The case of a more realistic drag model is examined in this chapter. The aerodynamic drag assumes the same form as in the case of constant C_D , but now the drag coefficient is assumed to depend on the Mach number according to the following relationship [49]:

$$C_D(M) = A_1 \tan^{-1}(A_2(M - A_3)) + A_4 \quad (5.1)$$

This formula generates a quick transition from one value of C_D in the subsonic region to another higher value of C_D in the supersonic region. A_1, A_2, A_3, A_4 are constants controlling when, and how fast, this transition takes place (figs.24-29). These constants were chosen such that the supersonic value of C_D coincides with the data for the case of constant drag coefficient, and their values are given below:

$$\begin{aligned}
A_1 &= 0.0095 \\
A_2 &= 25 \\
A_3 &= 0.953467778 \\
A_4 &= 0.036
\end{aligned}$$

The rest of the aerodynamic parameters, and the initial and final values of the state variables, remain the same as given in Chapter 3. For simplicity it was assumed that the speed of sound remains constant with altitude, an assumption which is actually valid only for stratospheric solutions.

In fig.30 is also shown that the assumption

$$v\left(\frac{\partial^2 D_o}{\partial v^2} + \frac{\partial D_o}{\partial v}c^{-1}\right) + \frac{D_o}{c} > 0 \quad \text{for} \quad v > 0$$

made by Munick and Lee and Markus on the requirements of an admissible drag model, is a very strong one, and it is rarely satisfied for realistic data.

For this drag model the partial derivatives of the drag required for the solution are given as follows:

$$\frac{\partial D}{\partial v} = 2C_D b |v| \exp(\beta(1-h)) + \frac{\partial C_D}{\partial v} b v |v| \exp(\beta(1-h)) \quad (5.2)$$

$$\frac{\partial D}{\partial h} = -C_D b v |v| \beta \exp(\beta(1-h)) \quad (5.3)$$

$$\begin{aligned}
\frac{\partial}{\partial v}\left(\frac{\partial D}{\partial v}\right) &= 2\text{sgn}(v)C_D b \exp(\beta(1-h)) + \\
&+ 4\frac{\partial C_D}{\partial v} b |v| \exp(\beta(1-h)) + \frac{\partial C_D^2}{\partial v^2} b v |v| \exp(\beta(1-h)) \quad (5.4)
\end{aligned}$$

$$\frac{\partial}{\partial h}\left(\frac{\partial D}{\partial v}\right) = -2C_D b |v| \beta \exp(\beta(1-h)) - \frac{\partial C_D}{\partial v} b v |v| \beta \exp(\beta(1-h)) \quad (5.5)$$

The partials of $C_D(M)$ with respect to the velocity can be easily evaluated, which, after algebraic manipulations, take the final form:

$$\frac{\partial C_D}{\partial v} = \frac{A_1 A_2}{1 + (A_2(M - A_3))^2} \frac{1}{\alpha} \quad (5.6)$$

$$\frac{\partial^2 C_D}{\partial v^2} = -\frac{2A_1 A_2^3}{\alpha^2} \frac{M - A_3}{(1 + (A_2(M - A_3))^2)^2} \quad (5.7)$$

where α denotes the speed of sound. The graphs of C_D , $\frac{\partial C_D}{\partial M}$, and $\frac{\partial^2 C_D}{\partial M^2}$ vs. the Mach number are given in figs.24-26.

Control-Logic Analysis

Only the free-time case was studied, but the method of solution is applicable also for any value of fixed final time.

As shown in fig.31, due to the sharp increase of $\partial C_D/\partial M$ near Mach 1, the singular surface witnesses also a peak in the same region. Moreover, projections of the singular surface into mass-velocity and altitude-velocity planes reveal the existence of a non-admissible portion of the variable-thrust arc, since it corresponds to increasing mass (shown by a dashed line in figs.32-33). Therefore, an optimal switching structure cannot include a singular arc in the transonic region, on account of this violation of assumption 8 of chapter 2.

The problem becomes more elegant and easier to treat, if one uses the transformation to z_1 and z_3 , state space described in the previous chapter. It should be noted however, that such an approach is equivalent to admitting jump discontinuities in the new control variable $z_2 = v$. Such discontinuities, occurring at corner points of the solution imply impulsive behavior of the thrust P (see eq.(4.6)). Such behavior would be admissible in the absence of the inequality constraint on P , which we have assumed from eq.(2.7), but in general, does not

apply to engineering applications, since there is always a limit on the available thrust of the engine. However, an optimal solution obtained in the z-space would still be of importance as an approximation to the case of a very high magnitude of the thrust of the rocket, and in addition to this, it could provide physical insight to the problem.

The analysis can be stated briefly as follows: examine the singular arc by transforming to z-space with a new control-like variable, z_2 , which maximizes the new Hamiltonian (eqs.(4.24),(4.25)). The variation of the Hamiltonian vs. the velocity along the extremal, corresponding to the singular arc of the original problem, is shown in fig.34. Notice that along this singular arc the Hamiltonian has three stationary values, corresponding to three solutions of the singular surface. Two of those correspond to a maximum, and the other corresponds to a minimum value of the Hamiltonian. The first maximum corresponds to the subsonic branch, the minimum corresponds to the transonic branch, screened out, and the second maximum corresponds to the supersonic branch of the singular surface. Henceforth we shall use the terms "subsonic maximum" or "subsonic solution", and "supersonic maximum" or "supersonic solution" to distinguish between the two cases of interest. Thus, points corresponding to the transonic solution cannot be included in an optimal trajectory for a second reason, since such points provide a local *minimum*, rather than a maximum, for the Hamiltonian.

From fig.34 we notice that there is a point in time t_{sw} when both solutions provide the same maximum to the Hamiltonian, and the velocity then *jumps* from the subsonic to the supersonic solution. That is,

$$\tilde{\mathcal{H}}(v_{sbsn}(t_{sw})) = \tilde{\mathcal{H}}(v_{sprsn}(t_{sw})) \quad (5.8)$$

where the subscript *sbsn* denotes the subsonic solution, and the subscript *sprsn* denotes the supersonic solution.

Hence,

$$z_2(t) = v_{sbsn} \quad \text{for} \quad t \leq t_{sw} \quad (5.9)$$

and

$$z_2(t) = v_{sprsn} \quad \text{for} \quad t \geq t_{sw} \quad (5.10)$$

That is because, although both the subsonic and the supersonic solution give a relative maximum, an optimal control should correspond to the *absolute* maximum of the Hamiltonian (eq.(2.25))

Composite Optimal Trajectory

The previous analysis indicates that an optimal trajectory should start with an impulsive boost until the subsonic solution of the singular surface is reached. Then a variable-thrust subarc using this solution is used up to the point when both the subsonic and the supersonic branches provide the same maximum to the Hamiltonian. A switching then to the supersonic branch occurs, and the trajectory remains on the singular surface until the time when the fuel is exhausted. Then a final coasting arc is used, until the terminal boundary conditions are satisfied. Note that this is exactly the result obtained by Garfinkel [14], with $N = 1$.

Although this thrust history would provide the optimal switching structure for the case of $P_{\max} = \infty$, this will not be necessarily true for the case of bounded thrust. In such a case discontinuities in the velocity are of course unacceptable, and the validity of the solution depends on the value of the upper bound of the thrust. Thus, the structure of the optimal trajectory is still in question. This is the topic of the following section.

Numerical solution and Computational Results

The analysis so far shows that the variational problem has a special mathematical structure, in so far as the occurrence of two optimal solutions of $E=0$ implies the existence of an infinite number of composite solutions, in the passing through the transonic region, all satisfying the same boundary conditions. The question is: which of this family of extremals is to be preferred from the point of view of maximizing the altitude? For the case of unbounded thrust the answer has already been given: At a time $t = t_{sw}$, when the Hamiltonian in the reduced z-space switches from its subsonic to its supersonic maximum. Although valid only for unbounded thrust, nevertheless, this remark gives us a hint: An optimal trajectory must *accelerate* from the subsonic to the supersonic region. Since the variable-thrust case must be ruled out, our only choice is the use of full thrust between the two solutions of $E=0$. Furthermore, because for a realistic case $P_{max} < \infty$, the switching from the variable-thrust to the second full-thrust subarc must take place somewhere *before* the time t_{sw} , and such that the switching function vanishes at the points of departure and arrival to the singular surface (points B and D in figs.35-36). In addition to this, it should remain positive all along the full-thrust subarc in order to satisfy the optimality condition of eq.(2.26).

Thus, a trial-and-error procedure is needed to determine the points B and D. The BOUNDSOL result obtained was rather disappointing; An optimal switching from the first variable-thrust subarc to the second full-thrust subarc (point B), should take place before the switching of the first full-thrust subarc to the first variable-thrust subarc (point A). Therefore, for the case of $P_{max} = 3.5$, an optimal trajectory cannot have this switching structure, but rather must have the simpler full-singular-coast sequence, with the singular subarc corresponding to the supersonic solution of $E=0$.

However, when an analogous calculation for the case $P_{\max} = 6$ was performed, the new, more complex, sequence of subarcs, full-singular-full-singular-coast, gave indeed a *higher* final altitude than the full-singular-coast sequence (table 3).

6. Conclusions

The problem of maximizing the final altitude of a vertically-ascending rocket has been first analyzed for the case of bounded thrust, and quadratic drag law. For the case of a constant drag coefficient, solutions were obtained for several values of the duration of the flight, and the analysis of the problem showed that a one-parameter family of singular extremals is generated, according to the prescribed value of the final time. Moreover, it has been shown that the final value of the time affects the switching structure of the problem, with the most interesting case the appearance of a second full-thrust subarc after the singular subarc, as a result of the boundedness of the available thrust. For the vertical-flight problem this is a new result, as far as the author knows.

Subsequently, a more realistic drag model was used, with the drag coefficient as a function of the Mach number, witnessing a sharp increase in the transonic region. A more complex switching structure, with an intermediate full-thrust subarc in transition through the transonic region, was needed owing to the requirement that the mass should be monotonically non-increasing. The results are identical with those of Garfinkel, for the $P_{\max} = \infty$ case, although a totally different approach was used. The solution obtained, using a transformation to a

reduced two-dimensional state space, showed that the optimality of the solution depends on the assumed upper bound on the thrust. Numerical results obtained verified the superior performance of the new thrust program, over the classical full-singular-coast sequence, at least for a *sufficiently high* upper bound on the thrust.

For both cases, the Kelley necessary condition for singular arcs, and the McDanell and Powers condition for joining singular and non-singular subarcs were checked, and were found to be satisfied. In addition to this, a Jacobi-like test was performed along the transformed singular extremal, for the case of constant C_D , and $P_{\max} = \infty$.

From the analysis of the problem it becomes evident that the composition of an optimal trajectory depends heavily on the drag model assumed for the solution. The results obtained in the present work may by no means apply to the case of a more complex or of a more "naive" drag model. In fact, as Leitmann [8] has suggested, for the particular case of a drag of the form

$$D = C_D(M)v^2 \quad (6.1)$$

i.e., independent of the air density, the full-thrust subarc in the transition through the transonic region should be replaced by a *coasting* subarc (fig.46). This is mainly due to the fact that the switching curve is independent of the altitude, and as a result, the vehicle *decelerates* along the singular subarc. Hence a coasting subarc is required for the transition from the supersonic branch to the subsonic branch of the solution of the switching surface.

Suggestions for Future Research

The case of prescribed final time for the Mach-dependent drag coefficient model may generate a more complex switching structure, with the possible appearance of a *third* full-thrust subarc due to the saturation of the thrust on

its upper bound, especially for sufficiently small values of final time. Also the more realistic case of a rocket in vertical flight with a drop-away booster and an upper limit on dynamic pressure are of prime importance in aerospace applications. The Jacobi-like test method described in chapter 4 is applicable only to the case $P_{\max} = \infty$. In such a case an impulsive burn could be used to satisfy the conditions at the entry into the singular subarc. However no such a test is so far available for the bounded-thrust case. A Jacobi-like condition applicable to broken extremals, although there are recent developments in this direction, still remains an open issue [42-47]. Even for the case of $P_{\max} = \infty$ the test does not include the coasting subarc.

Such problems pose interesting research questions.

References

1. Goddard, R.H., "A Method of Reaching Extreme Altitudes", *Smithsonian Inst. Misc. collections* 71,1919 and reprint by Amer. Rocket Soc., 1946.
2. Hamel, G., "Über eine mit dem Problem der Rakete Zusammenhängende Aufgabe der Variationsrechnung", *Zeitschrift für angewandte Mathematik und Mechanik*, Vol.7, no.6, Dec. 1927, pp. 451-452, (in German).
3. Tsien, H.S., and Evans, R.C., "Optimum Thrust Programming for a Sounding Rocket", *Journal of American Rocket society*, Vol.21, no.5, Sept. 1951, pp. 99-107.
4. Leitmann, G., "A Calculus of Variations Solution of Goddard's Problem", *Astronautica Acta*, Vol.II, no.2, 1956, pp. 55-62.
5. Leitmann, G., "Optimum Thrust Programming for High Altitude Rockets", *Aeronautical Engineering Review*, Vol.16, no.6, June 1957, pp. 63-66.
6. Leitmann, G., "Stationary Trajectories for a High-Altitude Rocket with Drop-Away Booster", *Astronautica Acta*, fasc.3, 1956, pp. 119-124.
7. Leitmann, G., "On a Class of Variational Problems in Rocket Flight", *Journal of Aero/Space Science*, Sept. 1959, pp. 586-591.
8. Leitmann, G., "An Elementary Derivation of the Optimal Control Conditions", *12th International Astronautical Congress*, Academic Press, New York, 1963.

9. Miele, A., and Cavoti, C.R., "Generalized Variational Approach to the Optimum Thrust Programming for the Vertical Flight of a Rocket", *ZFW*, Vol.6, no.4, March 1958, pp. 102-109.
10. Miele, A., "Optimum Climbing Technique for a Rocket-Powered Aircraft", *Jet Propulsion*, August 1955, pp. 385-391.
11. Bryson, A.Jr., and Ross, S.E., "Optimum Rocket Trajectories with Aerodynamic Drag", *Jet Propulsion*, July 1958, pp. 465-469.
12. Miele, A., "Extremization of Linear Integrals by Green's Theorem", *Optimization Techniques with Applications to Aerospace Systems*, Academic Press, New York, 1962, pp. 69-98.
13. Miele, A., and Cicala, P., "Generalized Theory of the Optimum Thrust Programming for the Level Flight of a Rocket-Powered Aircraft", *Jet Propulsion*, Vol.26, no.6, June 1956, pp. 443-455.
14. Garfinkel, B., "A Solution of the Goddard Problem", *SIAM Journal on Control*, Vol.1, no.3, 1963, pp. 349-368.
15. Munick, H., "Goddard Problem with Bounded Thrust" *AIAA Journal*, Vol.3, no.7, 1965, pp. 1283-1287.
16. Lee, E.B., and Markus, L., "Foundations of Optimal Control Theory", John Wiley and Sons Inc., New York, 1967, pp. 456-466.
17. Miele, A., "Stationary Conditions for Problems Involving Time Associated with Vertical Rocket Trajectories", *Journal of Aero/Space Sciences*, July 1958, pp. 467-469.
18. Miele, A., "On the Brachistochronic Thrust Program for a Rocket Powered Missile Traveling in an Isothermal Medium", *Jet Propulsion*, Vol. 28, no. 10, Oct. 1958, pp. 675-684.
19. Faulkner, F., "The Problem of Goddard and Optimum Thrust Programming", *Advances in the Astronautical Sciences*, Vol.1, Plenum Press, New York, 1957, pp. 43-51.
20. Ewing, G.M., and Haseltine, W.R., "Optimal Programs for an Ascending Missile", *SIAM Journal on Control*, Vol.2, no.1, 1964, pp.66-88.
21. Zlatskiy, V.T., and Kiforenko, B.N., "Computation of Optimal Trajectories with Singular-Control Sections", *Vychislitel'naia i Prikladnaia Matematika*, no.49, 1983, pp. 101-108 (in Russian).

22. Bliss, G.A., "Lectures on the Calculus of Variations", Un. of Chicago Press, Chicago Illinois, 1946.
23. Pontryagin, L.S., et al., "The Mathematical Theory of Optimal Processes", Interscience, New York, 1962.
24. Johnson C.D., and Gibson J.E., "Singular Solutions in Problems of Optimal Control", *IEEE Transactions on Automatic Control*, January 1963, pp. 4-15.
25. *Jane's all the World's Aircraft*, McGraw Hill, New York, pp. 521-522, 1967-1968.
26. Bulirsch, R., "Einführung in die Flugbahnoptimierung die Mehrzielmethode zur Numerischen Lösung von Nichtlinearen Randwertproblemen und Aufgaben der Optimalen Steuerung", *Lehrgang Flugbahnoptimierung*, Carl-Cranz-Gesellschaft e.v., October 1971, (in German).
27. Kelley, H.J., "A Second-Variation Test for Singular Extremals", *AIAA Journal*, Vol. 2, no. 8, August 1964, pp.1380-1382.
28. Robbins, H.M., "Optimality of intermediate-thrust arcs of rocket trajectories", *AIAA Journal*, Vol. 3, June 1965, pp.1094-1098.
29. Robbins, H.M., "A Generalized Legendre-Clebsch Condition for the Singular Cases of Optimal Control", *IBM Journal of Research*, Vol.11, 1967, pp. 361-372.
30. Kelley, H.J., Kopp, R.E., and Moyer, H.G., "Singular Extremals", *Topics in Optimization*, G. Leitmann, ed., Academic Press, New York, 1967.
31. Kelley, H.J., "A Transformation Approach to Singular Subarcs in Optimal Trajectory and Control Problems", *SIAM Journal on Control*, Vol.2, no.2, 1964, pp. 234-240.
32. Breakwell, J.V., "Approximations in Flight Optimization Techniques", *Aerospace Engineering*, Vol.20, no.9, 1961, pp.26-27.
33. Cicala P., "An Engineering Approach to the Calculus of Variations", Levrotto e Bella, Turin, 1957.
34. Mason, J.D., "Transformations and Discontinuities for Optimal Space Trajectories", Ph.D. Dissertation, Dept. of Aerospace and Mechanical Engineering, University of Arizona, 1967.

35. Ewing G.M., "Necessary Conditions for an Extremum", *Calculus of Variations and Applications*, Dover Publications, New York, 1969, pp. 26-51.
36. Johnson, C.D., "Singular Solutions in Problems of Optimal Control", *Advances in Control Systems*, C.T. Leondes, ed., Vol.2, Academic Press, New York, 1967,
37. McDanell, J.P., and Powers, W.F., "Necessary Conditions for Joining Optimal Singular and Nonsingular Subarcs", *SIAM Journal on Control*, Vol.9, no.2, 1971, pp.161-173.
38. Bershchanskiy, Y.M., "Conjugation of Singular and Nonsingular Parts of Optimal Control", *Automation and Remote Control*, Vol.40, no.3, March 1979, pp.325-330.
39. Kelley, H.J., and Moyer, H.G., "Computational Jacobi-Test Procedure", Proceedings of Workshop, *Current Trends in Control*, Dubrovnik, Yugoslavia, June 29-30, 1984, JUREMA, Zagreb, 1985.
40. Larew, G.A., "Necessary Conditions in the Problem of Mayer in the Calculus of Variations", *Transactions of the American Mathematical Society*, Vol. 20, 1919, pp. 1-22.
41. Reid, W.T., "Discontinuous Solutions in the Nonparametric Problem of Mayer in the Calculus of Variations", *American Journal of Mathematics*, Vol. 57, 1935.
42. Moyer, H.G., "Optimal Control Problems that Test for Envelope Contacts", *Journal of Optimization Theory and Applications*, Vol.6, no.4, Oct. 1970, pp. 287-298. pp. 209-267.
43. Moyer, H.G., "Minimum Impulse Coplanar Circle-Ellipse Transfer", *Journal of AIAA*, Vol. 3, no. 4, 1965.
44. McDanell, J.P., and Powers, W.F., "New Jacobi-type Necessary and Sufficient Conditions for Singular Optimization Problems", *AIAA Journal*, Vol.8, 1970, pp. 1416-1420.
45. Speyer, J.L., and Jacobson, D.H., "Necessary and Sufficient Conditions for Optimality for Singular Control Problems: A Transformation Approach", *Journal of Mathematical Analysis and Applications*, Vol. 33, 1971, pp. 163-187.
46. Speyer, J.L., and Jacobson, D.H., "Necessary and Sufficient Conditions for Optimality for Singular Control Problems: A limit Approach",

Journal of Mathematical Analysis and Applications, Vol. 34, 1971, pp. 239-266.

47. Moyer, H.G., "Sufficient Conditions for a Strong Minimum in Singular Control Problems", *Journal SIAM on Control*, Vol.11, no.4, Nov. 1973, pp. 620-636.
48. Caratheodory, C., "Calculus of Variations and Partial Differential Equations of the First Order", Vol. 2, Holden-Day, San Fransisco, 1967, (English translation of 1935 German-language original)
49. Shankar, U.J., "Periodic Solutions in Aircraft Cruise - Dash Optimization", Ph.D. Dissertation, Dept. of Aerospace and Ocean Engineering, Virginia Polytechnic Institute and State University, Sept. 1987.
50. Ross, S.E., "Minimality for Problems in Vertical and Horizontal Rocket Flight", *Jet Propulsion*, 1958, pp. 55-56.

Final Time	Full Thrust Subarc	Singular Thrust Subarc	Full Thrust Subarc
0.058	0.99378	-	-
0.080	0.71428	-	-
0.100	0.57142	-	-
0.120	0.47619	-	-
0.130	0.33827	0.36742	0.44114
0.140	0.25679	0.39305	0.42377
0.150	0.19787	0.40441	-
0.170	0.16153	0.38898	-
0.198	0.11822	0.36541	-
0.220	0.09784	0.35164	-
0.250	0.07760	0.33553	-
0.280	0.06350	0.32227	-
0.320	0.05031	0.30788	-
0.350	0.04313	0.29855	-

Table 1: Variation of Switching points with final time

Final Time	Final Altitude	Final Velocity
0.058	1.00405	0.14324
0.080	1.00683	0.10788
0.100	1.00877	0.08612
0.120	1.01028	0.06596
0.130	1.01090	0.05621
0.140	1.01142	0.04789
0.150	1.01173	0.03579
0.170	1.01249	0.02367
0.198	1.01283	0.00000
0.220	1.01265	-0.01772
0.250	1.01173	-0.04340
0.280	1.01004	-0.06932
0.320	1.00659	-0.10224
0.350	1.00330	-0.11215

Table 2: Variation of final altitude and final velocity with final time

	Final Time	Final Altitude
F-S-C :	0.197374	1.0132976
F-S-F-S-C:	0.198978	1.0133038

Table 3: Comparison of the two thrust programs for $P_{\max} = 6$

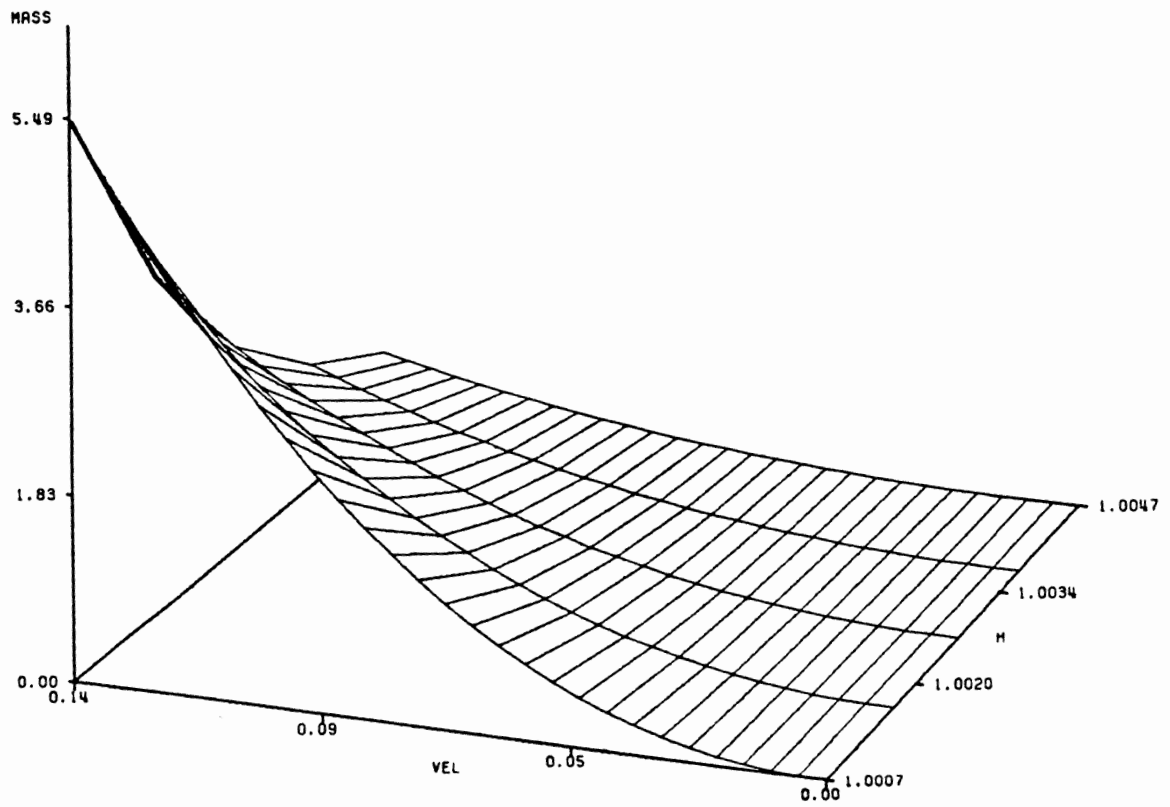


Fig.1: Singular surface in h, m, v space

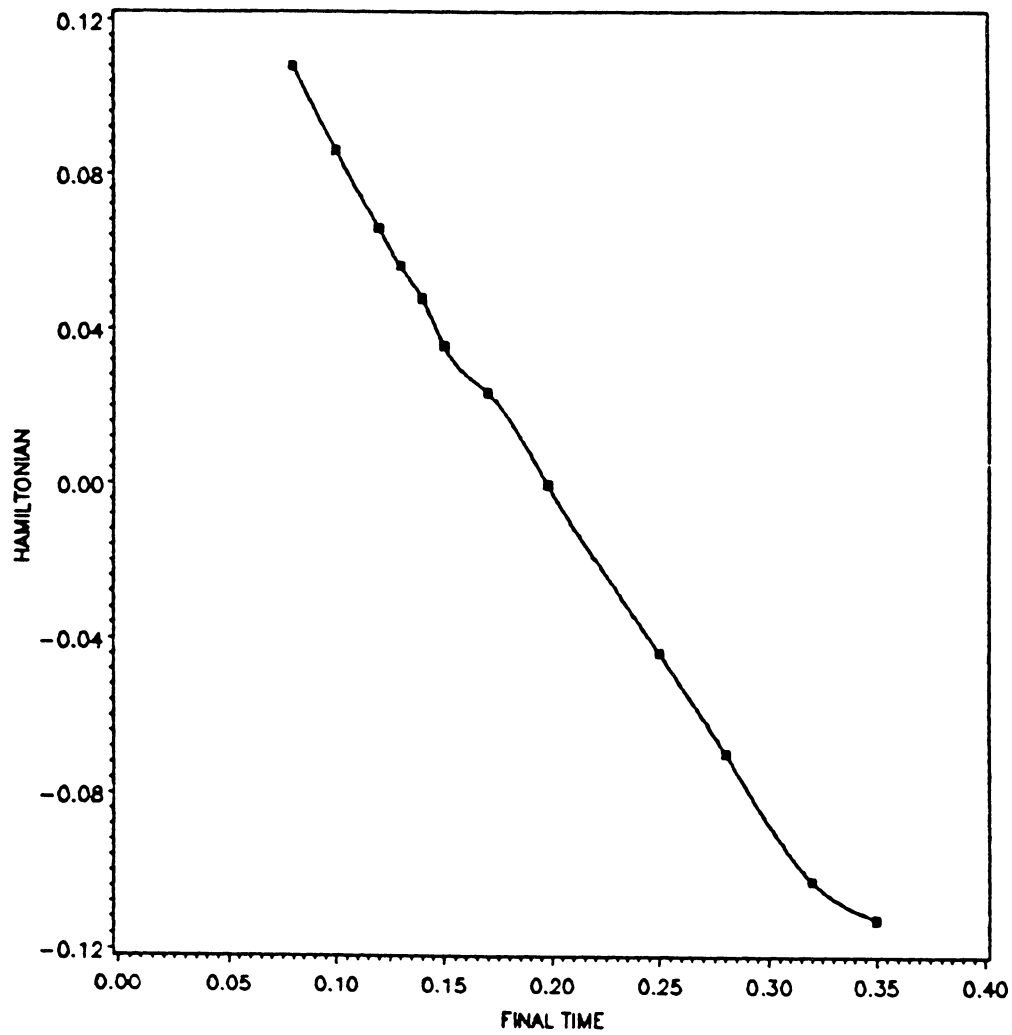


Fig.2: Variation of Hamiltonian with final time

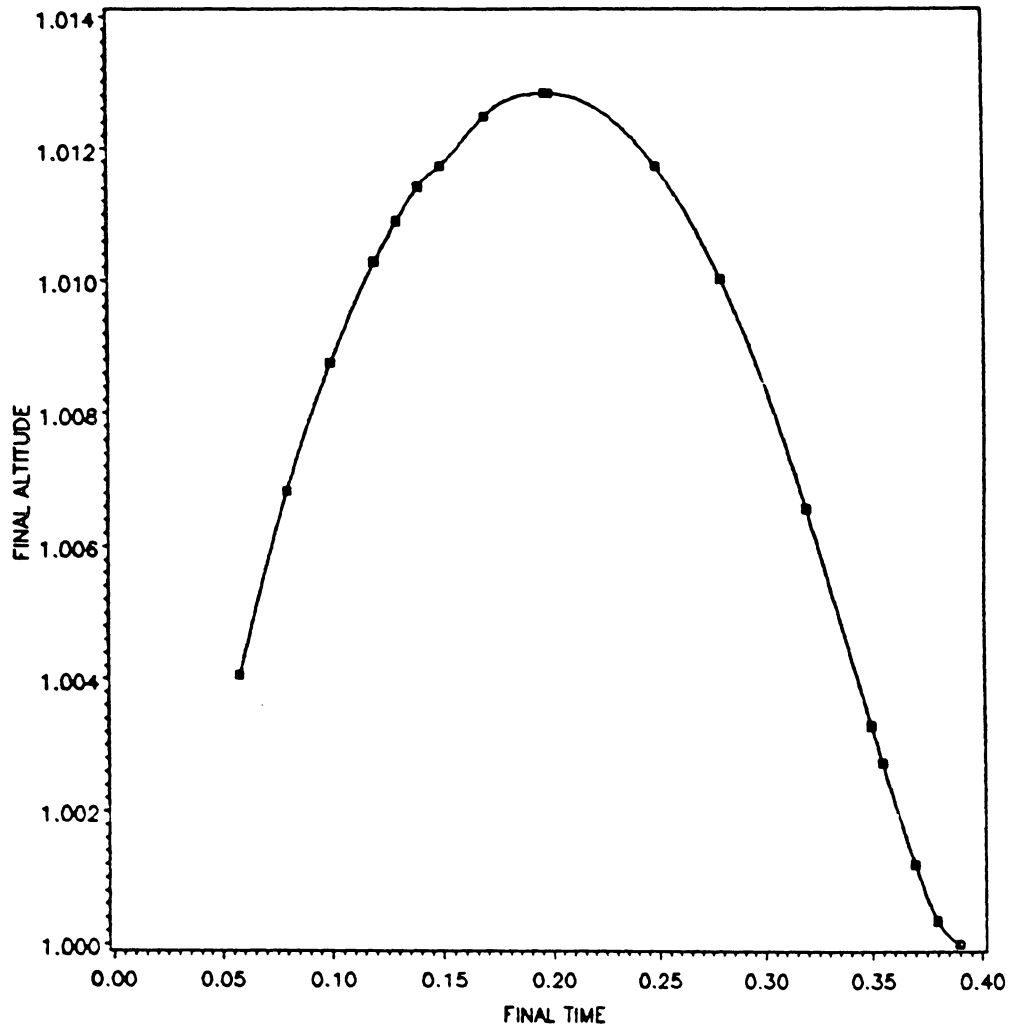


Fig.3: Variation of final altitude with final time

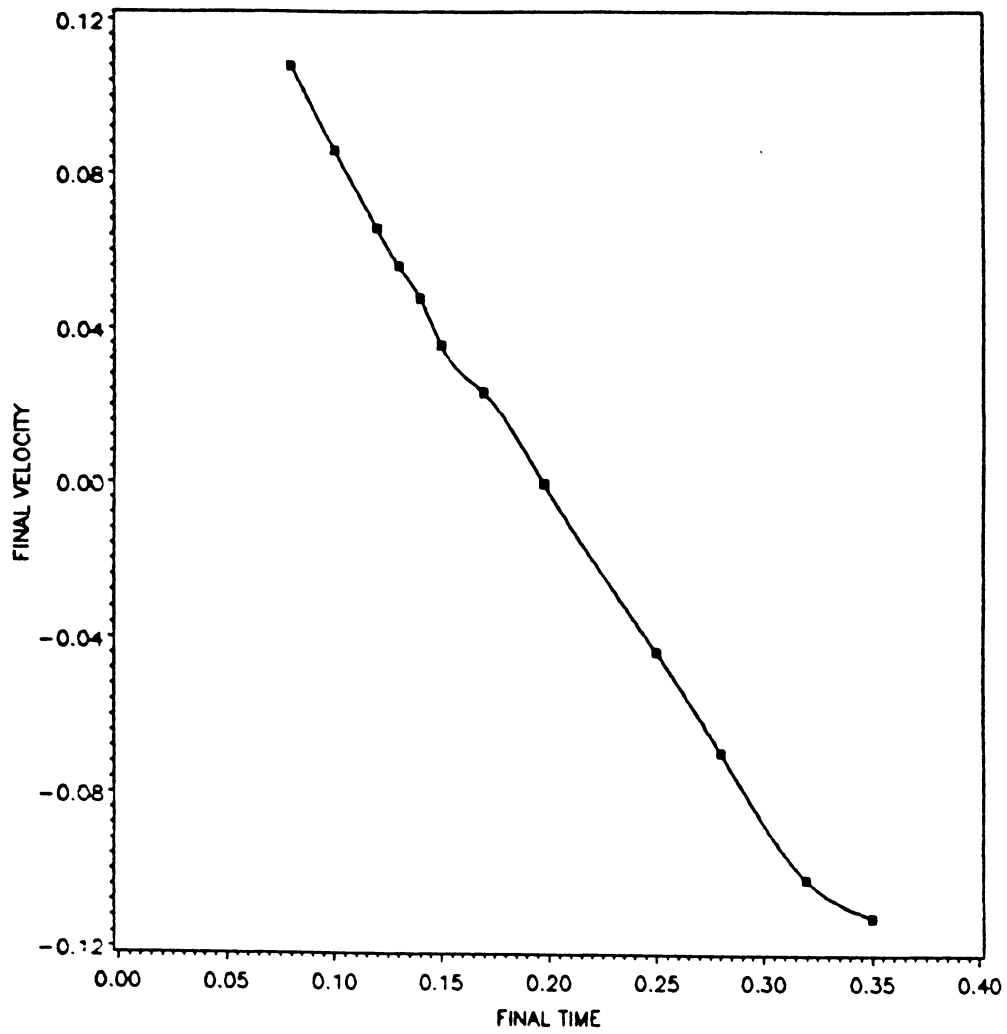


Fig.4: Variation of final velocity with final time

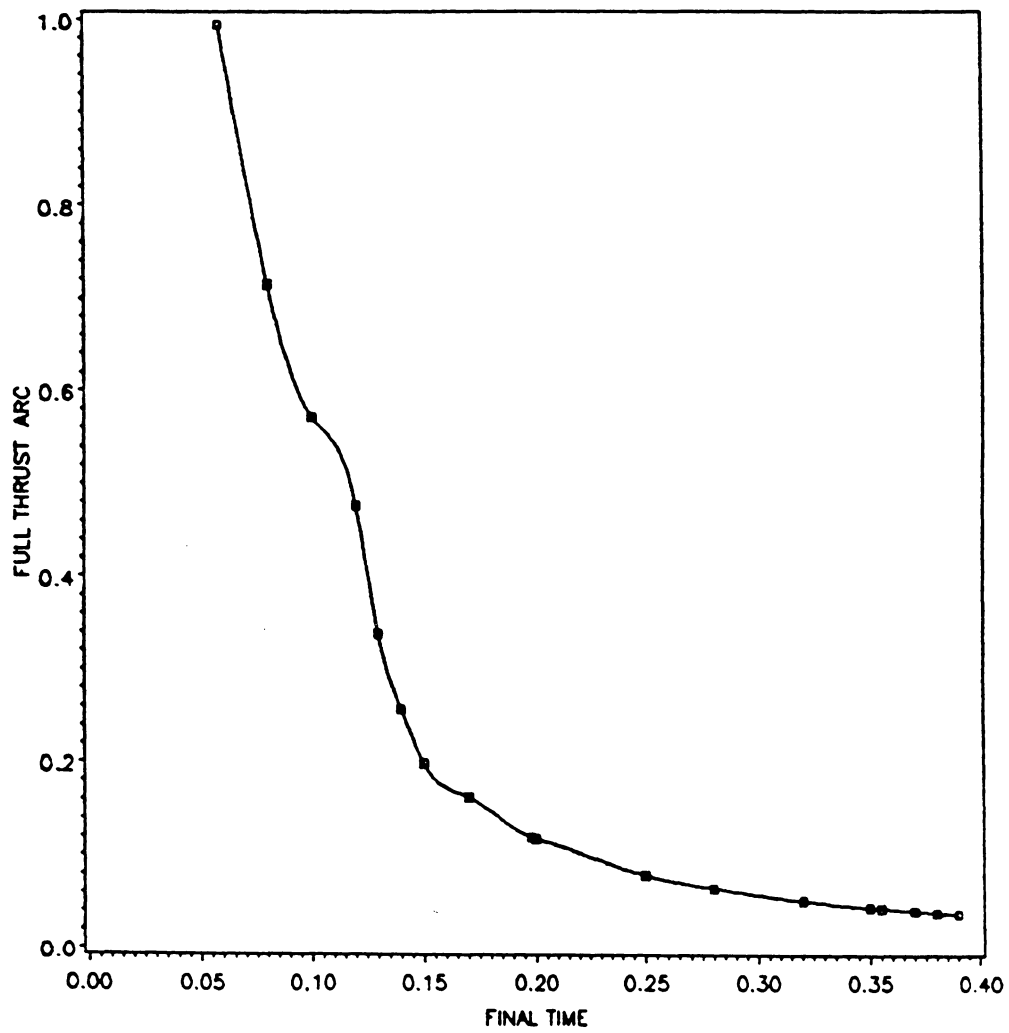


Fig.5: Variation of full-thrust subarc with final time

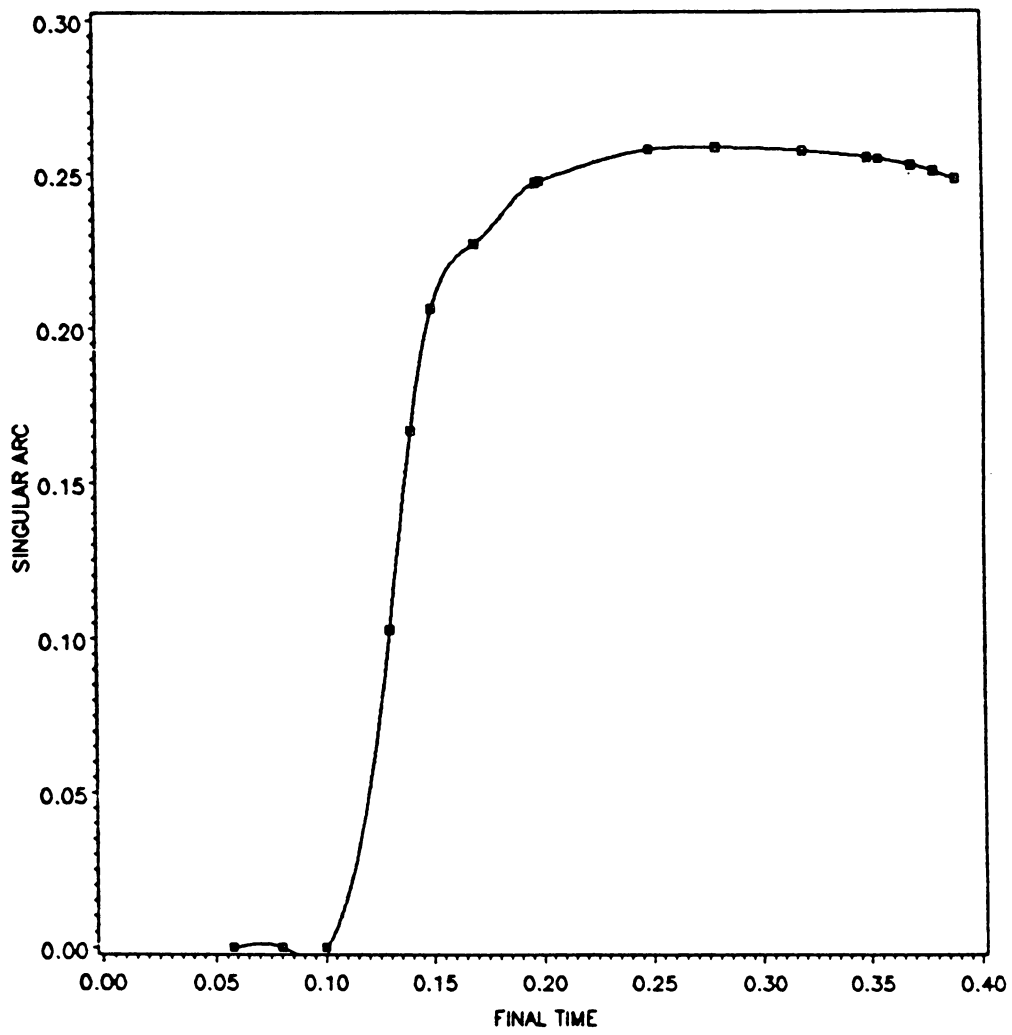


Fig.6: Variation of singular-thrust subarc with final time

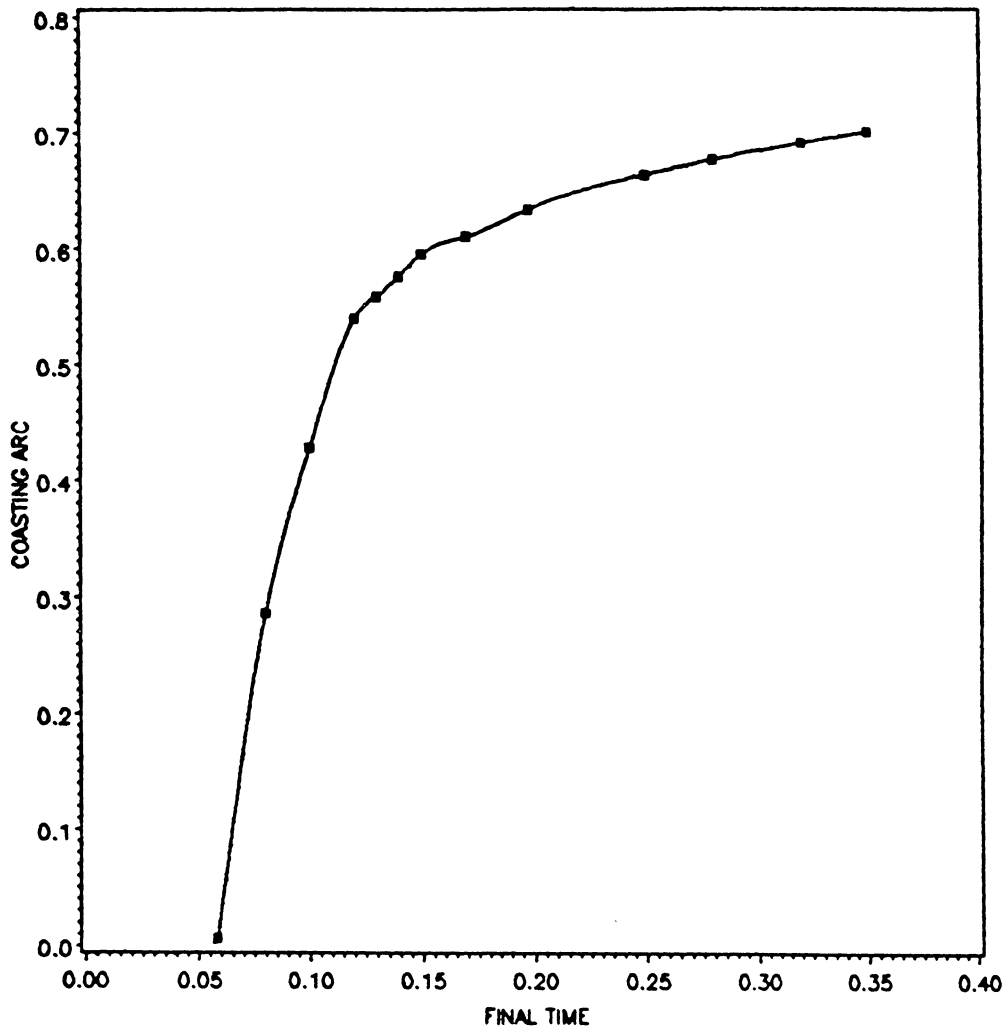


Fig.7: Variation of zero-thrust subarc with final time

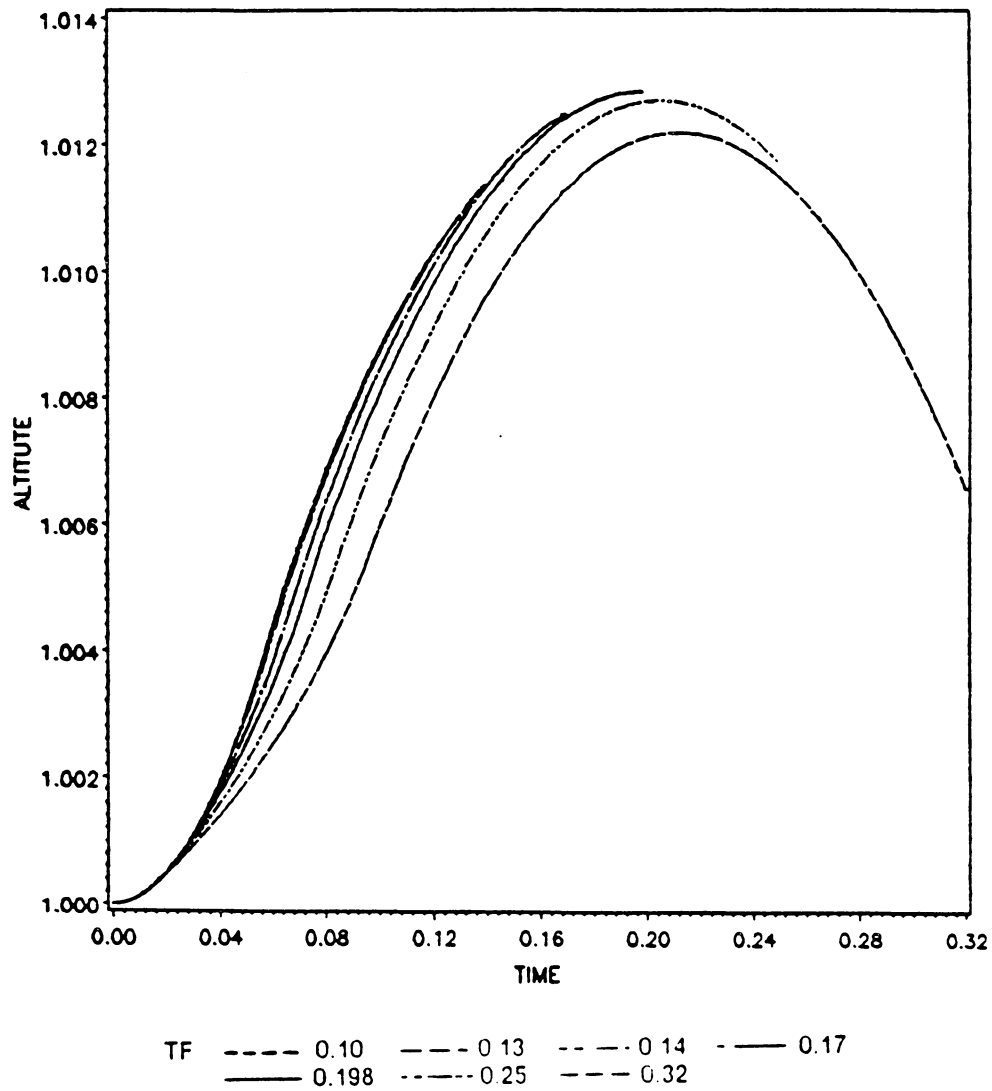


Fig.8: Variation of altitude h with time

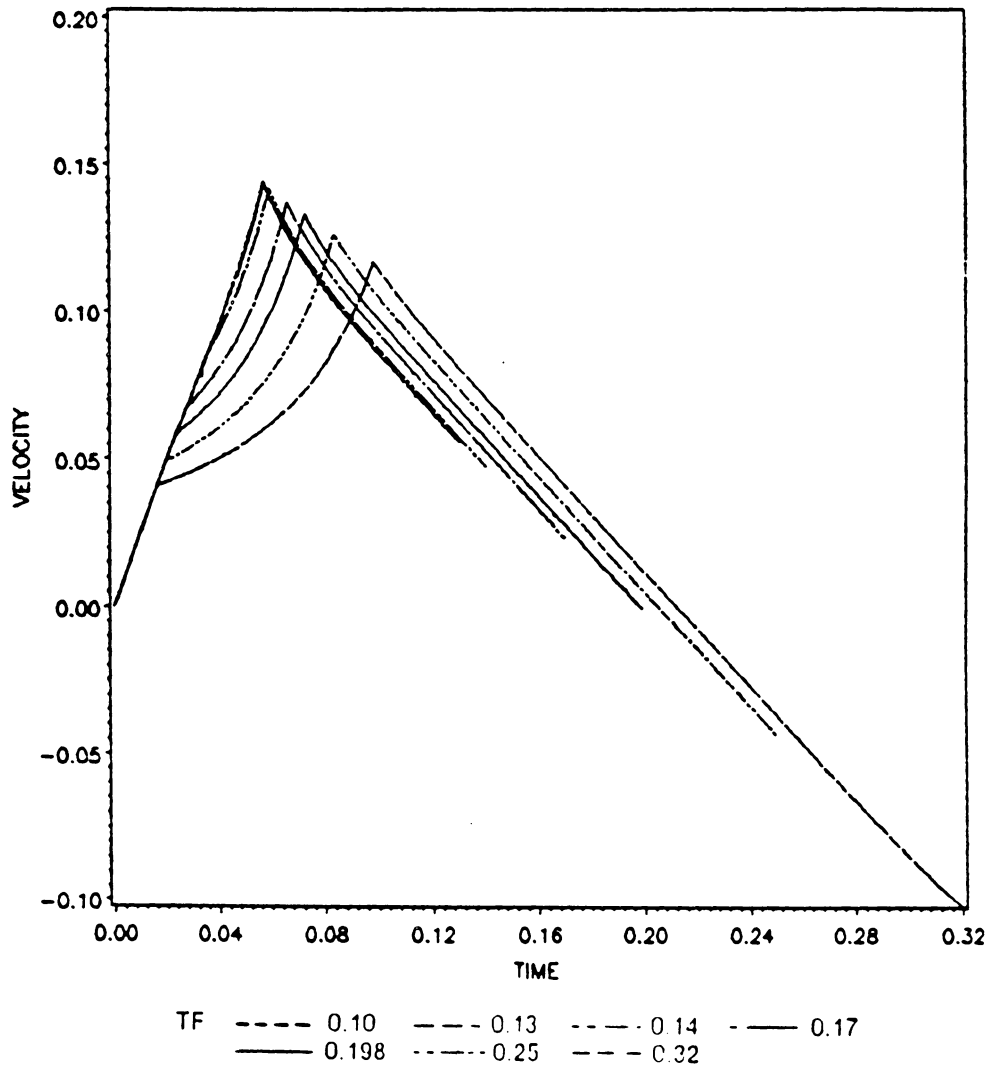


Fig.9: Variation of velocity v with time

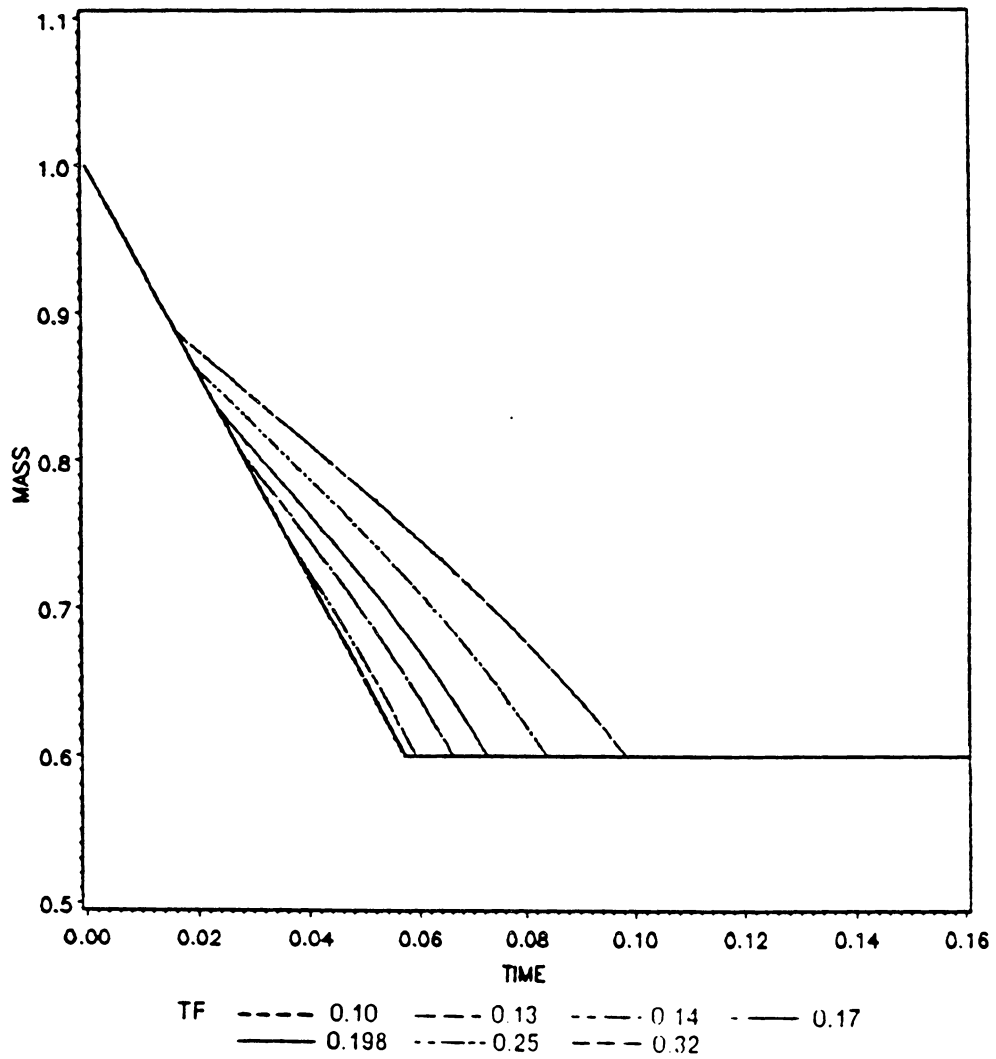


Fig.10: Variation of mass m with time

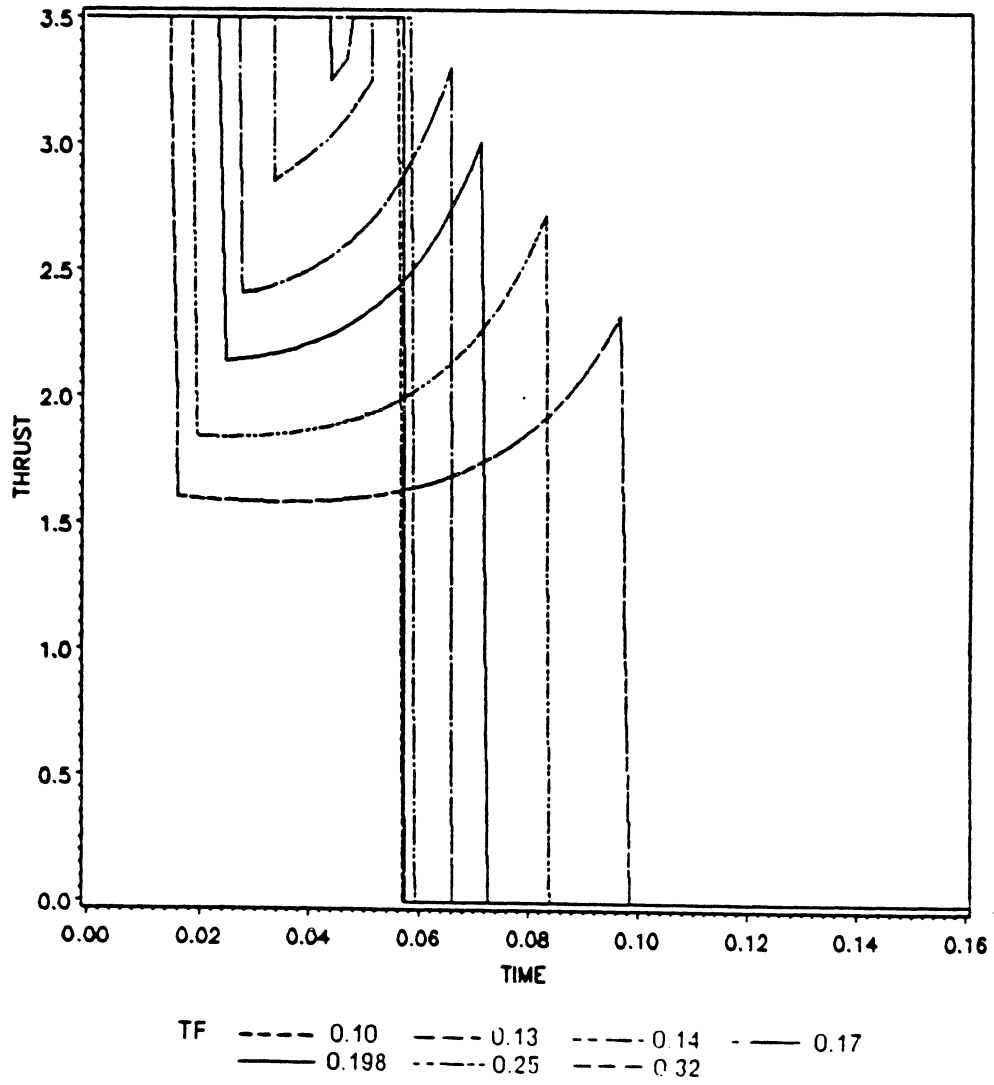


Fig.11: Variation of thrust P with time

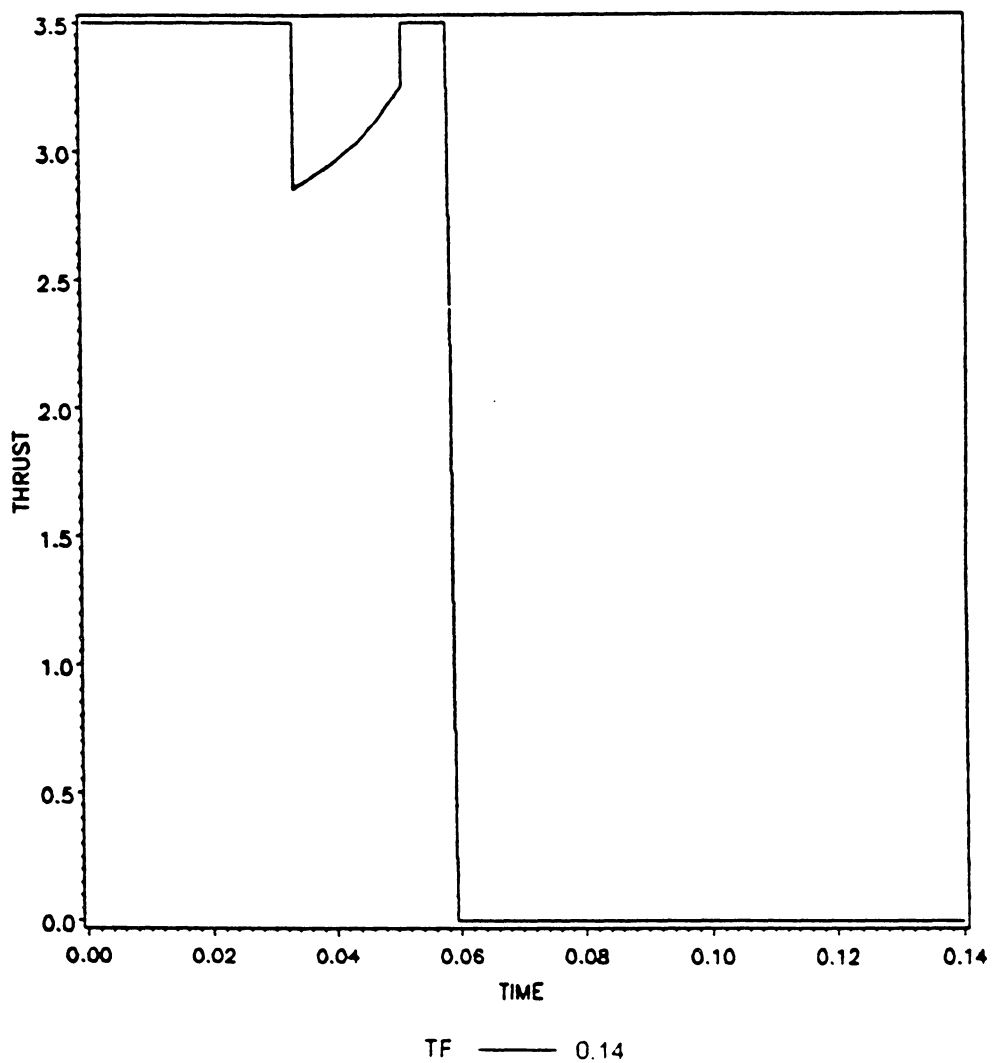


Fig.12: Variation of thrust P with time for full-singular-full-coast sequence

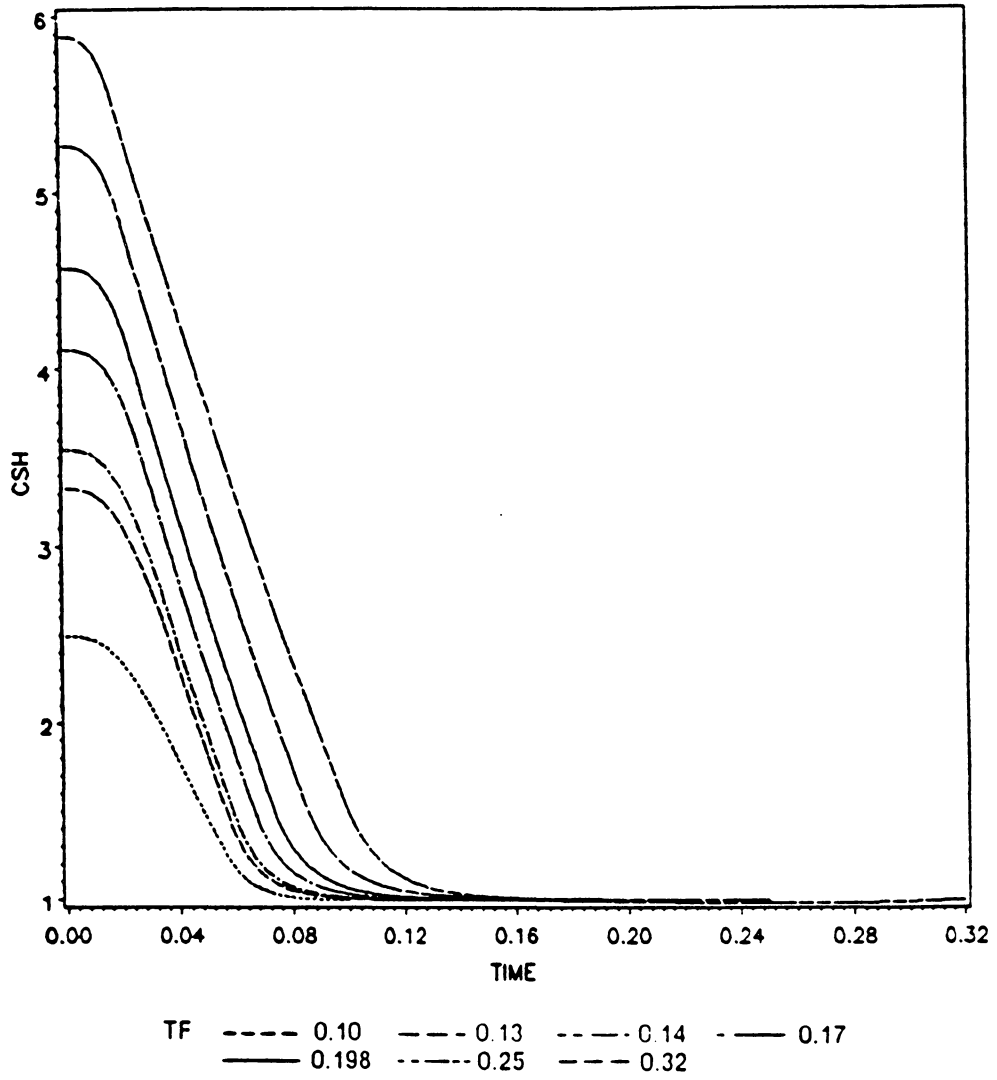


Fig.13: Variation of costate λ_h with time

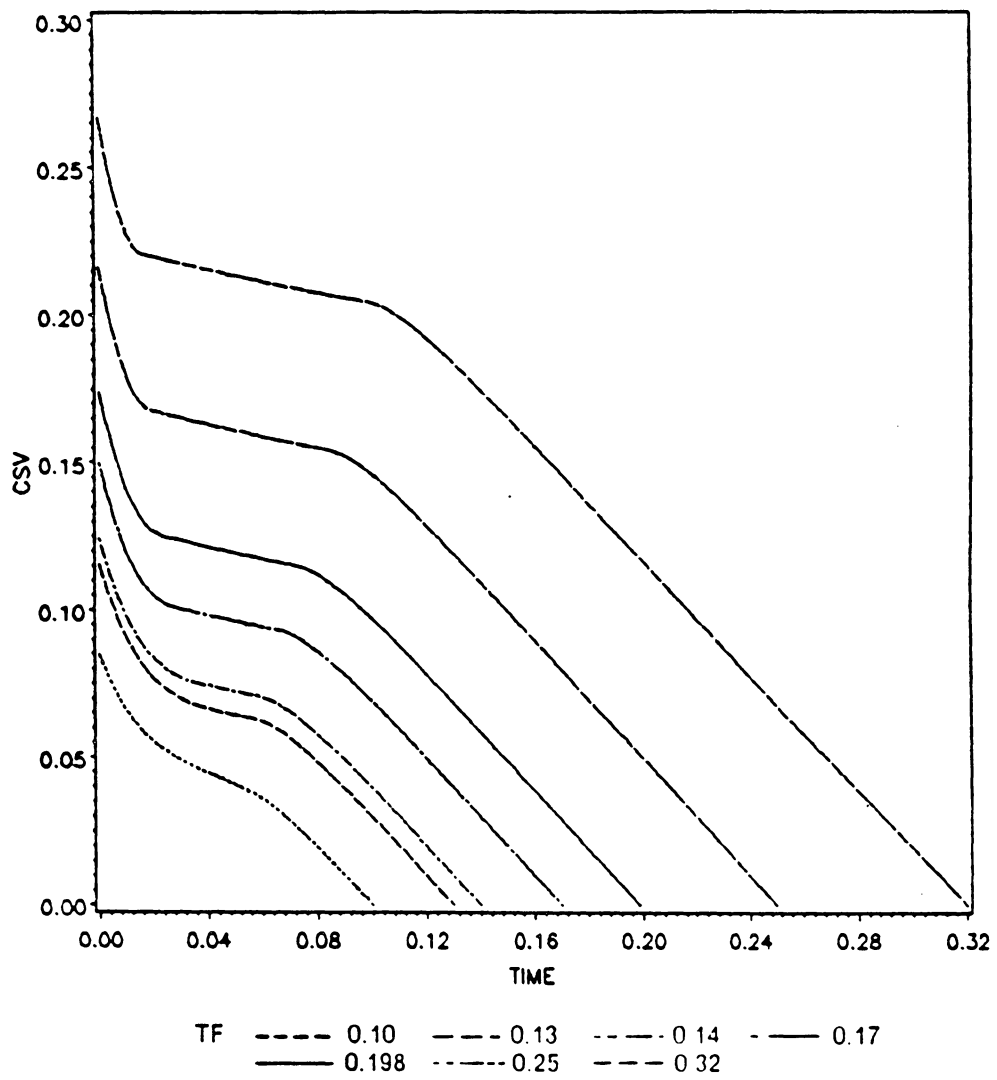


Fig.14: Variation of costate λ_1 with time

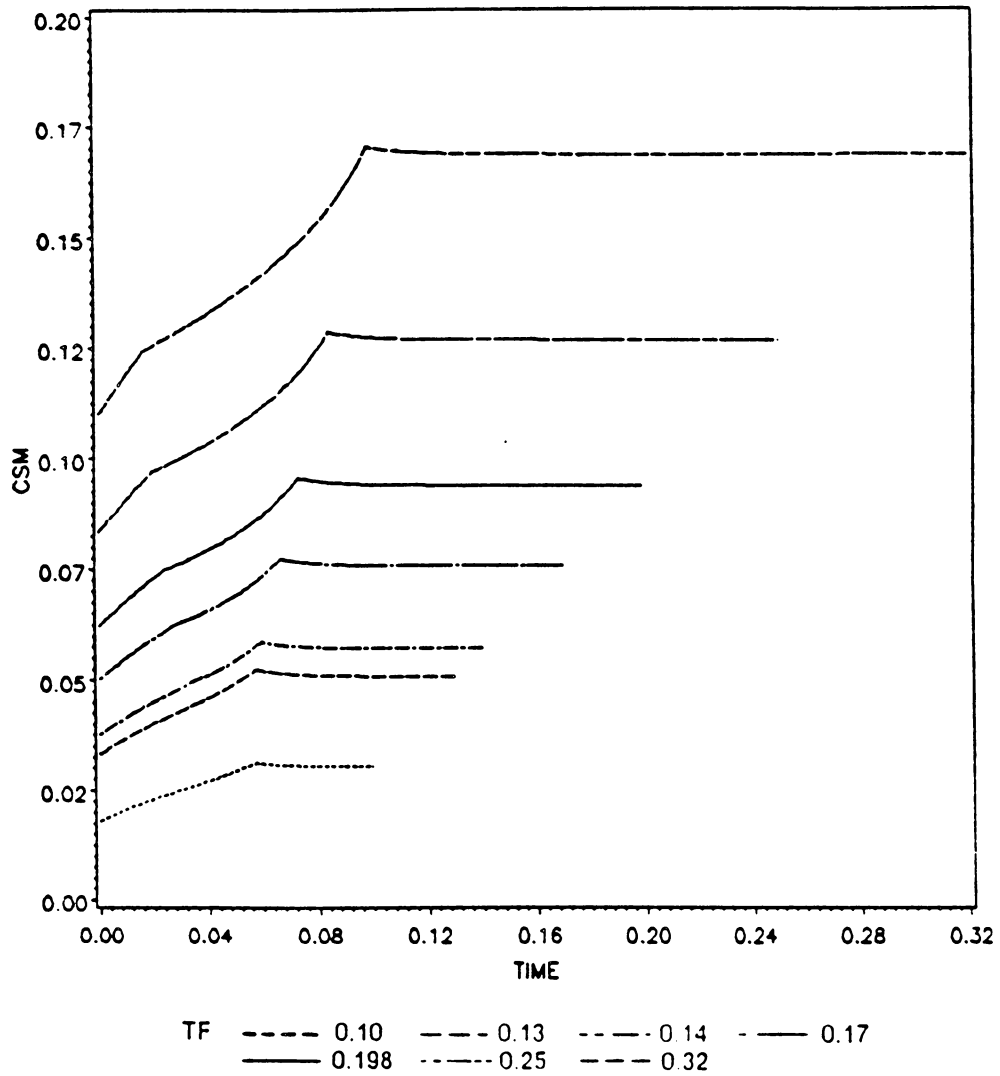


Fig.15: Variation of costate λ_m with time

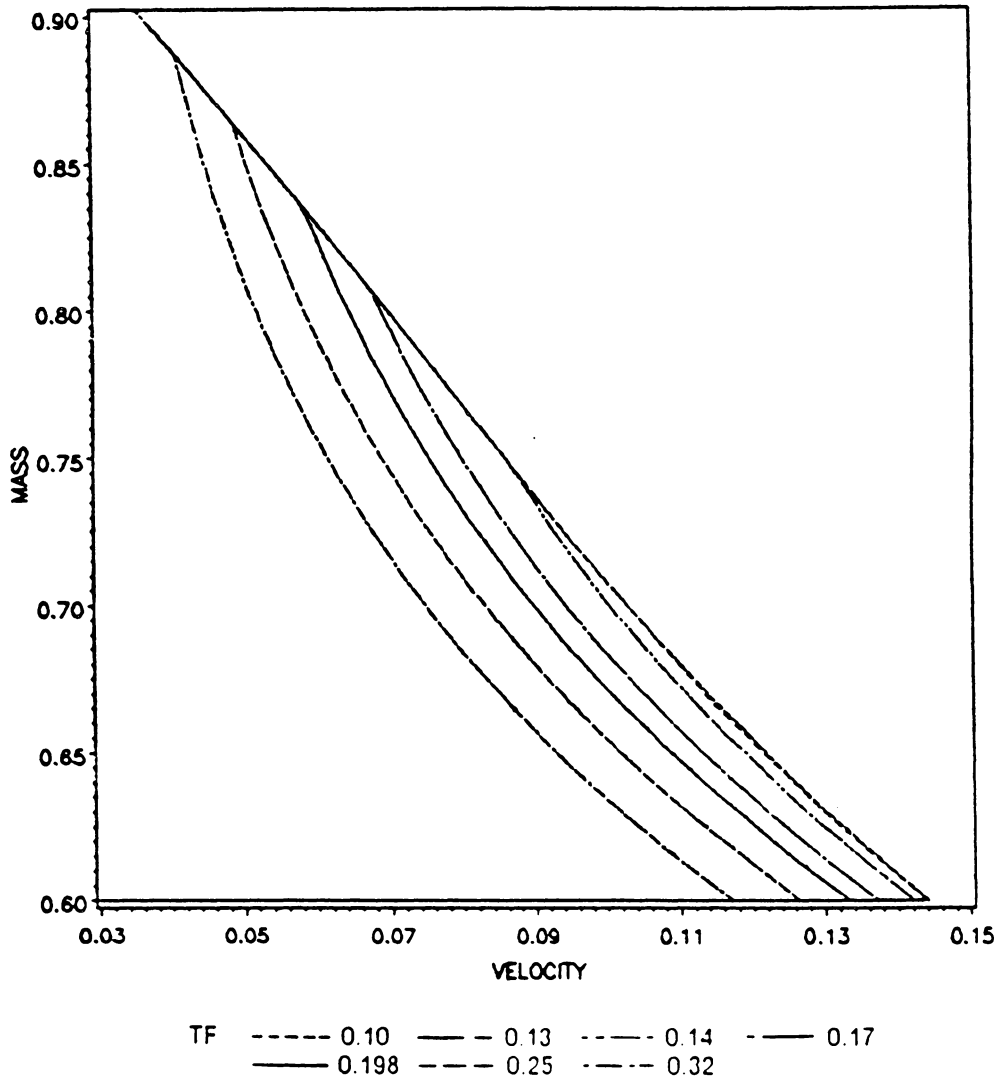


Fig.16: Variation of mass m with velocity v

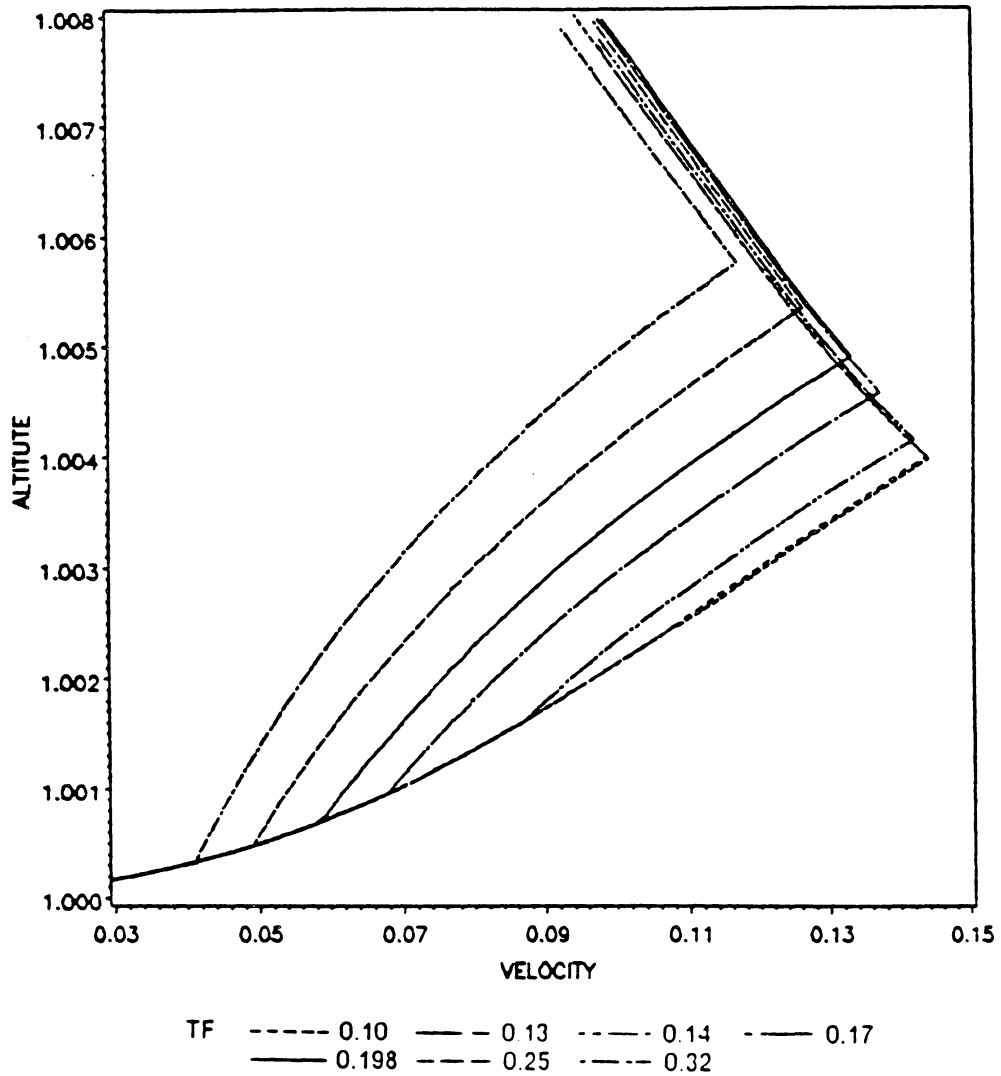
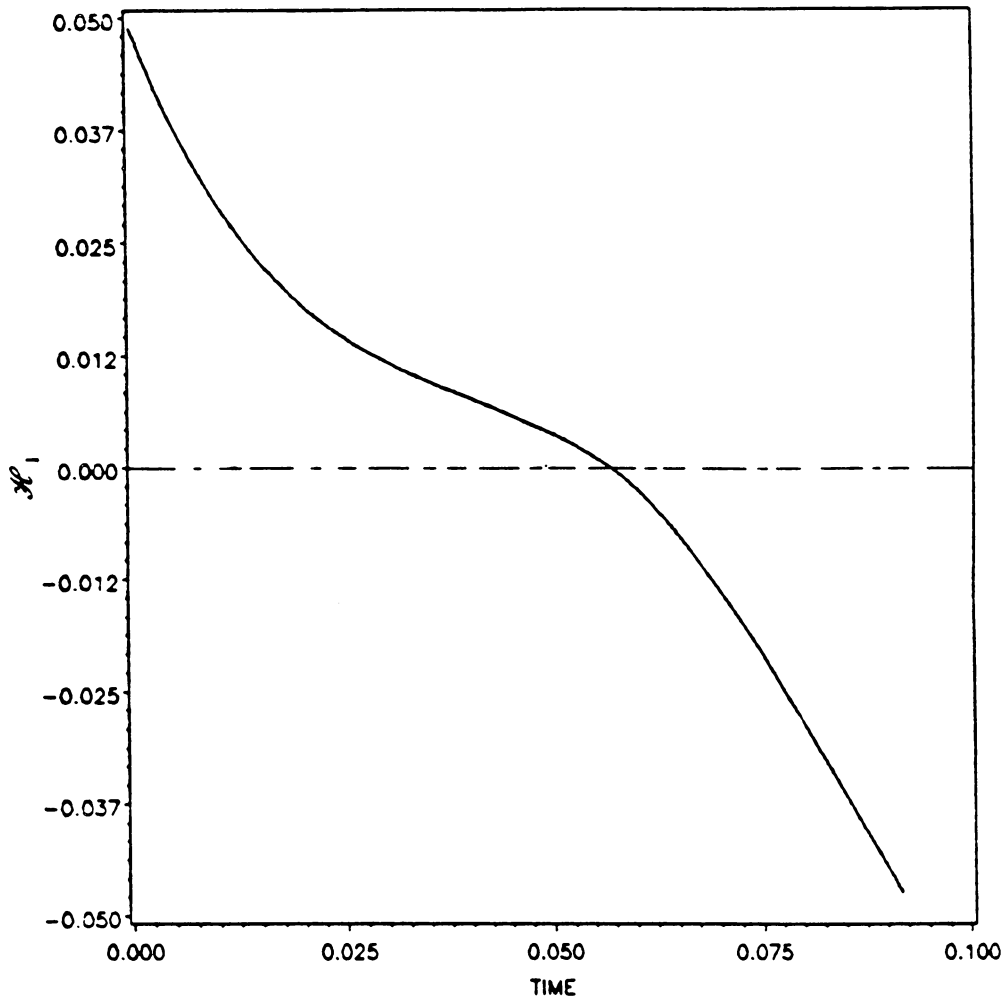


Fig.17: Variation of altitude h with velocity v



TF ——— 0.10

Fig.18: Switching function \mathcal{H}_1 vs. time for full-coast sequence

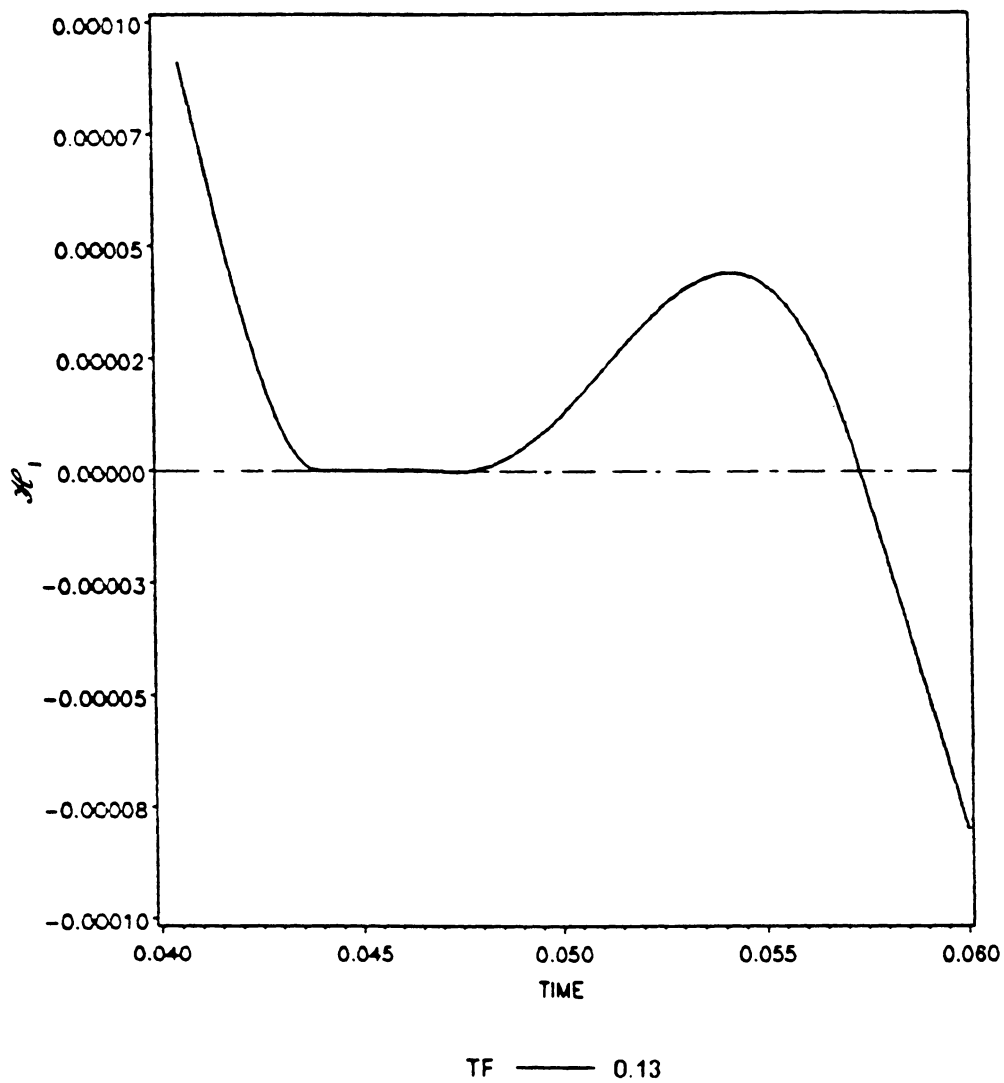


Fig.19: Switching function \mathcal{H}_1 vs. time for full-singular-full-coast sequence

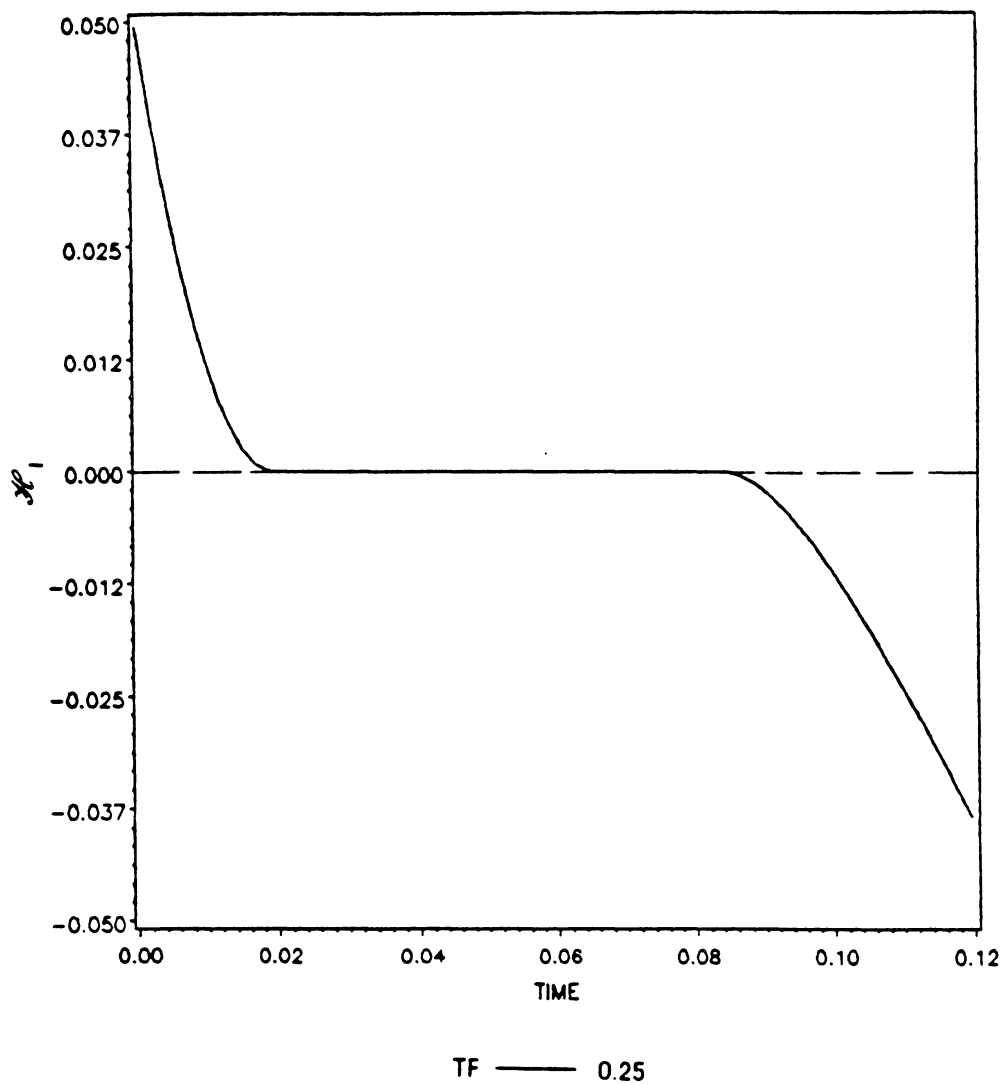


Fig.20: Switching function \mathcal{H}_1 vs. time for full-singular-coast sequence

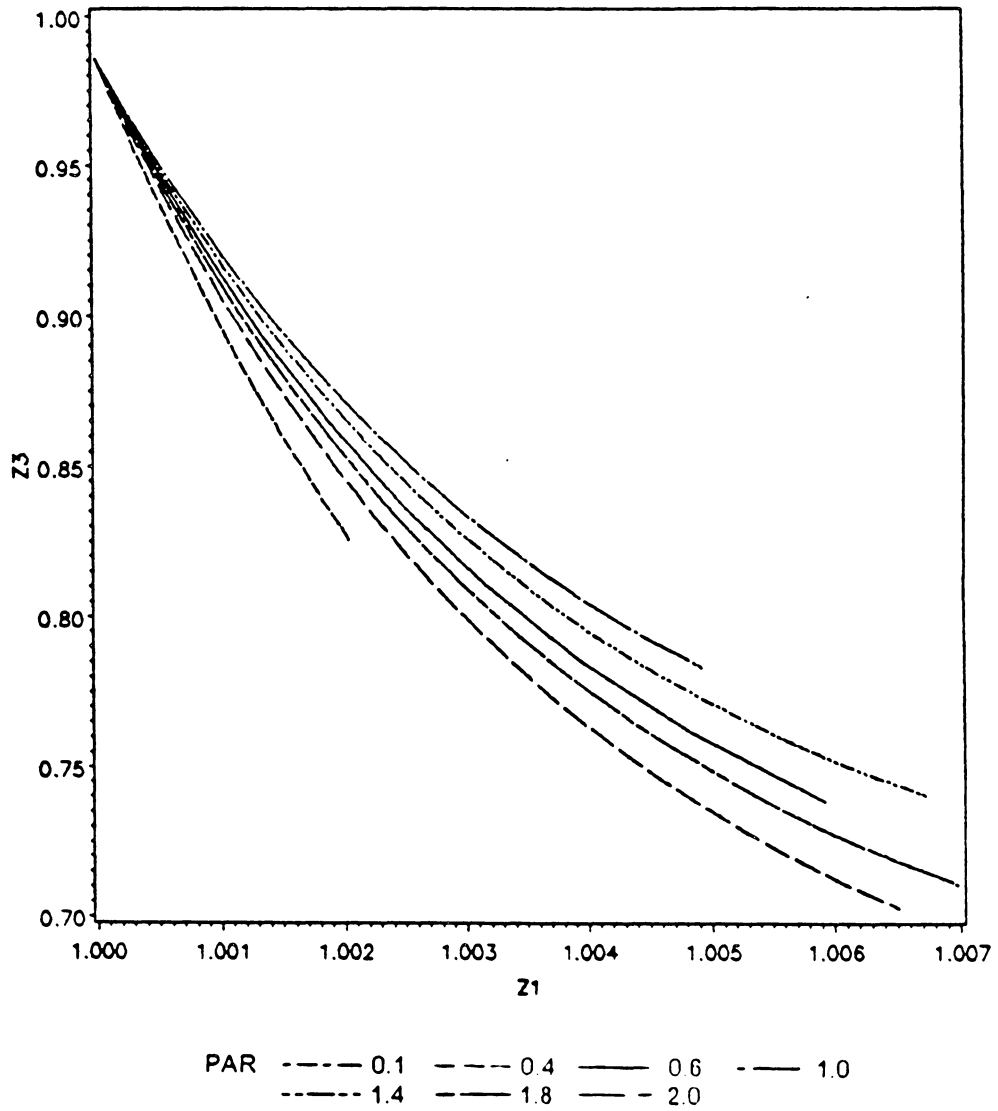


Fig.21: Variation of z_1 with z_3

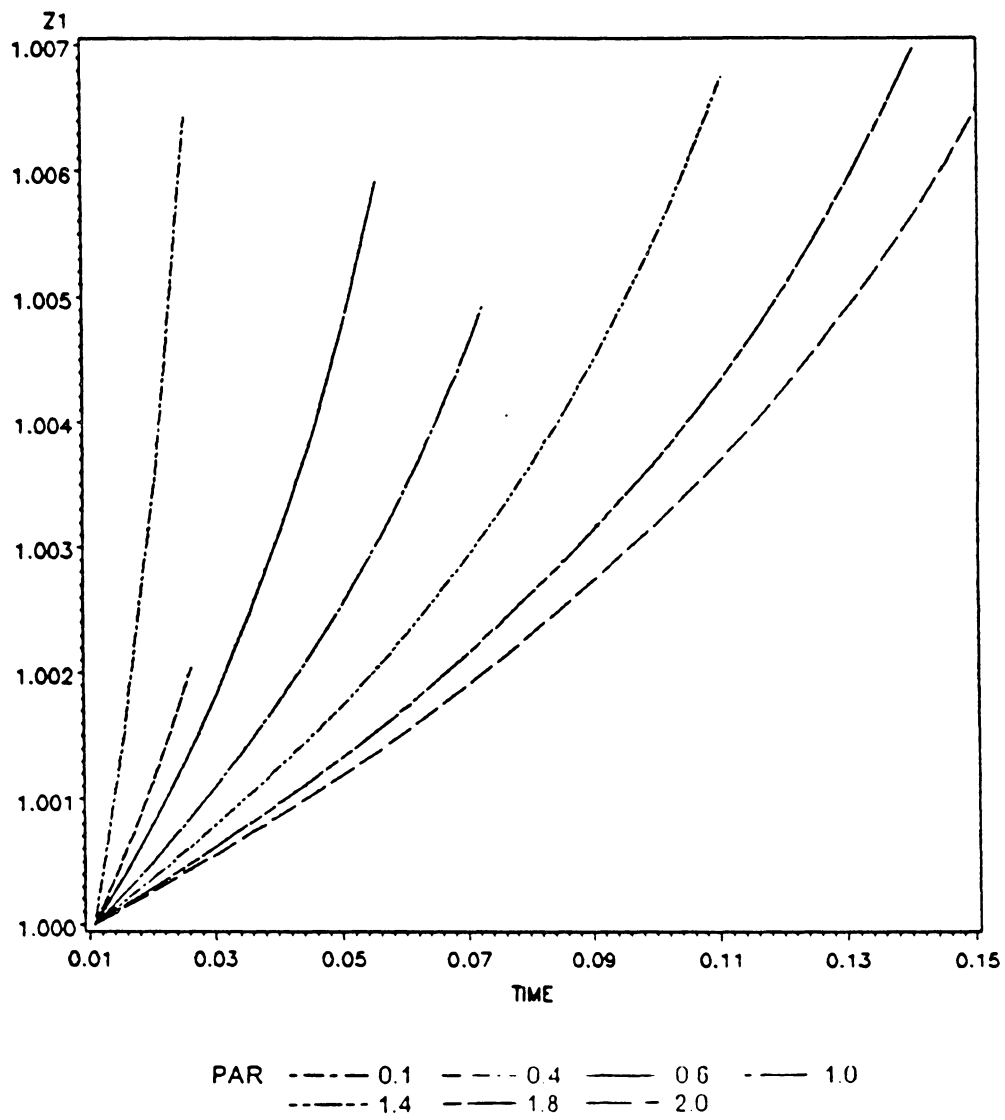


Fig.22: Variation of z_1 with time

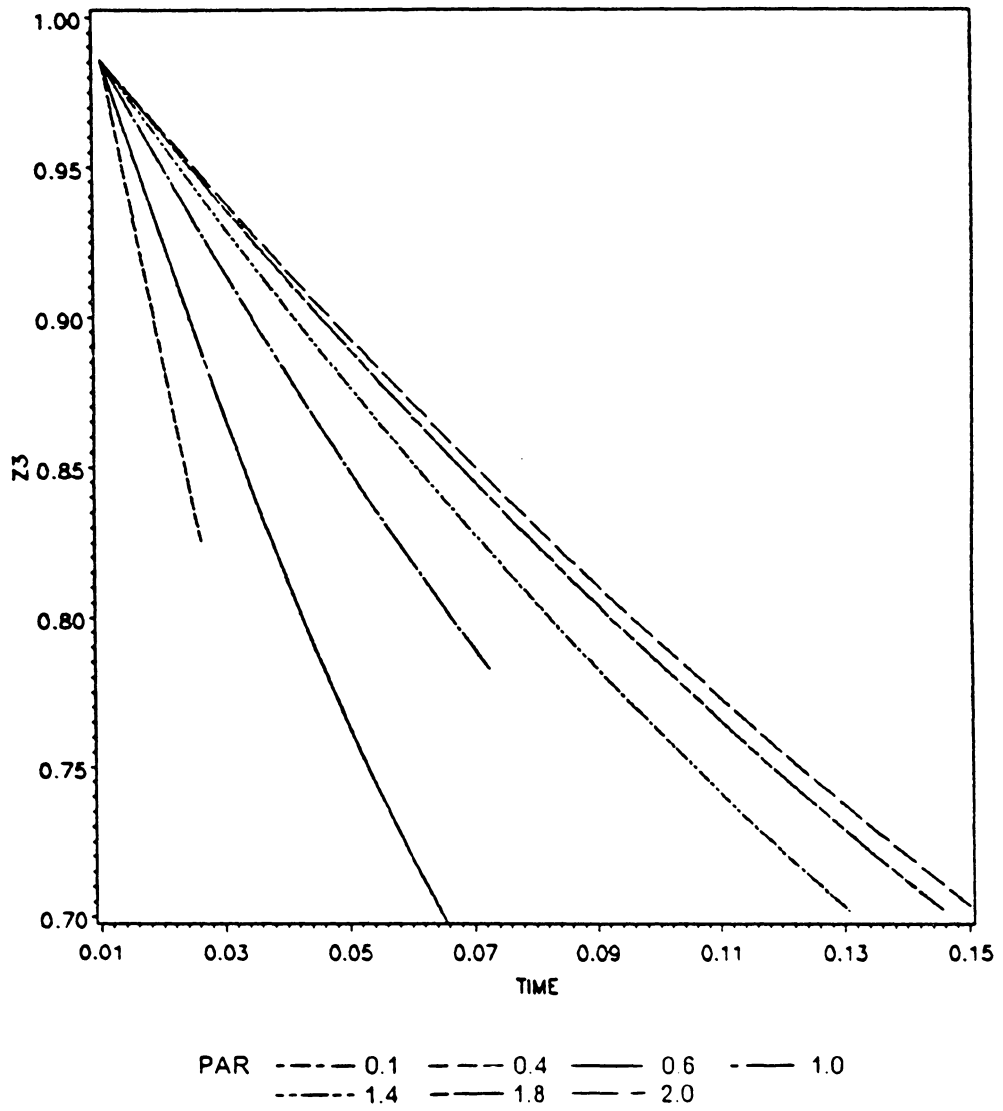


Fig.23: Variation of z_3 with time

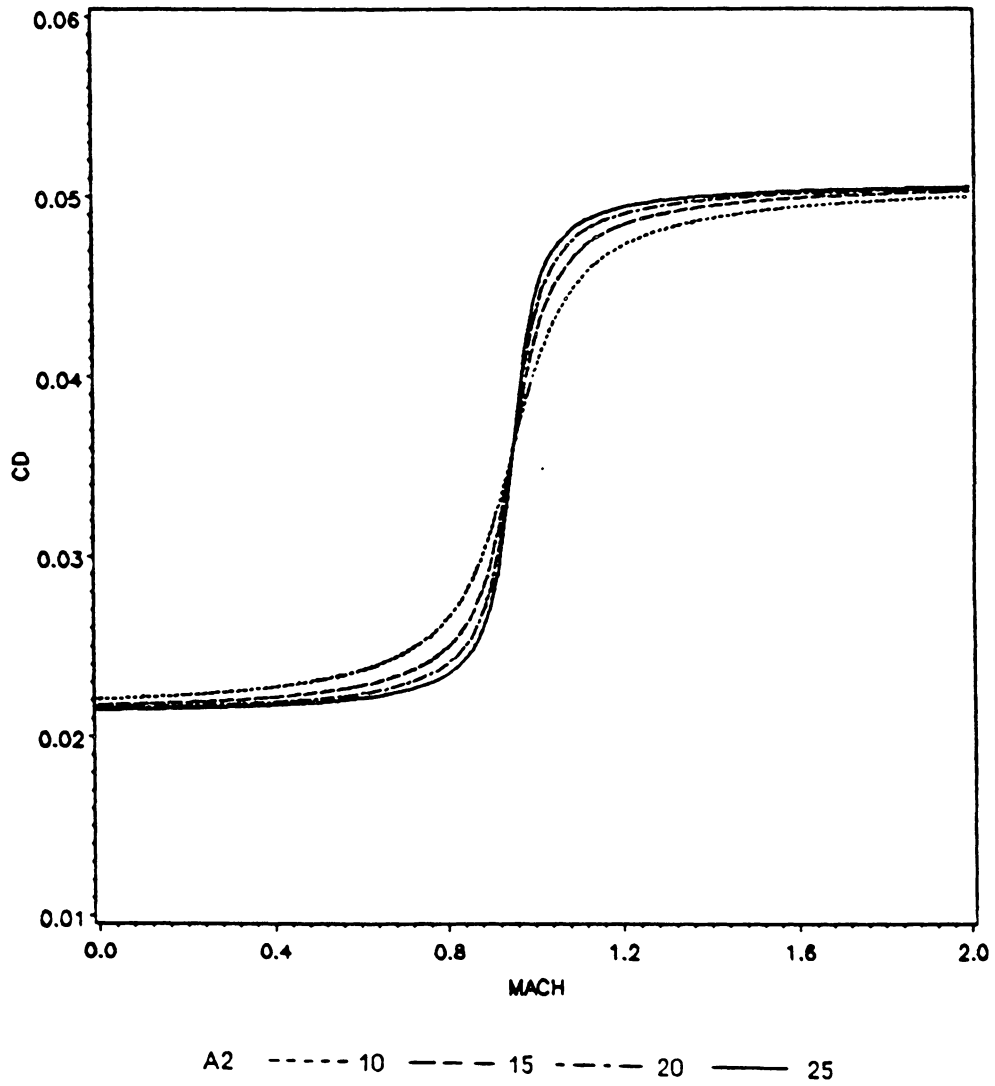


Fig.24: Variation of drag coefficient with Mach number

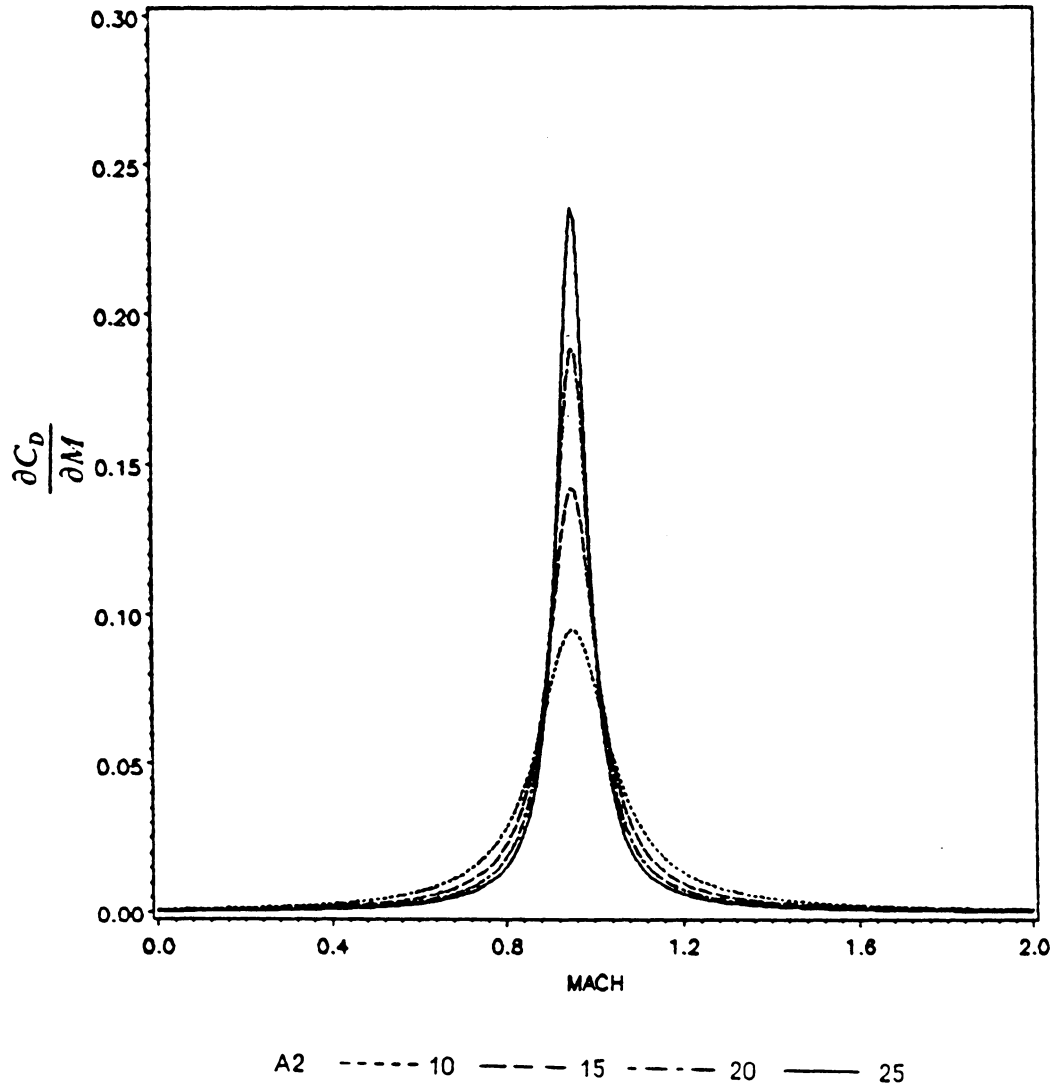


Fig.25: Variation of $\frac{\partial C_D}{\partial M}$ with Mach number

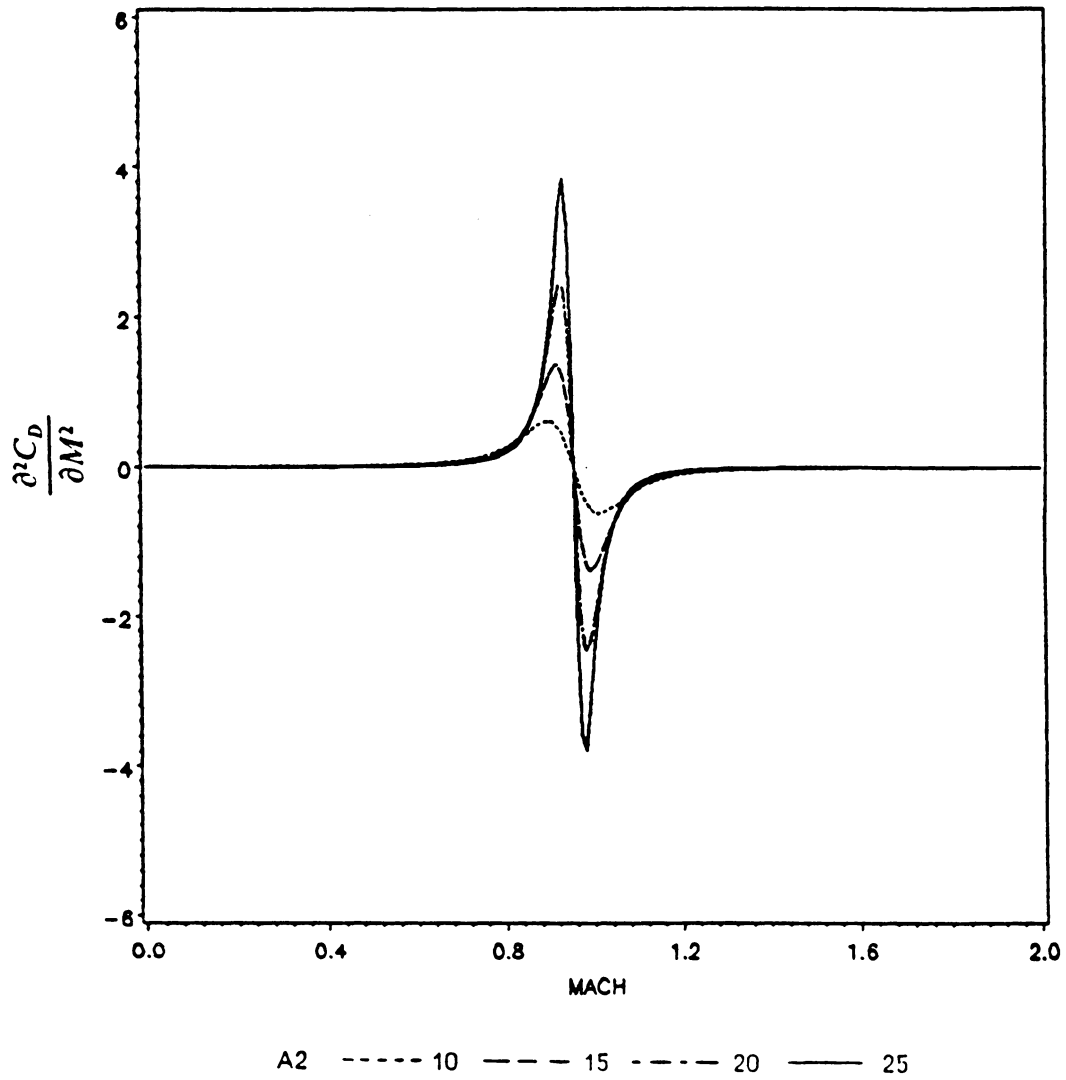


Fig.26: Variation of $\frac{\partial^2 C_D}{\partial M^2}$ with Mach number

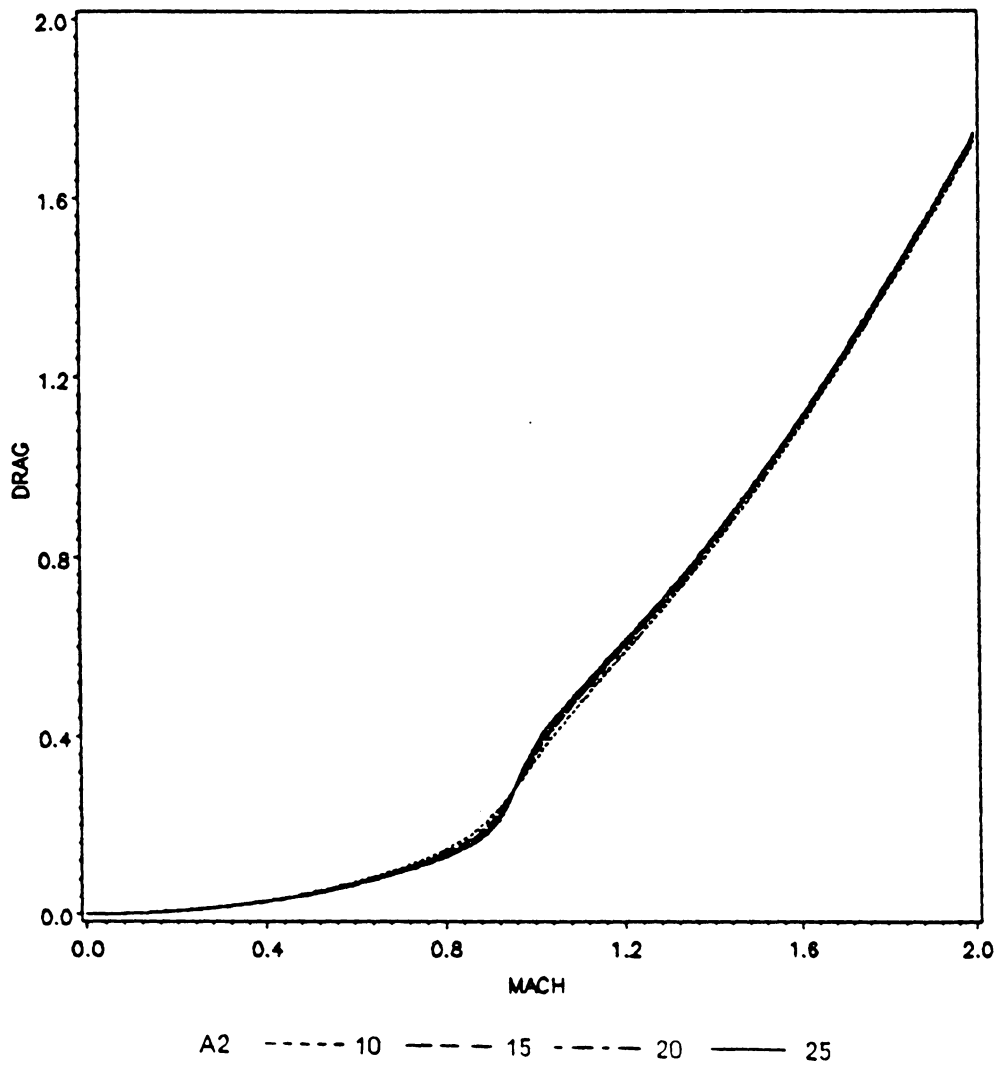


Fig.27: Variation of Drag with Mach number

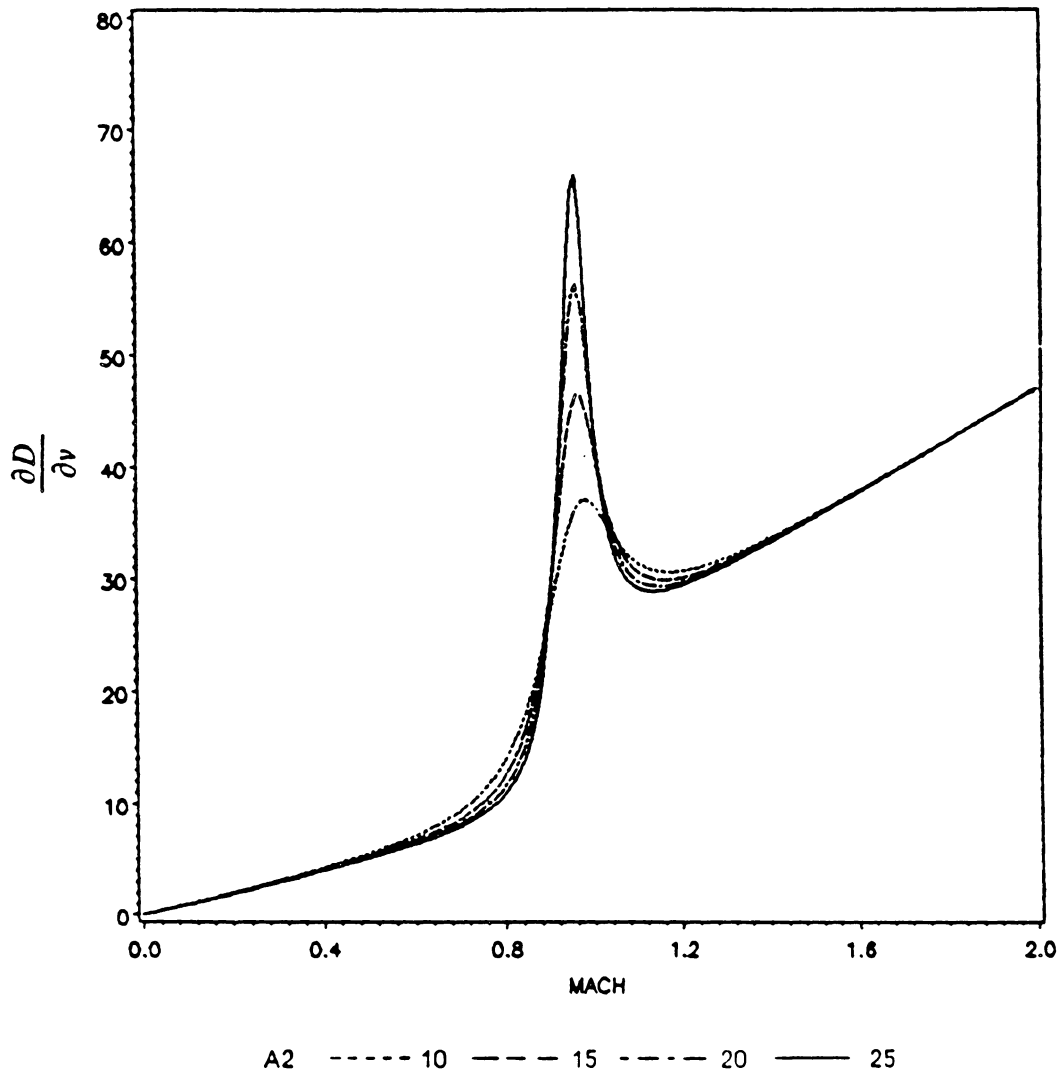


Fig.28: Variation of $\frac{\partial D}{\partial v}$ with Mach number

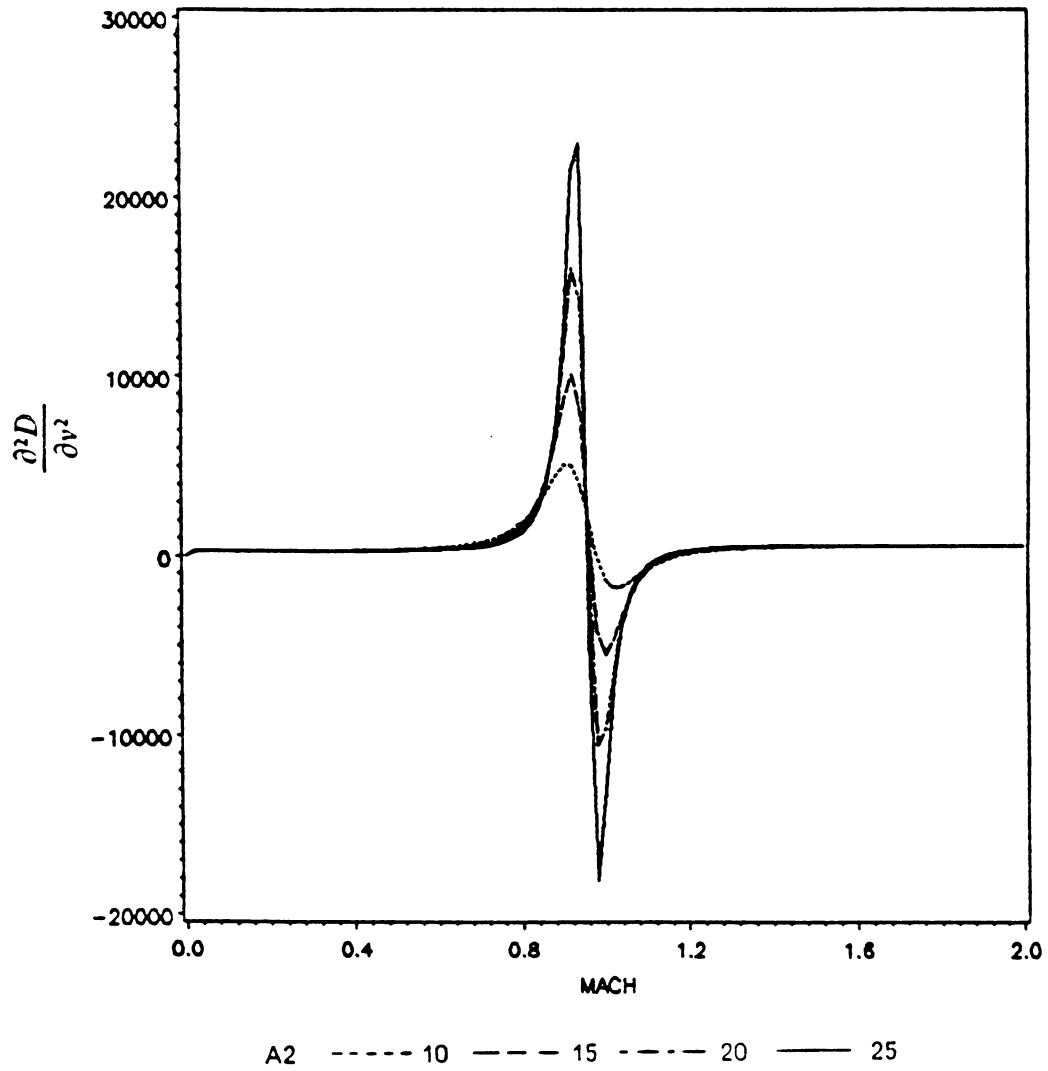


Fig.29: Variation of $\frac{\partial^2 D}{\partial v^2}$ with Mach number

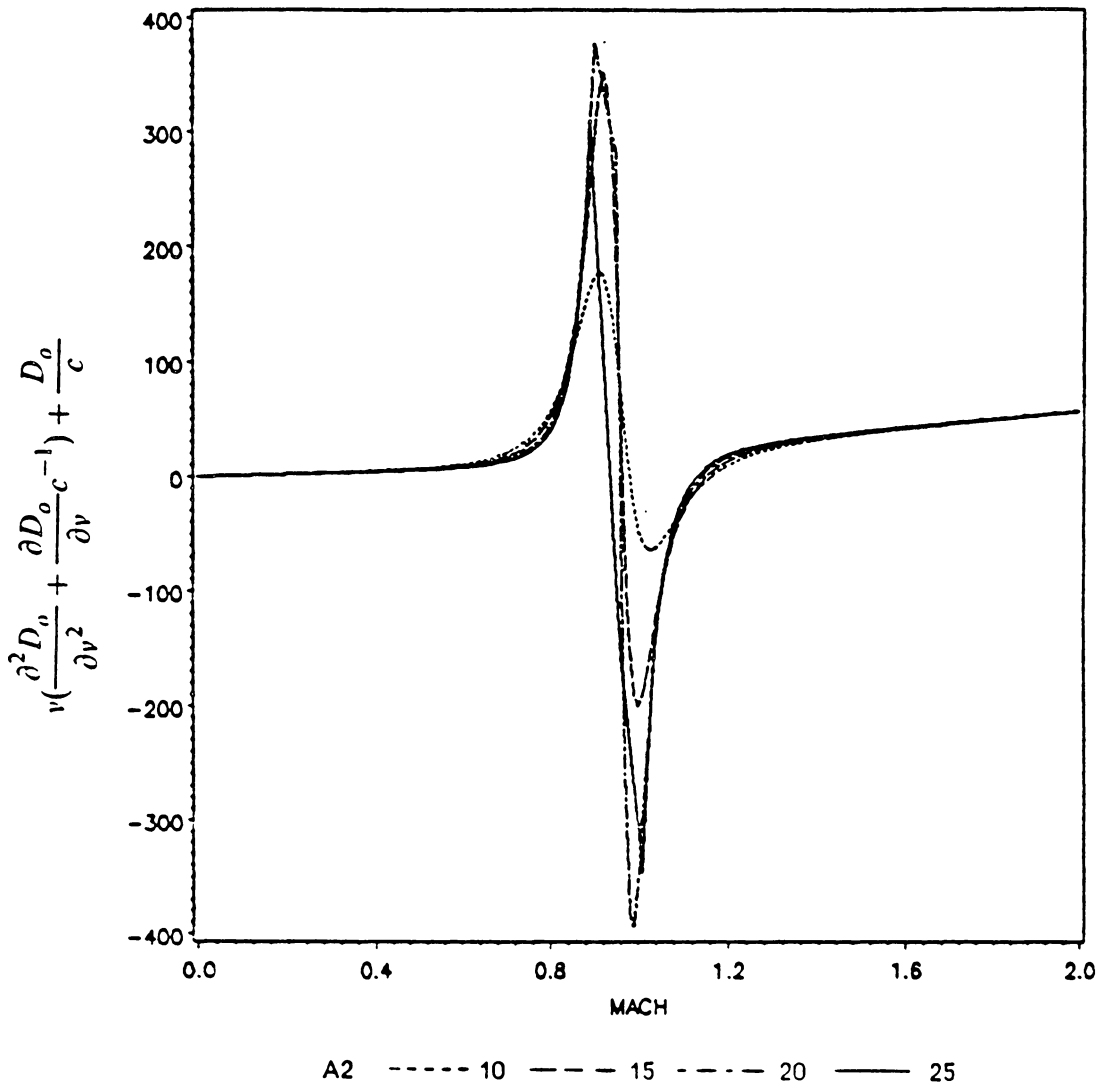


Fig.30: Variation of $v\left(\frac{\partial^2 D_o}{\partial v^2} + \frac{\partial D_o}{\partial v} c^{-1}\right) + \frac{D_o}{c}$ with Mach number

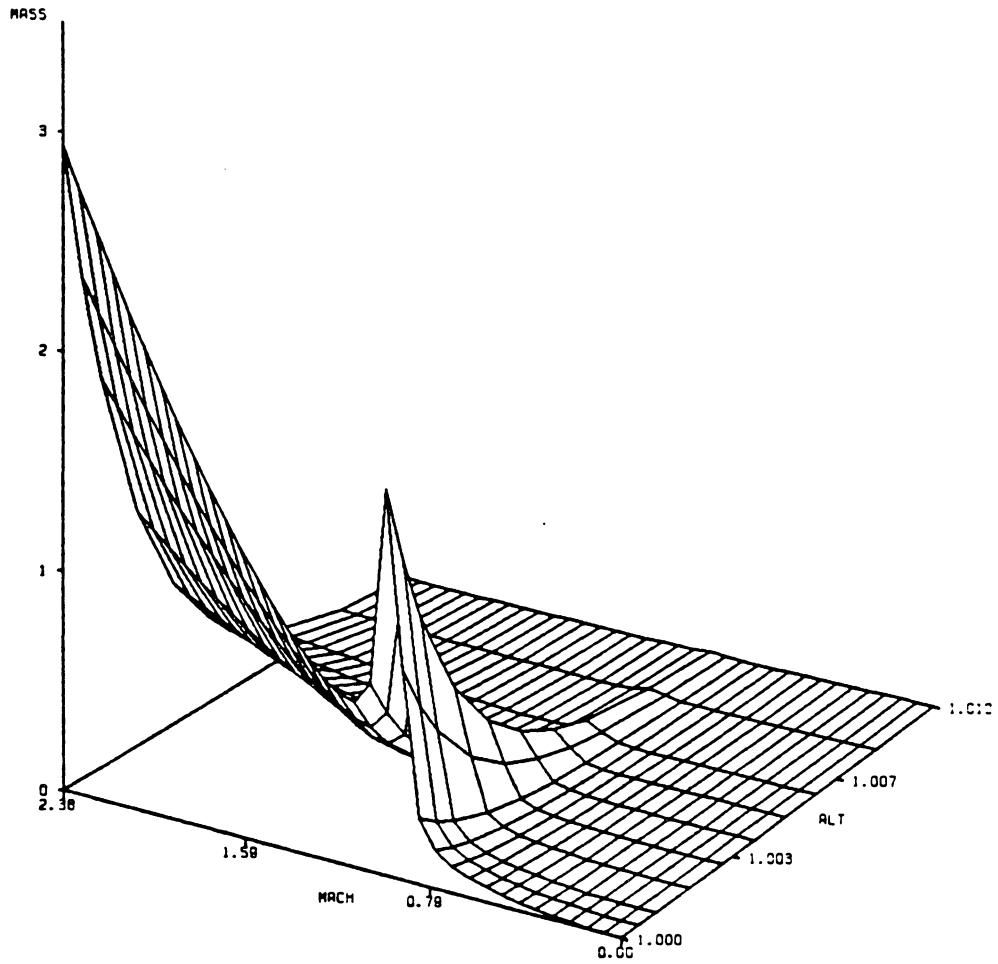


Fig.31: Singular surface for Mach dependent drag coefficient

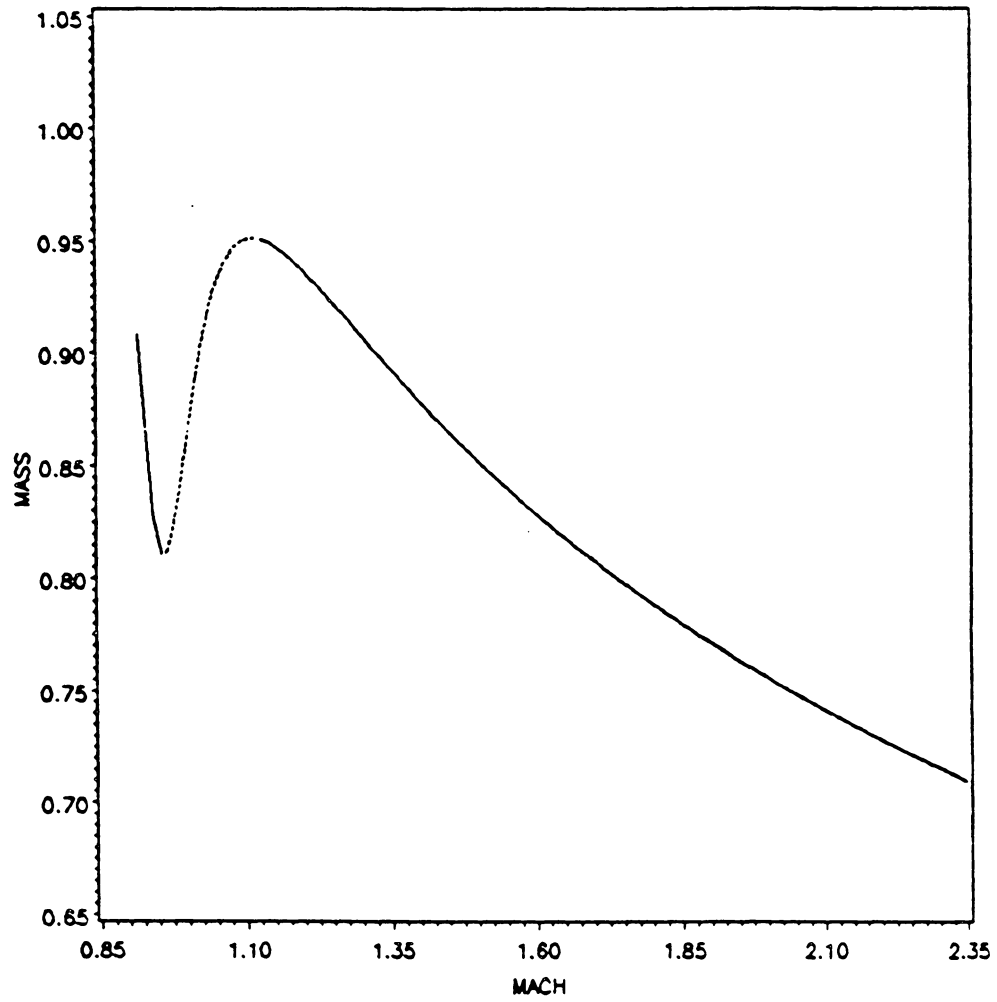


Fig.32: Projection of singular path on mass-velocity plane

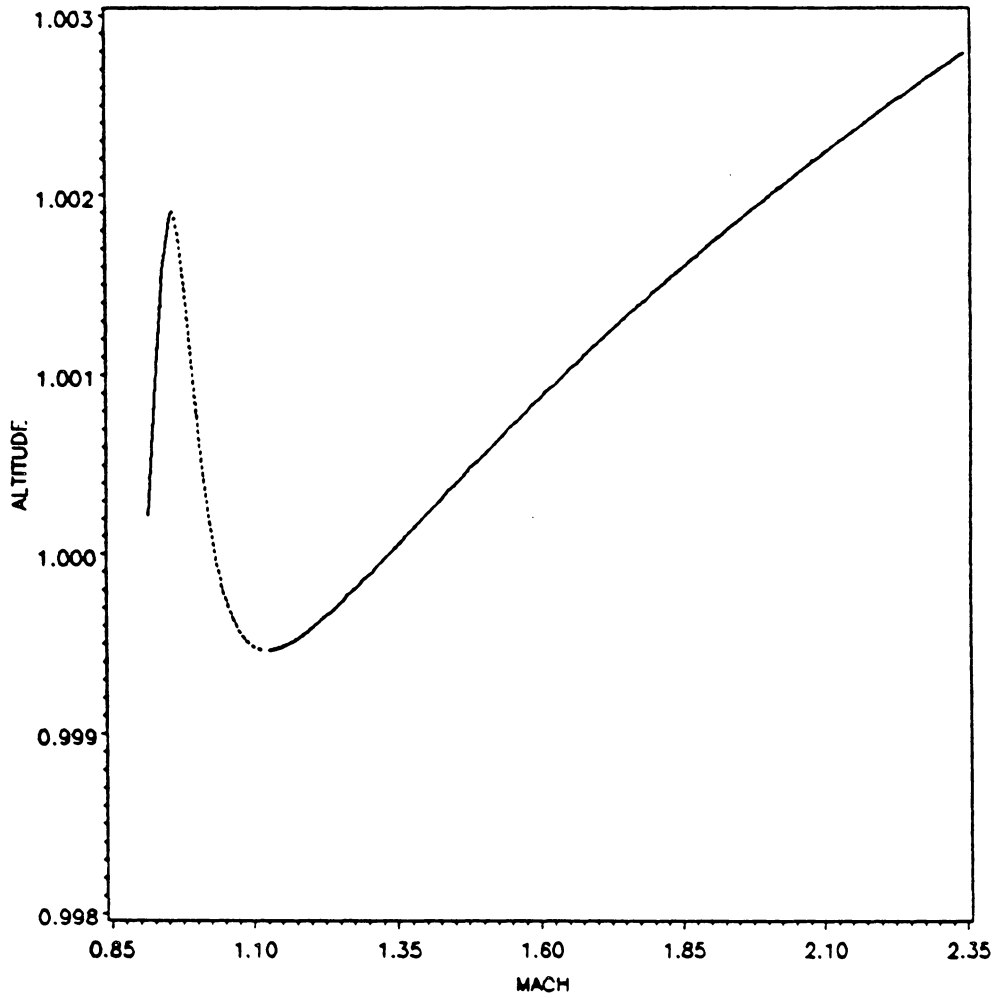


Fig.33: Projection of singular path on altitude-velocity plane

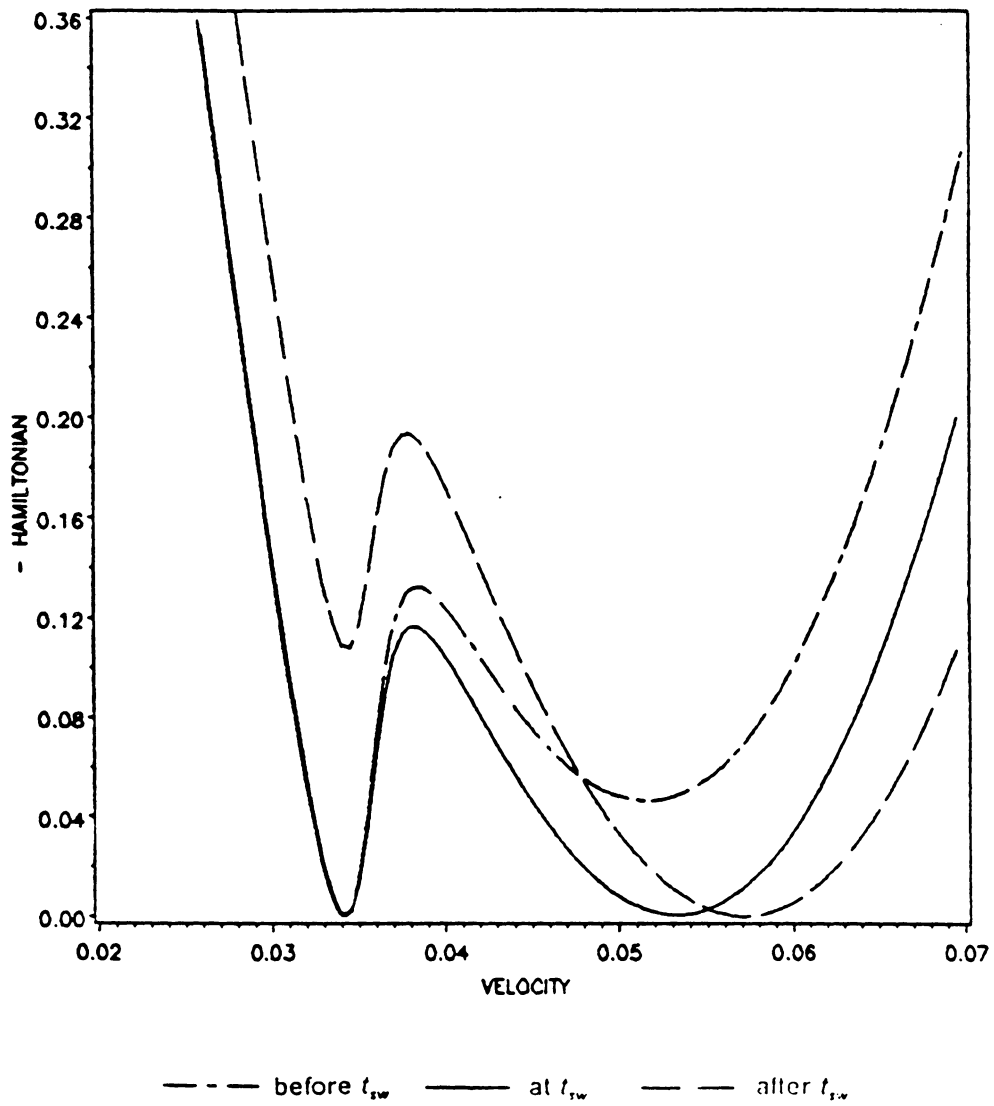


Fig.34: Variation of $-\tilde{\mathcal{H}}$ with $z_2 = v$

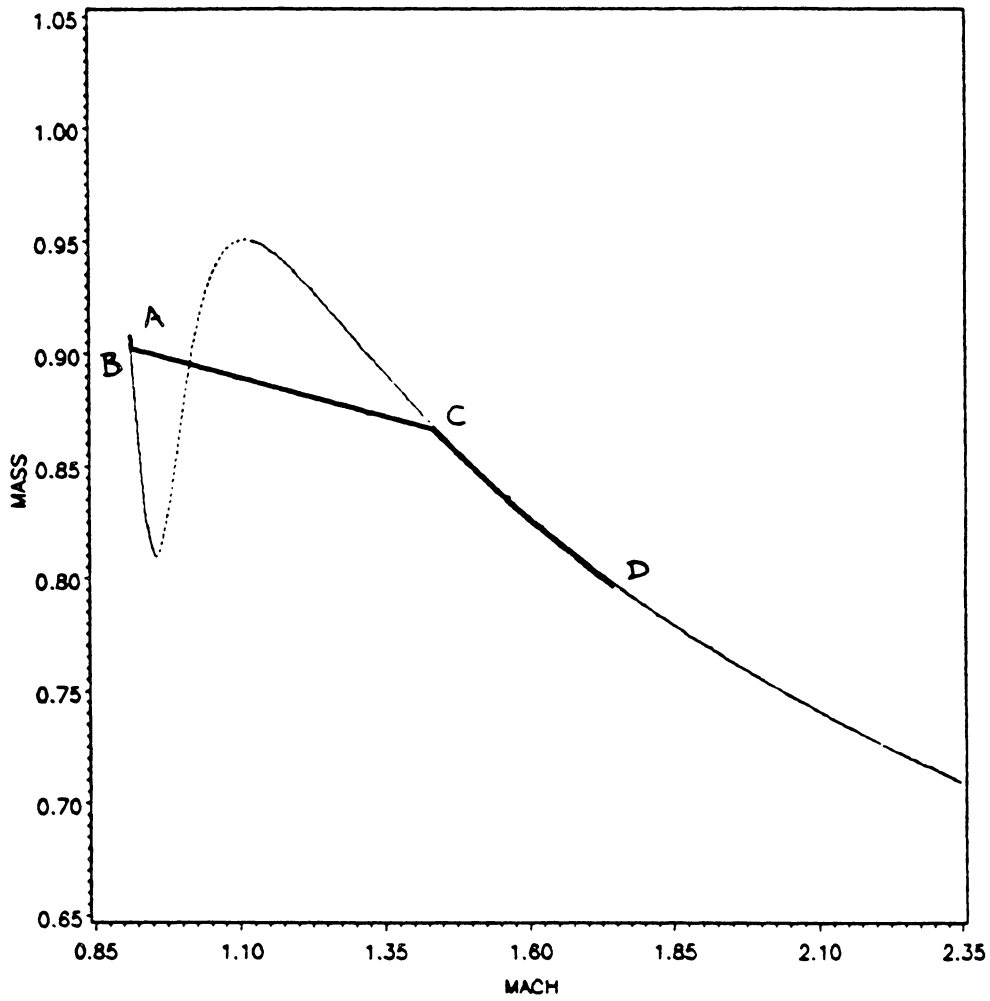


Fig.35: Projection of the trajectory on mass-velocity plane for $P_{\max} = \infty$

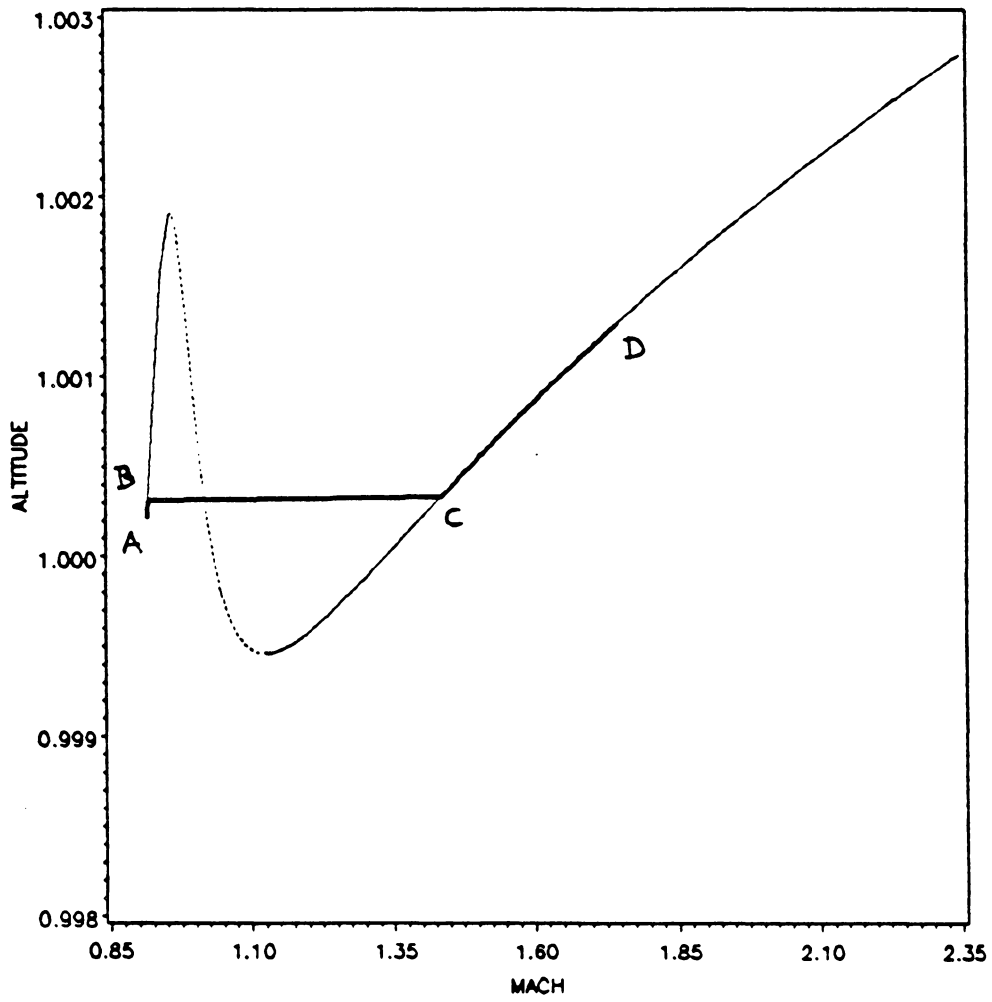


Fig.36: Projection of the trajectory on altitude-velocity plane for $P_{\max} = \infty$

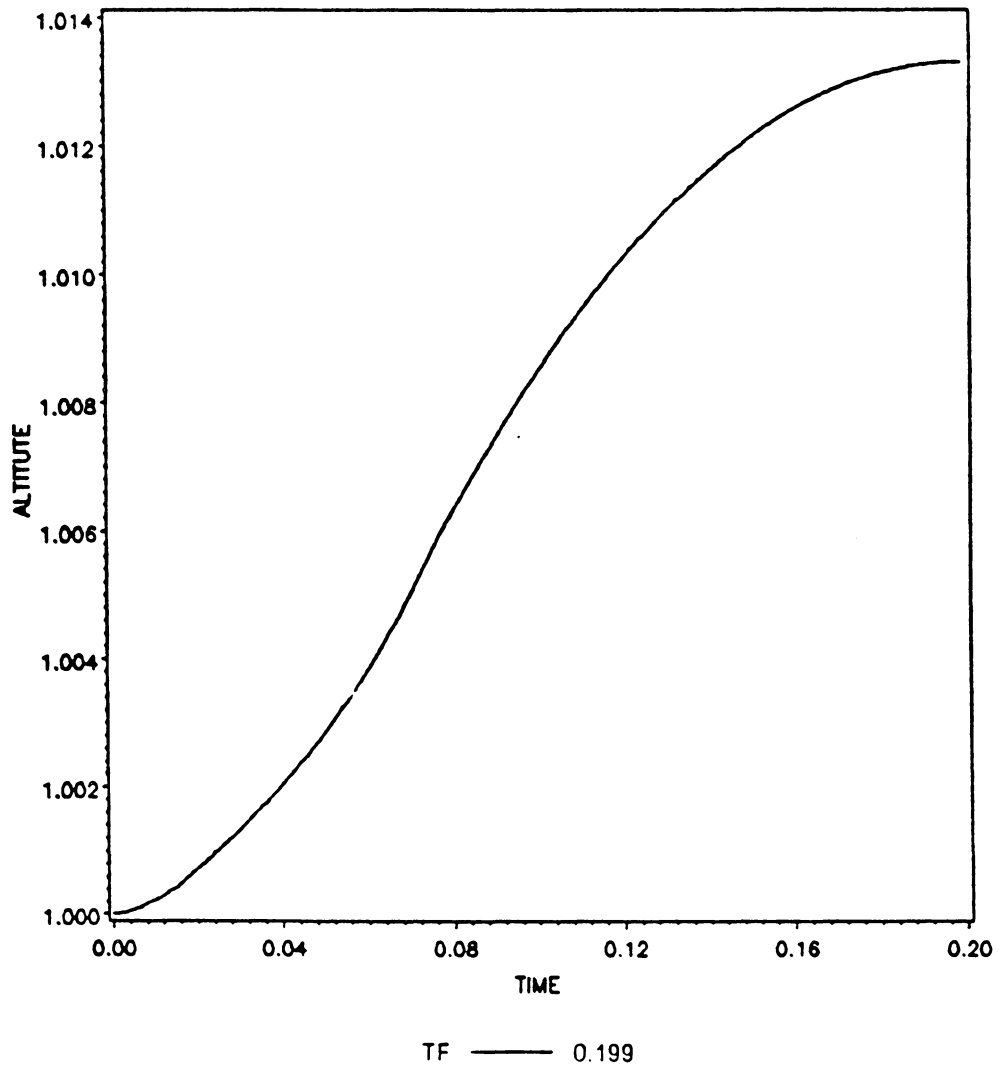


Fig.37: Variation of altitude h with time for $P_{\max} = 6$

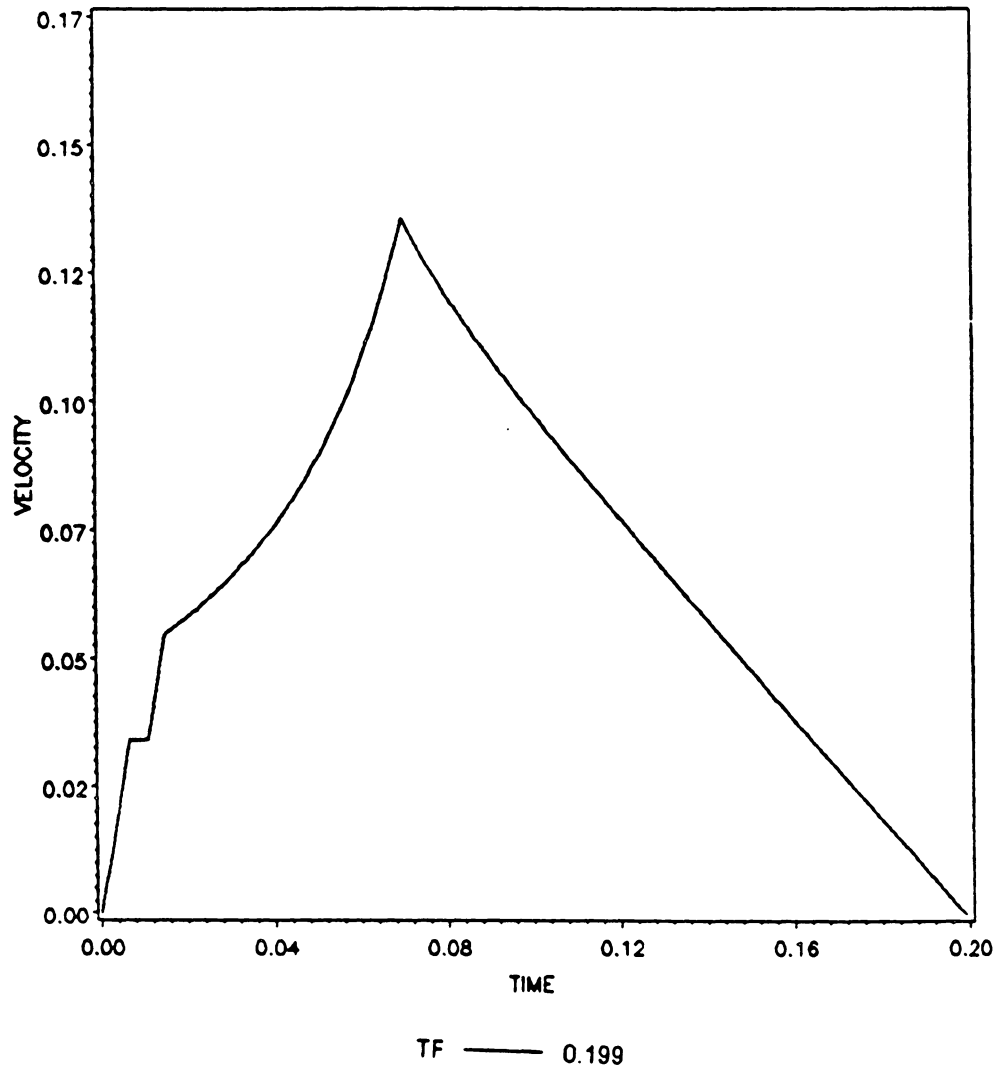


Fig.38: Variation of velocity v with time for $P_{\max} = 6$

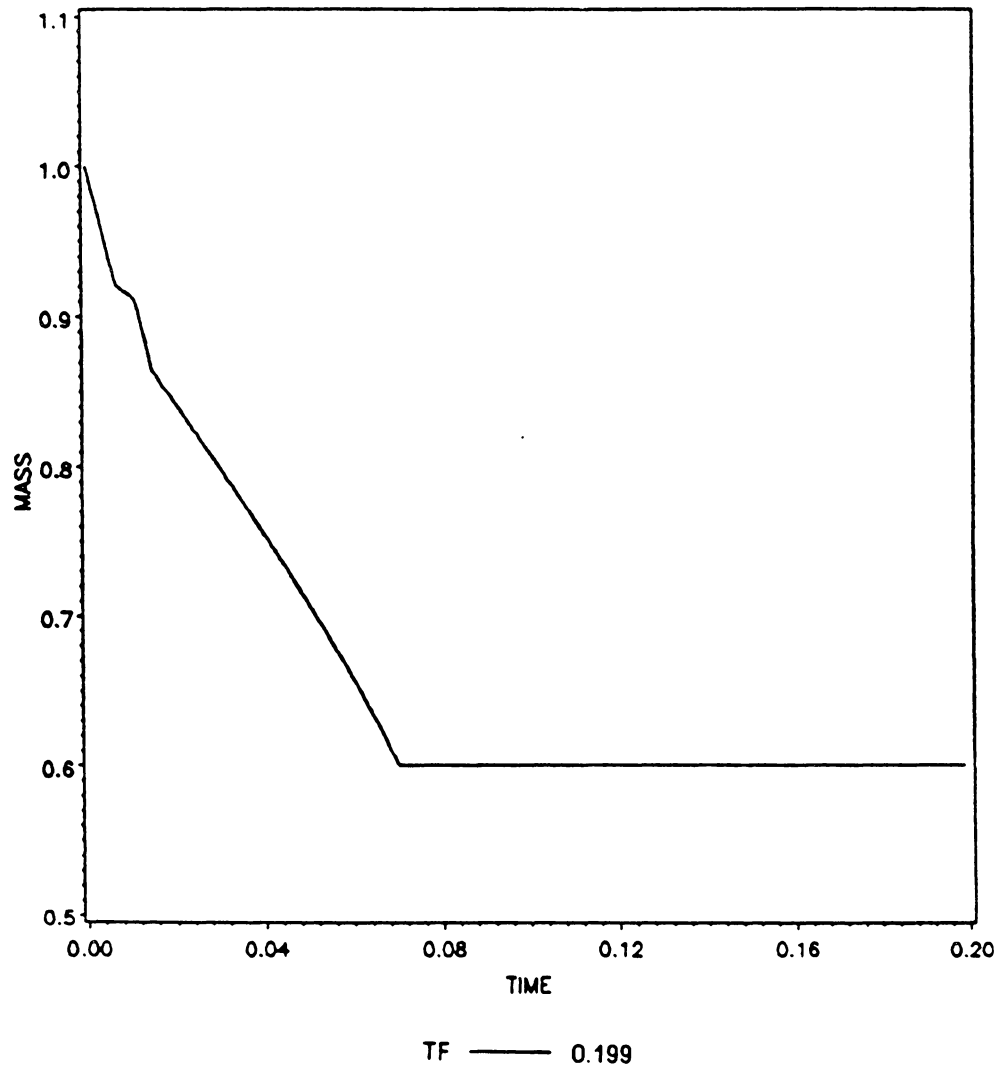


Fig.39: Variation of mass m with time for $P_{\max} = 6$

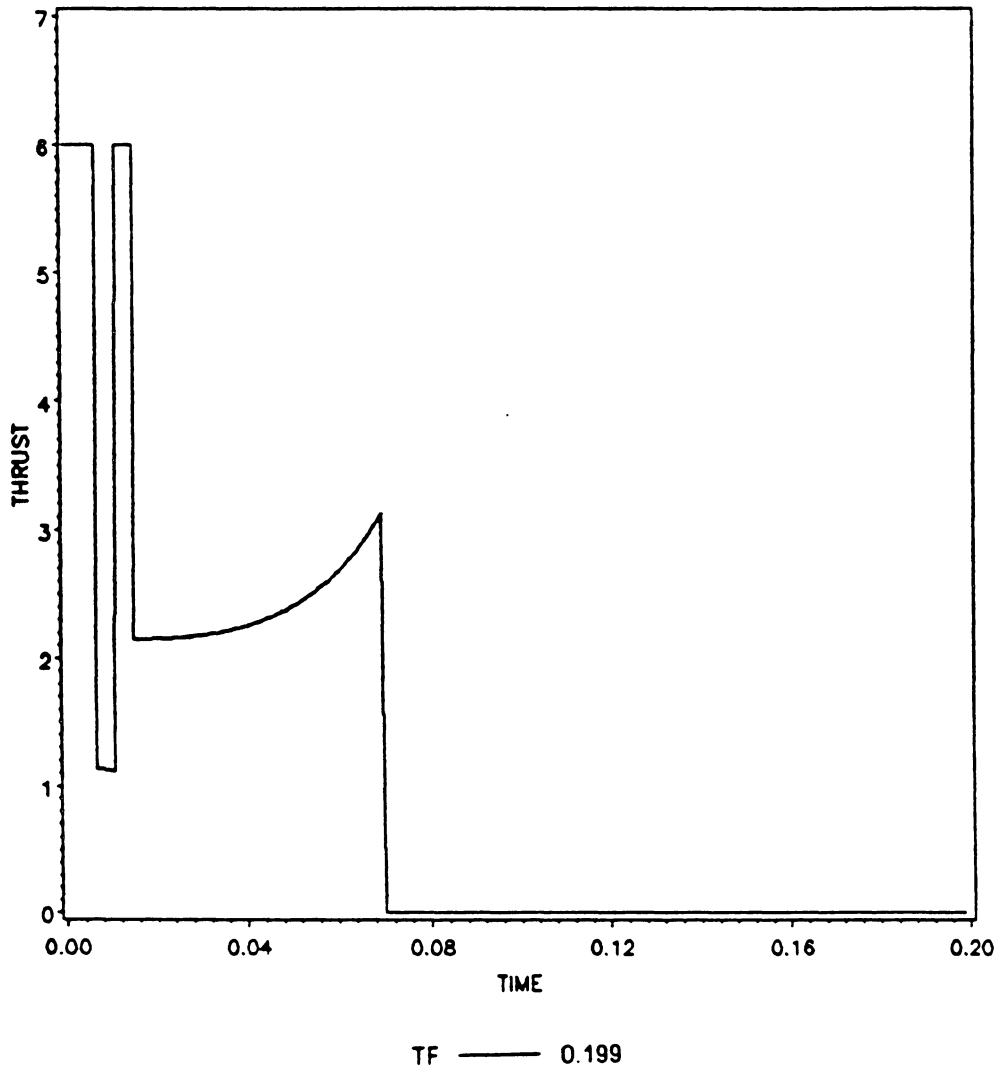


Fig.40: Variation of thrust P with time for $P_{max} = 6$

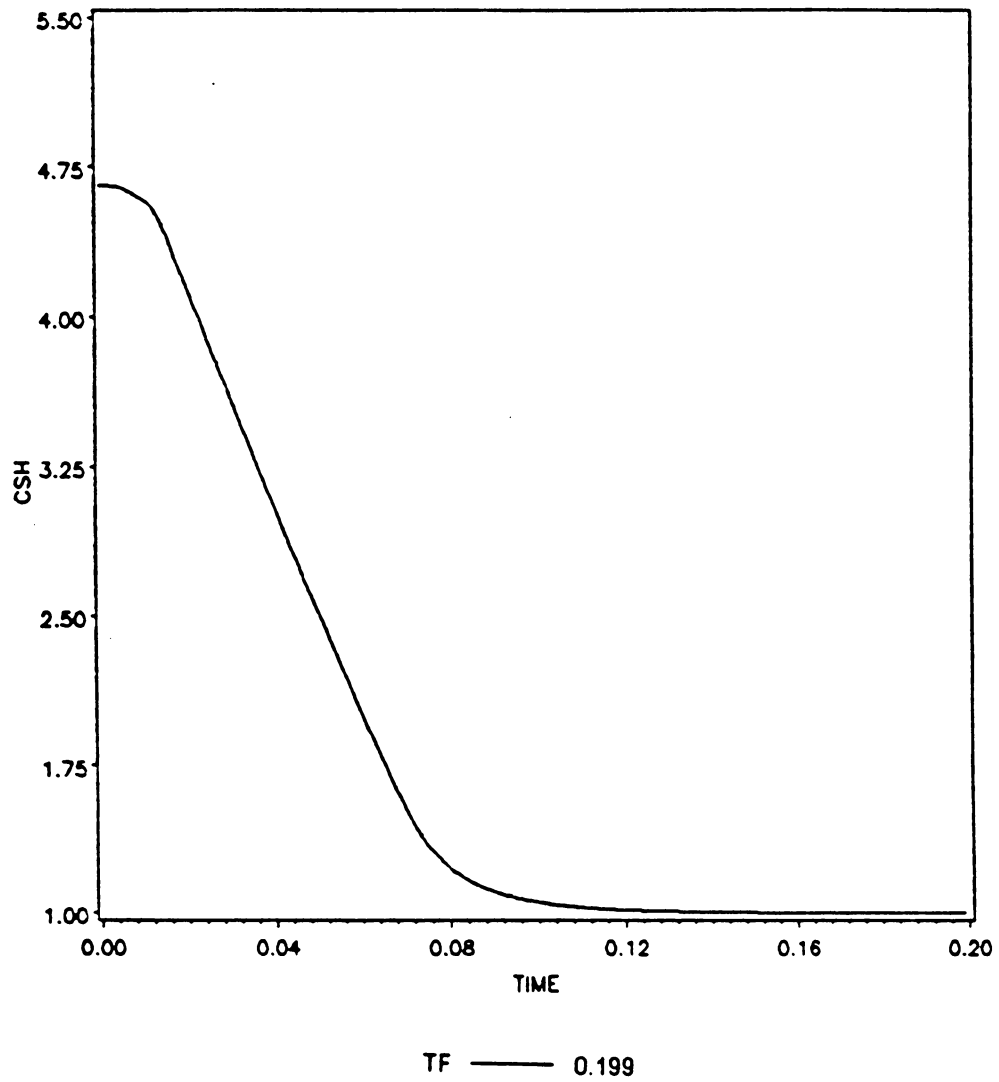


Fig.41: Variation of costate λ_h with time for $P_{\max} = 6$

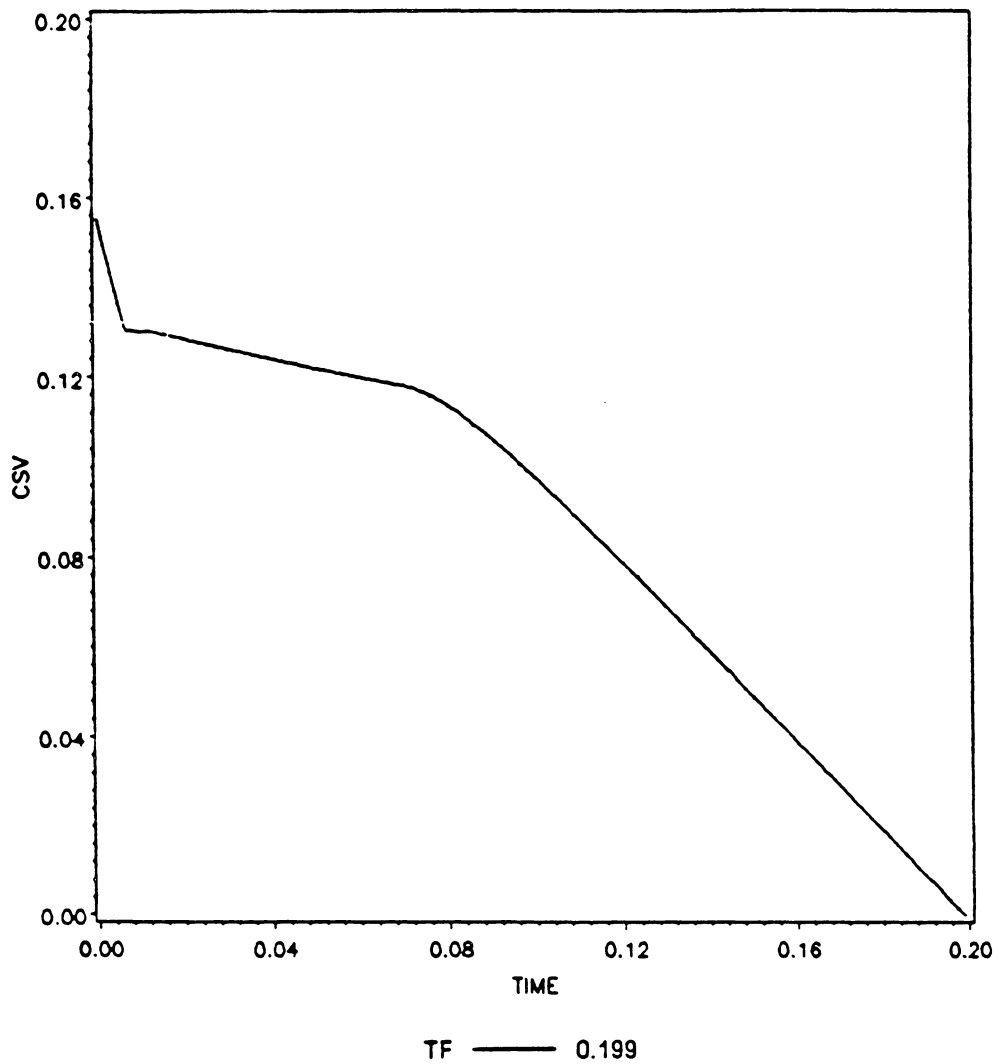


Fig.42: Variation of costate λ_v with time for $P_{\max} = 6$

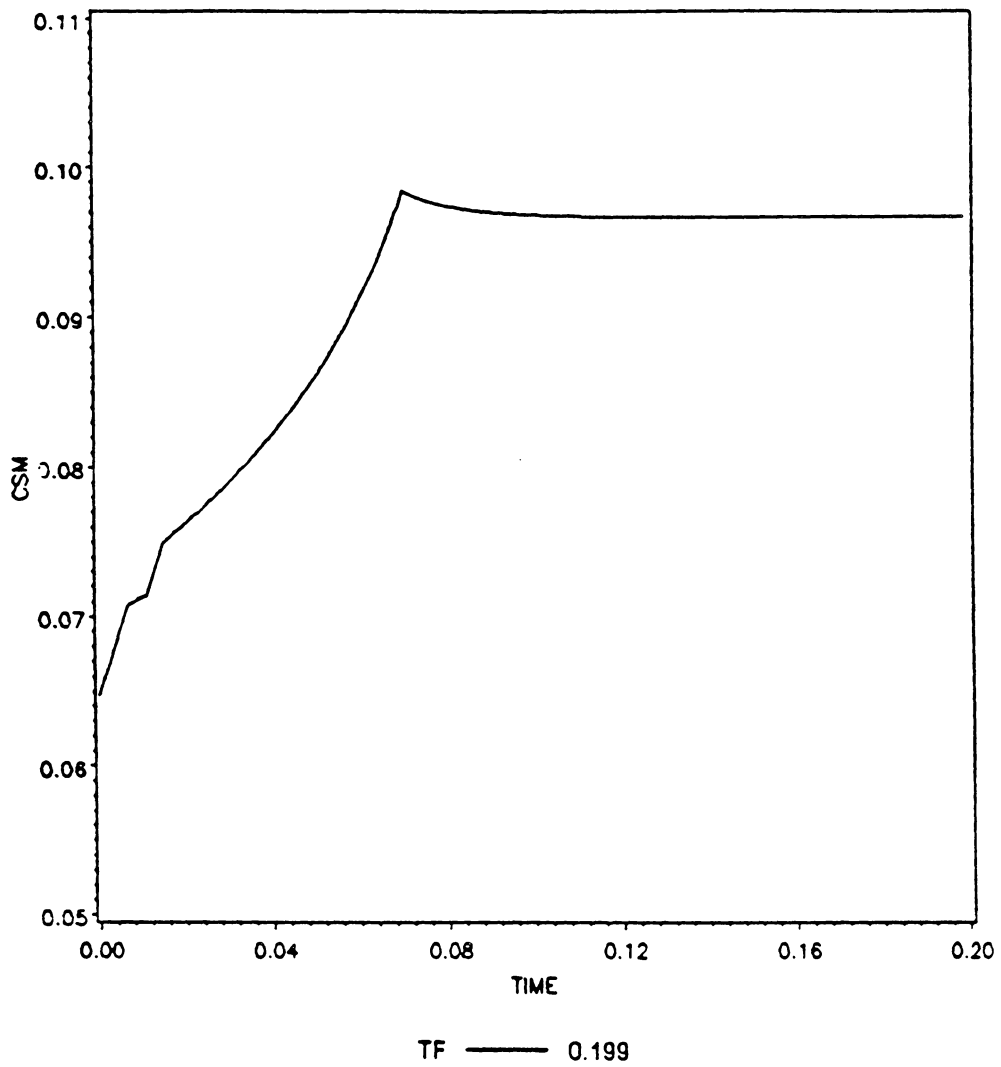


Fig.43: Variation of costate λ_m with time for $P_{\max} = 6$

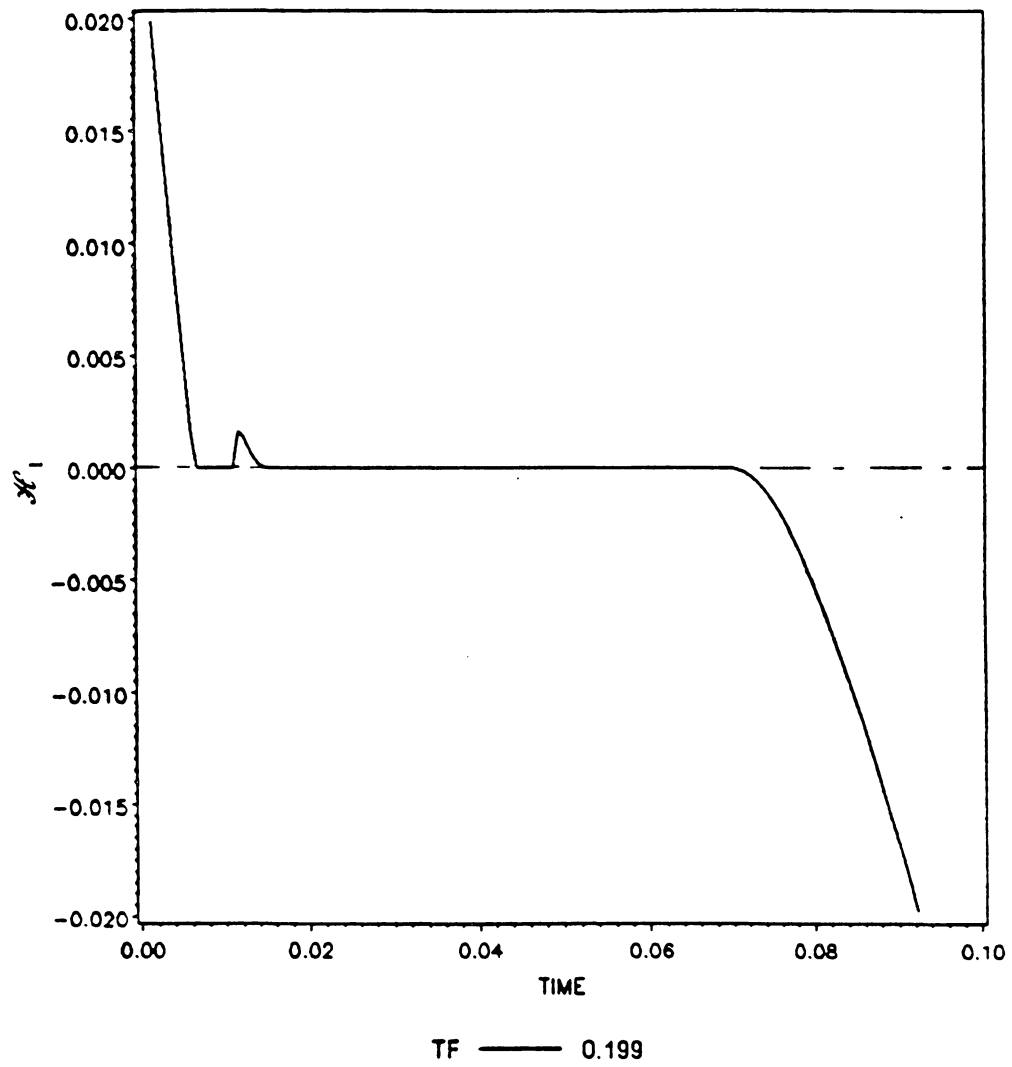


Fig.44: Switching function \mathcal{H}_1 vs. time for $P_{\max} = 6$

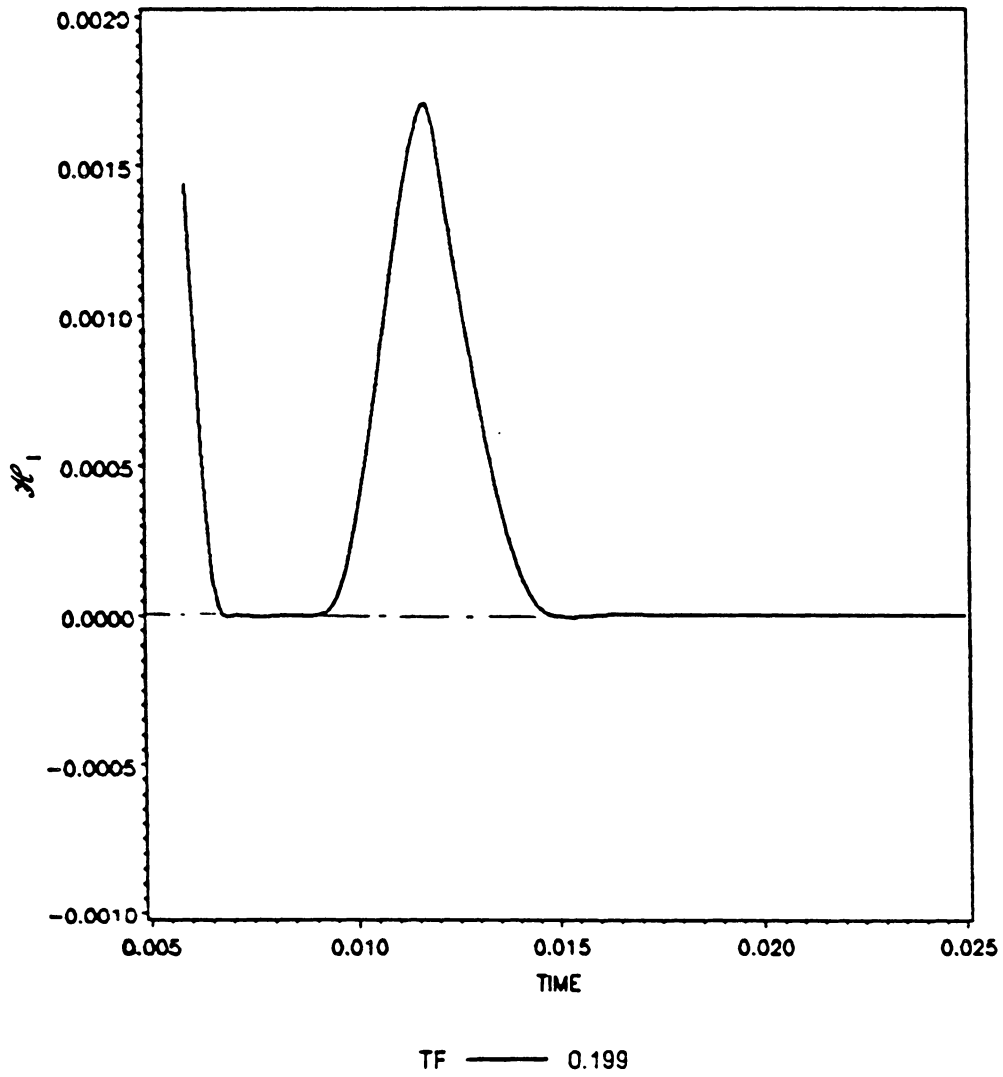


Fig.45: Switching function \mathcal{H}_1 vs. time for $P_{\max} = 6$

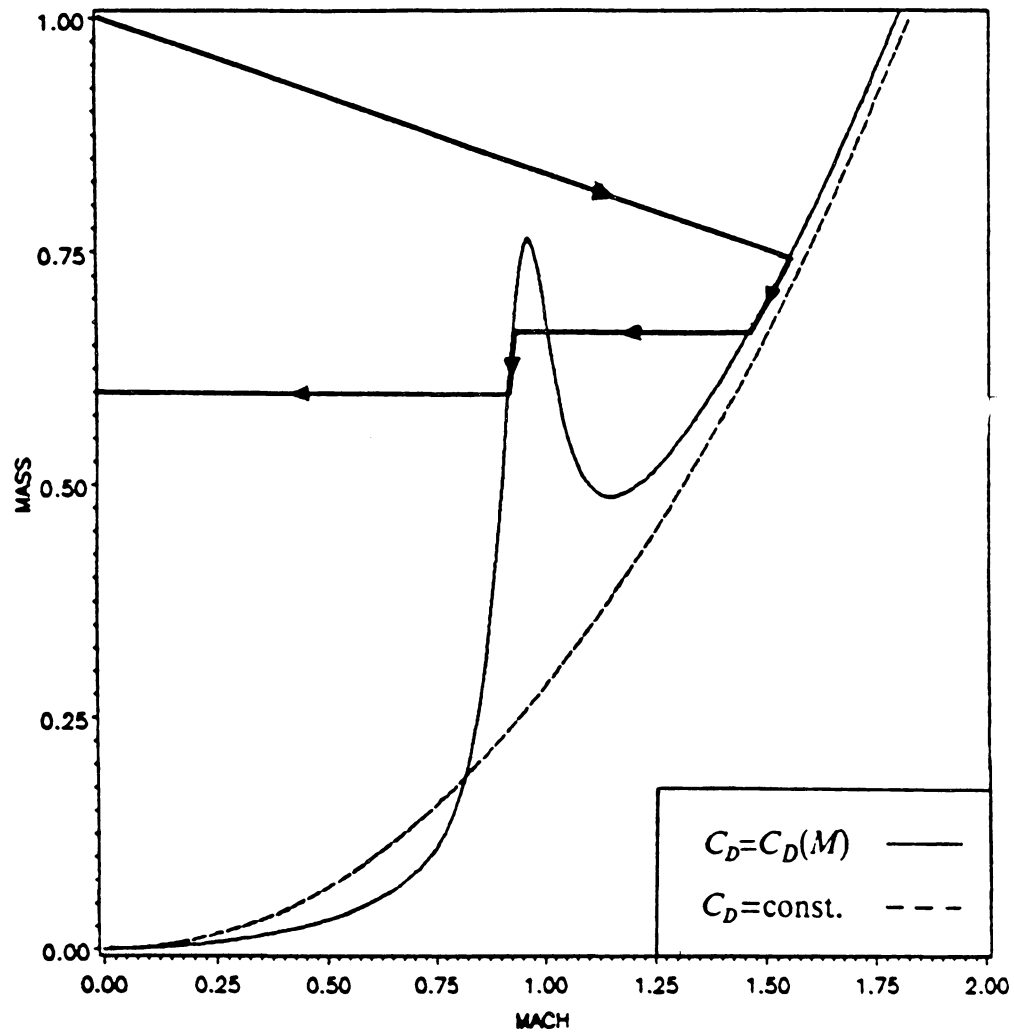


Fig.46: Singular surface for drag independent of air density

**The vita has been removed from
the scanned document**